

Human Toxicogenomic Analysis of the Monohaloacetic Acids

Web Report #4132

 Subject Area: Water Quality



Human Toxicogenomic Analysis of the Monohaloacetic Acids



About the Water Research Foundation

The Water Research Foundation is a member-supported, international, 501(c)3 nonprofit organization that sponsors research that enables water utilities, public health agencies, and other professionals to provide safe and affordable drinking water to consumers.

The Foundation's mission is to advance the science of water to improve the quality of life. To achieve this mission, the Foundation sponsors studies on all aspects of drinking water, including resources, treatment, and distribution. Nearly 1,000 water utilities, consulting firms, and manufacturers in North America and abroad contribute subscription payments to support the Foundation's work. Additional funding comes from collaborative partnerships with other national and international organizations and the U.S. federal government, allowing for resources to be leveraged, expertise to be shared, and broad-based knowledge to be developed and disseminated.

From its headquarters in Denver, Colorado, the Foundation's staff directs and supports the efforts of more than 800 volunteers who serve on the Board of Trustees and various committees. These volunteers represent many facets of the water industry, and contribute their expertise to select and monitor research studies that benefit the entire drinking water community.

Research results are disseminated through a number of channels, including reports, the Website, Webcasts, workshops, and periodicals.

The Foundation serves as a cooperative program providing subscribers the opportunity to pool their resources and build upon each others' expertise. By applying Foundation research findings, subscribers can save substantial costs and stay on the leading edge of drinking water science and technology. Since its inception, the Foundation has supplied the water community with more than \$460 million in applied research value.

More information about the Foundation and how to become a subscriber is available at www.WaterRF.org.

Human Toxicogenomic Analysis of the Monohaloacetic Acids

Prepared by:

Michael J. Plewa and Elizabeth D. Wagner

Department of Crop Sciences, College of Agricultural, Consumer and Environmental Sciences
University of Illinois at Urbana-Champaign, 1101 West Peabody Dr., Urbana, IL 61801

Sponsored by:

Water Research Foundation

6666 West Quincy Avenue, Denver, CO 80235

Published by:



DISCLAIMER

This study was funded by the Water Research Foundation (Foundation). The Foundation assumes no responsibility for the content of the research study reported in this publication or for the opinions or statements of fact expressed in the report. The mention of trade names for commercial products does not represent or imply the approval or endorsement of the Foundation. This report is presented solely for informational purposes.

Copyright © 2012
by Water Research Foundation

ALL RIGHTS RESERVED.
No part of this publication may be copied, reproduced
or otherwise utilized without permission.



Printed on recycled paper

CONTENTS

LIST OF TABLES	iv
LIST OF FIGURES	VIII
FOREWORD	XI
ACKNOWLEDGMENTS	XIII
EXECUTIVE SUMMARY	xv
CHAPTER 1: INTRODUCTION	1
Background	1
Monohaloacetic Acids	2
Comparative Mammalian Cell Toxicological Responses: Mechanisms of Action	3
Toxicogenomics	4
Hypothesis	5
Objectives	5
CHAPTER 2: MATERIALS AND METHODS	7
Introduction	7
Reagents	7
Cultured Cells	7
Chinese Hamster Ovary Cells	7
Human Small Intestine Epithelial Cells	8
Cell Viability	8
Single Cell Gel Electrophoresis (SCGE) Assay	9
DNA Repair Experiment Treatment Conditions	10
MonoHAA Toxicogenomic Analysis	11
MonoHAA Treatment of Human FHs Cells and RNA Isolation and Purification	11
cDNA Synthesis	11
Real Time PCR Analyses	11
Human DNA Damage/Repair Genes and Human Toxic Response Genes	12
Quality Assurance/Quality Control	15
Data Analysis	15
Safety	16
CHAPTER 3: HUMAN FHS CELLS AND TOXICOGENOMIC ANALYSES	17
SCGE Analysis of IAA, BAA, and CAA Using Human FHs Cells	15
Iodoacetic Acid	18
Bromoacetic Acid	19
Chloroacetic Acid	20
Equivalent Genotoxic Effects Among the Monohaloacetic Acids	21
Comparison of DNA Damage Induction by MonoHAAs in CHO and FHs Cells	21
Comparison of the Human FHs Cell Densities After Exposure to MonoHAAs	23

CHAPTER 4: BROMOACETIC ACID TOXICOGENOMICS	25
Introduction.....	25
General Requirements and Limits for Toxicogenomic Experimental Designs	25
Toxicogenomic Analysis of Bromoacetic Acid.....	26
Treatment of FHs Cells.....	26
RNA Isolation and DNase Treatment.....	26
RNA Quantity and Quality Assessment	26
cDNA Synthesis.....	27
Real Time PCR Analysis	28
Statistical Analysis.....	29
FHs Cell Genotoxicity	29
Real-Time qRT-PCR Array Analysis	29
Interpretation of Bromoacetic Acid Toxicogenomic Results	31
CHAPTER 5: MONOHALOACETIC ACID COMPARATIVE TOXICOGENOMICS.....	39
Quantitative Comparative Toxicogenomics of the MonoHAAs	39
Comparative Cytotoxicity, Genotoxicity and Teratogenicity of the Monohaloacetic Acids	39
Cytotoxicity and Genotoxicity Measurements Associated with Toxicogenomic Experiments	43
MonoHAA Treatment for Toxicogenomic Analyses, RNA Isolation and Purification ...	43
cDNA Synthesis.....	46
qRT-PCR Array	47
Comparative Analyses of Human Transcriptome Profiles	47
Functional Grouping of Genes in the DNA Damage-DNA Repair qRT-PCR Array	47
Human Transcriptome Profiles after MonoHAA Exposure	47
CHAPTER 6: REPAIR KINETICS OF DNA DAMAGE INDUCED BY THE MONOHALOACETIC ACIDS.....	59
Introduction.....	59
Comparative Analyses of DNA Repair Kinetics	59
Liquid Holding Time and Cytotoxicity.....	60
DNA Repair Kinetics.....	61
Frequency Distribution of DNA Repair.....	69
Statistical Analyses of DNA Repair	71
CHAPTER 7: MONOHALOACETIC ACID GENOMIC DAMAGE, ALTERED GENE EXPRESSION AND DNA REPAIR KINETICS.....	73
Possible Mechanisms to Integrate MonoHAA-Mediated DNA Damage, Altered Gene Expression and DNA Repair.....	73
CHAPTER 8 CONCLUSIONS	75
REFERENCES	77
ABBREVIATIONS	87

TABLES

1.1	Physicochemical properties of monoHAAs.....	3
2.1	Description of the mono-haloacetic acids.....	7
2.2	DNA damage and repair related genes analyzed in this study.....	13
3.1	Concentration of monoHAAs that induce equivalent levels of genomic DNA damage in non-transformed human FHs cells.....	21
4.1	Gene expression changes in human FHs cells after 30 min BAA exposure.....	34
4.2	Gene expression changes in human FHs cells after 4 h BAA exposure.....	35
5.1	RNA concentration and purity for each monoHAA treatment group.....	45
5.2	SuperArray PAHS-029 gene array with genes assigned to functional groups.....	48
5.3	Changes in gene expression from concurrent negative controls after 30 min of monoHAA exposure.....	50
5.4	Changes in gene expression from concurrent negative controls after 4 h of monoHAA exposure.....	52
5.5	MonoHAA-induced transcriptome profiles analyzed using the Database for Annotation, Visualization and Integrated Discovery.....	54
6.1	DNA repair t_{50} values of genomic damage induced by IAA, BAA or CAA.....	70
6.2	Two-way Analysis of Variance for DNA repair of CHO cells treated with IAA, BAA or CAA (Holm-Sidak pairwise multiple comparison).....	71

FIGURES

1.1	Log-linear plots illustrating the chronic cytotoxic capacity of IAA, BAA and CAA in CHO cells.....	2
1.2	Log-linear plots illustrating the genomic DNA damaging capacity of IAA, BAA and CAA in CHO cells	3
2.1	Microphotograph of CHO cells clone 11-4-8.	8
2.2	Microphotograph of human embryonic FHs 74int cells.	9
2.3	PCR Gene Array™ Experimental Design with Human FHs Cells.....	12
3.1	Flow chart of the SCGE assay	17
3.2	Acute cytotoxicity and genotoxicity induced by iodoacetic acid in human FHs cells.	18
3.3	Acute cytotoxicity and genotoxicity induced by bromoacetic acid in human FHs cells. .	19
3.4	Acute cytotoxicity and genotoxicity induced by chloroacetic acid in human FHs cells. .	20
3.5	Log-linear plots illustrating the genomic DNA damaging capacity of iodoacetic acid, bromoacetic acid and chloroacetic acid in CHO cells (Panel A) and FHs cells (Panel B).	22
3.6	Cell density analyses of FHs cells exposed to monoHAAs for 30 min or 4 h and incubated for 24 h	24
4.1	RNA gel from BAA treated FHs cells demonstrating the 28S and 18S bands with a 2:1 ratio.	27
4.2	Example of an amplification plot generated by the Stratagene MxPro Software.....	28
4.3	Example of a dissociation curve used to verify functioning primers.....	29
4.4	A dendrogram based on relative fold-change of genes after 30 min (left panel) and 4 hours (right panel) exposure of BAA in human FHs cells.....	30
4.5	Frequency distributions of BAA-induced modulation of gene transcript expression assorted by pathway related functional groups.....	36
4.6	Frequency distribution of a gene functional group expression index for DNA damage/repair, cell cycle regulation and apoptosis, and stress response and xenobiotic metabolism groups.....	37
5.1	MonoHAA induction of neural tube damage in mouse embryos.	40

5.2	MonoHAA induction of mutagenic potency in <i>S. typhimurium</i> strain TA100.....	41
5.3	MonoHAA induction of mutagenic potency at the HGPRT locus in CHO-K1 cells	42
5.4	Histograms of the distribution of SCGE genomic DNA damage in human FHs cells for the negative control, and for cells that expressed an average value of 50 %Tail DNA for BAA, CAA and IAA-induced genotoxic damage.	44
5.5	Electrophoresis of RNA samples isolated from control and FHs cells treated with IAA.	45
5.6	Capillary electrophoresis of RNA isolated from concurrent negative controls and IAA-treated human FHs cells.....	46
5.7	Global gene expression changes for gene functional groups involving DNA damage/repair, cell cycle regulation and apoptosis for human FHs cells exposed to the monoHAAs.	49
5.8	Changes in gene expression within gene functional groups in human FHs cells induced by BAA, CAA, or IAA.....	55
5.9	Changes in gene expression in human FHs cells induced by the monoHAAs as a function of treatment time.....	56
6.1	CHO cell viability throughout a 60 h time period with cells maintained under liquid holding conditions (F12 medium without FBS).	60
6.2	Histograms illustrating the distributions of SCGE % tail DNA values from the CHO cell negative controls at 0 h, 5 h and 24 h liquid-holding recovery.....	61
6.3	Histograms illustrating the distributions of SCGE % tail DNA values from CHO cells treated with bromoacetic acid (BAA), chloroacetic acid (CAA) and iodoacetic acid (IAA) at 0-h liquid-holding recovery.	62
6.4	Histograms illustrating the distributions of SCGE % tail DNA values from CHO cells treated with bromoacetic acid (BAA), chloroacetic acid (CAA) and iodoacetic acid (IAA) at 1-h liquid-holding recovery.	63
6.5	Histograms illustrating the distributions of SCGE % tail DNA values from CHO cells treated with bromoacetic acid (BAA), chloroacetic acid (CAA) and iodoacetic acid (IAA) at 2-h liquid-holding recovery.	64
6.6	Histograms illustrating the distributions of SCGE % tail DNA values from CHO cells treated with bromoacetic acid (BAA), chloroacetic acid (CAA) and iodoacetic acid (IAA) at 3-h liquid-holding recovery.	65

6.7	Histograms illustrating the distributions of SCGE % tail DNA values from CHO cells treated with bromoacetic acid (BAA), chloroacetic acid (CAA) and iodoacetic acid (IAA) at 4-h liquid-holding recovery.	66
6.8	Histograms illustrating the distributions of SCGE % tail DNA values from CHO cells treated with bromoacetic acid (BAA), chloroacetic acid (CAA) and iodoacetic acid (IAA) at 5-h liquid-holding recovery	67
6.9	Histograms illustrating the distributions of SCGE % tail DNA values from CHO cells treated with bromoacetic acid (BAA), chloroacetic acid (CAA) and iodoacetic acid (IAA) at 24-h liquid-holding recovery	68
6.10	Comparative genomic DNA repair kinetics in CHO cells for chloroacetic acid (CAA), iodoacetic acid (IAA), and bromoacetic acid (BAA)	70

FOREWORD

The Water Research Foundation (Foundation) is a nonprofit corporation that is dedicated to the implementation of a research effort to help utilities respond to regulatory requirements and traditional high-priority concerns of the industry. The research agenda is developed through a process of consultation with subscribers and drinking water professionals. Under the umbrella of a Strategic Research Plan, the Research Advisory Council prioritizes the suggested projects based upon current and future needs, applicability, and past work; the recommendations are forwarded to the Board of Trustees for final selection. The Foundation also sponsors research projects through the unsolicited proposal process; the Collaborative Research, Research Applications, and Tailored Collaboration programs; and various joint research efforts with organizations such as the U.S. Environmental Protection Agency, the U.S. Bureau of Reclamation, and the Association of California Water Agencies.

This publication is a result of one of these sponsored studies, and it is hoped that its findings will be applied in communities throughout the world. The following report serves not only as a means of communicating the results of the water industry's centralized research program but also as a tool to enlist the further support of the nonmember utilities and individuals.

Projects are managed closely from their inception to the final report by the Foundation's staff and large cadre of volunteers who willingly contribute their time and expertise. The Foundation serves a planning and management function and awards contracts to other institutions such as water utilities, universities, and engineering firms. The funding for this research effort comes primarily from the Subscription Program, through which water utilities subscribe to the research program and make an annual payment proportionate to the volume of water they deliver and consultants and manufacturers subscribe based on their annual billings. The program offers a cost-effective and fair method for funding research in the public interest.

A broad spectrum of water supply issues is addressed by the Foundation's research agenda: resources, treatment and operations, distribution and storage, water quality and analysis, toxicology, economics, and management. The ultimate purpose of the coordinated effort is to assist water suppliers to provide the highest possible quality of water economically and reliably. The true benefits are realized when the results are implemented at the utility level. The Foundation's trustees are pleased to offer this publication as a contribution toward that end.

Roy L. Wolfe, Ph.D.
Chair, Board of Trustees
Water Research Foundation

Robert C. Renner, P.E.
Executive Director
Water Research Foundation

ACKNOWLEDGMENTS

The Authors wish to express our thanks for the many efforts of our current and former graduate students, Dr. M. G. Muellner, Dr. M. S. Attene-Ramos, Ms. Y. Komaki and Mr. J. Pals. We sincerely appreciate the scientific advice provided by our colleagues Dr. M. E. Hudson, and Dr. B. J. Marinas. In addition to the Water Research Foundation we acknowledge financial support by the Center of Advanced Materials for the Purification of Water with Systems, National Science Foundation Science and Technology Center, under Award CTS-0120978. The Heiwa Nakajima Foundation Fellowship Program is gratefully acknowledged for financial support to Y. Komaki.

We wish to sincerely thank the members of the Project Advisory Committee for their efforts on this project: Dr. Anthony DeAngelo from the U.S. Environmental Protection Agency (NHEERL), Research Triangle Park, NC, Dr. Seth W. Kullman from North Carolina State University, Raleigh, NC and Dr. William Mitch from Yale University, New Haven, CT. We especially thank the Water Research Foundation project manager, Jonathan Cuppett, for his thoughtful help during the project.

EXECUTIVE SUMMARY

OBJECTIVES

The goal of this project was to generate the first human toxicogenomic structure-activity relationship analysis comparing the monohaloacetic acids (monoHAAs). The specific objectives of this project and the chapters in which the detailed information is located is included in the following list.

1. Determine the DNA repair kinetics for iodoacetic, bromoacetic and chloroacetic acids in Chinese hamster ovary (CHO) cells (Chapter 6).
2. Determine the chronic cytotoxicity of iodoacetic acid (IAA), bromoacetic acid (BAA) and chloroacetic acid (CAA) to non-transformed normal human embryonic cells (Chapter 3).
3. Compare the cytotoxic sensitivity of human cells with that of CHO cells (Chapter 3).
4. Determine the acute genomic DNA damaging capacity of IAA, BAA and CAA to non-transformed, normal human embryonic cells (Chapter 3).
5. Compare the genotoxic sensitivity of human cells with that of CHO cells (Chapter 3).
6. Using gene array technologies, determine if nontoxic concentrations of each monoHAA differentially alters the expression of human genes involved in DNA damage/repair and human toxic responses (Chapters 2, 4, 5).
7. Determine the human functional gene assemblies and metabolic pathways that are altered after exposure to monoHAAs (Chapters 5, 7).
8. Explore if these gene expression changes may ultimately result in human disease and if specific gene functional groups may lead to the development human biomarkers (Chapter 5).

BACKGROUND

The disinfection of drinking water is acknowledged as an outstanding public health success of the 20th Century that reduced the transmission of deadly waterborne diseases. The generation of DBPs is an unintended consequence of disinfection. Although the benefits of disinfection are universally recognized, the undesirable health effects of DBPs generated by the reaction between disinfectants and organic and inorganic material in source water constitutes a public health concern. Toxicogenomics is the combination of genetic microarray technology and toxicological methods and is the study of the relationship between the structure and activity of the genome and the adverse biological effects of toxic agents. The goal of toxicogenomics is to better understand mechanisms of toxicity and to identify gene expression patterns that lead to adverse disease outcomes. These data would establish the molecular role of each halogen species on the toxicology of DBPs and may be useful in defining molecular human biomarkers that could enhance the resolution of epidemiological studies on the health effects of disinfected water.

APPROACH

Toxicogenomic analyses is a powerful quantitative molecular biological tool that resolves altered gene expression after cells, tissues, or intact organisms, are exposed to xenobiotics. For the systematic analyses of the monoHAAs we conducted *in vitro* cytotoxicity and genotoxicity assays first. The toxicogenomic study focused on DBP concentrations that were non-cytotoxic and thus biologically meaningful because the cells were not undergoing overt toxic stress. Therefore the resulting modulation in gene expression was directly associated with the monoHAAs. These experimental designs identified functional gene groups and metabolic pathways that participated in the genetic toxicology and chronic toxic response of these important DBPs. We developed a system that integrated high resolution *in vitro* human cell chronic cytotoxicity and acute genotoxicity with human toxicogenomic analysis.

RESULTS/CONCLUSIONS

The haloacetic acids (HAAs) are the second most common class of chlorinated water disinfection by-products. We demonstrated that the monoHAAs were direct-acting genotoxins in mammalian cells and in human cells. Genotoxic hazard is a function of the induction DNA damage as well as the capacity of the cells to repair the induced genomic insult. As part of this study we determined the rates of DNA repair of the monoHAA-generated genomic DNA damage. The single cell gel electrophoresis (SCGE) assay using CHO cells was modified to include liquid holding recovery time to measure genomic DNA damage and repair kinetics of CAA, BAA, and IAA. Previous research defined that the rank order of genotoxic potency was IAA > BAA >> CAA. In these experiments the concentration of each monoHAA was chosen to generate approximately the same level of genotoxic damage. No cytotoxicity was expressed during the 24-h liquid holding period. Nuclei from CHO cells treated with BAA showed the lowest rate of DNA repair ($t_{50} = 296$ min) compared to CAA or IAA ($t_{50} = 134$ and 84 min, respectively). The different rates of genomic repair expressed by IAA or CAA versus BAA suggest that different distributions of DNA lesions are induced or that the cellular environment that enhances DNA repair is differentially modified by individual monoHAAs.

The monoHAAs are toxic disinfection byproducts. *In vitro* cytotoxicity and genotoxicity end points were integrated with DNA damage and repair pathway-focused toxicogenomic analyses to evaluate monoHAA-induced alterations of gene expression in normal non-transformed human cells. When compared to concurrent control transcriptome profiles, metabolic pathways involved in the cellular responses to toxic agents were identified and provided insight into the biological mechanisms of toxicity. Using the Database for Annotation, Visualization and Integrated Discovery to analyze the gene array data, the majority of the altered transcriptome profiles were associated with genes responding to DNA damage or those regulating cell cycle or apoptosis. The major pathways involved with altered gene expression were ATM, MAPK, p53, BRCA1, BRCA2, and ATR. These latter pathways highlight the involvement of DNA repair, especially the repair of double strand DNA breaks. All of the resolved pathways are involved in human cell stress response to DNA damage and regulate different stages in cell cycle progression or apoptosis.

Although IAA is a more potent genotoxin as compared to BAA, BAA-induced genomic DNA damage required more time to repair than damage induced by IAA. These data suggest that BAA may be inducing a higher frequency of unrepaired dsDNA lesions.

We also observed an interesting correlation that the monoHAAs, at equivalent genotoxic responses without acute cytotoxicity may generate different levels of cell cycle inhibition. IAA and CAA induced a reduction in cell density without a high level of dead cells, while BAA did not show a decline in cell density. This response may be associated with the control of cell cycle inhibition. The foundation of this cellular response may be that the toxicogenomic data demonstrated that IAA and CAA modulated a larger number of cell cycle control genes than BAA. We speculate that the reduction in the repair of BAA-induced lesions may, in part, be due to a lack of cell cycle inhibition. This temporal effect may result in reducing the time available for DNA liquid holding repair.

The use of DNA repair coupled with genomic technologies may lead to the understanding of the biological and genetic response mechanisms that are involved in the toxicity induced by DBPs. Such knowledge may lead to the identification of biomarkers to identify susceptible subpopulations which may be employed in biological information feed-back loops to aid water chemists and engineers in the overall goal of producing safer drinking water.

APPLICATIONS/RECOMMENDATIONS

Overall this work represents the first non-transformed human cell toxicogenomic study with regulated drinking water DBPs. We linked the biological endpoint of DNA damage (SCGE) with toxicogenomic arrays featuring primers for genes related to human DNA damage and repair, and general cellular responses to toxicity. This research is a leap forward in understanding the link between *in vitro* cytotoxicity and genotoxicity assays with that of investigating the impact of DBPs on the expression of human toxic response gene pathways that may be involved in the etiology of disease. In addition toxicogenomic research may provide information that could aid in identifying individuals who are especially sensitive to the toxic impacts of specific DBP classes. By appropriate intervention it may be possible to reduce even more the level of adverse health impacts associated with exposure to DBPs.

With the implementation of the U.S. EPA Stage 2 DBP Rule and with energy and cost considerations, drinking water utilities will continue providing high quality, tasteful potable water for the nation. However, there are health concerns for emerging DBPs especially iodinated DBPs and nitrogen-containing DBPs (N-DBPs). With the best characterized disinfectant, chlorine, only approximately 50% of the DBPs are chemically identified. Even less is known of the DBPs generated with other disinfectants. Our knowledge concerning the toxicity of DBPs, although expanding, is woefully inadequate. Along with basic information that has accumulated on the adverse biological effects and health implications of DBPs, toxicogenomics provides insight into the impacts that DBPs impart upon the modulation of gene expression. With the information generated by the structure activity response between the chemistry and biology of DBPs coupled with the DBP-mediated transcriptome profiles, we have greater insight as to which molecular pathways impacted by DBPs may be associated with human disease.

In the future this information will be useful as part of the decision making process on the development and implementation of disinfection practices. Having an understanding of the unique characteristics of the source water, utilities ultimately will employ molecular markers for

disease to choose disinfection methods that generate the least toxic DBPs in their finished drinking water.

We are now at the time in which a DBP toxicity library must be developed using both traditional short-term *in vitro* toxicology methods and quantitative high throughput screening methodologies as advocated by such agencies as the National Institutes of Health. The merger of analytical chemistry, analytical biology and toxicogenomics will allow for precisely tuning the disinfection of source waters to generate even higher quality, economic, and safe drinking water while protecting the public health and the environment.

CHAPTER 1

INTRODUCTION

BACKGROUND

One important outcome from the 2006 Gordon Research Conference on Drinking Water Disinfection By-Products (DBPs) was the need to integrate analytical chemistry, analytical biology, epidemiological studies and engineering practice. *In vitro* and *in vivo* toxicological studies are useful in identifying the relative potencies of individual DBPs but they do not predict adverse human health outcomes (Plewa and Wagner 2009). In-depth, mechanistic biological information is required to develop human biomarkers for susceptible populations and to identify those DBPs that pose serious threats to the public health and the environment.

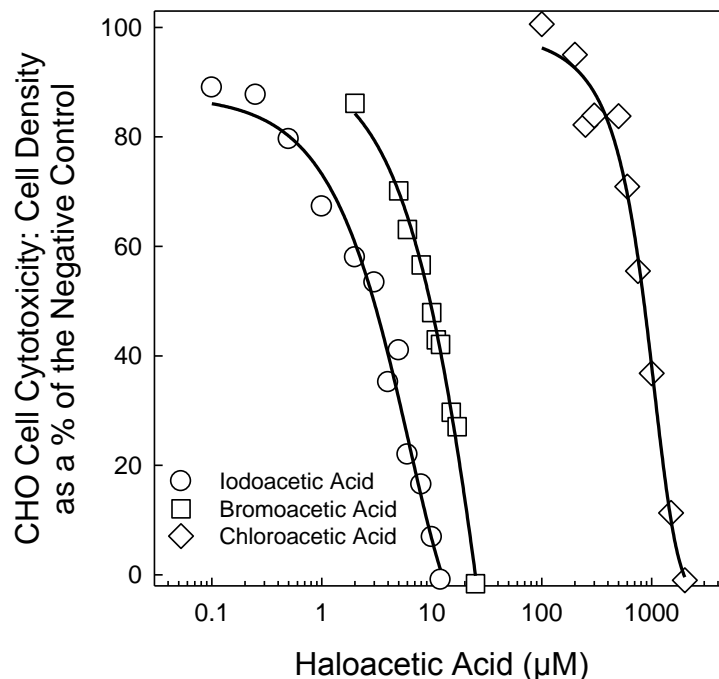
With the advent of more rigorous system-wide regulations promulgated by the U.S. Environmental Protection Agency (U.S. EPA) for DBPs, many drinking water utilities have changed their disinfection practices (U. S. Environmental Protection Agency 2006). Often, the primary disinfectant is changed from chlorine to alternative disinfectants (including ozone, chlorine dioxide, and chloramines), and in some cases, chlorine is used as a secondary disinfectant following primary treatment with an alternative disinfectant. Alternative disinfectants can substantially change the distribution of the DBP chemical classes present in the finished water (Andrews and Ferguson 1996; Glaze and Weinberg 1993; Zhang et al. 2000; Hua and Reckhow 2007; Stevens et al. 1989). Presently there is a research gap in the kinds of DBPs generated with alternative disinfectants especially with the increasing diversity of DBP precursors afforded by an ever increasing burden of synthetic contaminants in source waters (Krasner 2009; Richardson 2009). Differences in source water conditions, including concentrations of bromide or iodide, concentrations of natural organic matter, and pH, also have dramatic effects on the DBP species and the levels formed (Richardson 2009). Using Structure-Activity Relationship analysis, a list of priority DBPs with high potential carcinogenicity were identified (Woo et al. 2002). The U.S. EPA Nationwide DBP Occurrence Study examined these priority DBPs as well as currently regulated DBPs (Krasner et al. 2006). Many priority DBPs did not track with the regulated ones, and in fact, increased in formation when the regulated DBPs decreased. The priority DBPs included iodo-trihalomethanes (I-THMs) and iodo-acids, which occurred at the highest levels with disinfection by chloramination. Brominated and especially iodinated DBPs express higher cytotoxicity and genotoxicity than their chlorinated analogues (Plewa et al. 2004; Komaki et al. 2009; Richardson et al. 2008; Richardson et al. 2007; Plewa and Wagner 2009). A mechanism for the differential formation of iodo-DBPs by chloramine disinfection versus chlorine disinfection has been proposed (Bichsel and von Gunten 2000, 1999).

Although currently there are approximately 600 DBPs identified and countless numbers not yet known, even more cogent questions remain on the role of DBPs on human health and disease. Trying to understand the impacts of DBPs on human health reveals a plethora of data gaps and research needs. For example, the types of cancer observed in animal studies (primarily liver) for the regulated DBPs do not correlate with the types observed in human epidemiology studies (bladder, colon). This begs the question, does regulating four THMs, five haloacetic acids (HAAs), bromate and chlorite adequately protect human health (Singer 2006)? Are human health effects due to other DBPs that are currently unregulated? More fundamentally, what is the

mechanism of action of DBPs on human genes and metabolic pathways? Answers to questions like these would be a first step in developing human biomarkers for susceptible populations and identifying the role of DBPs in human disease states.

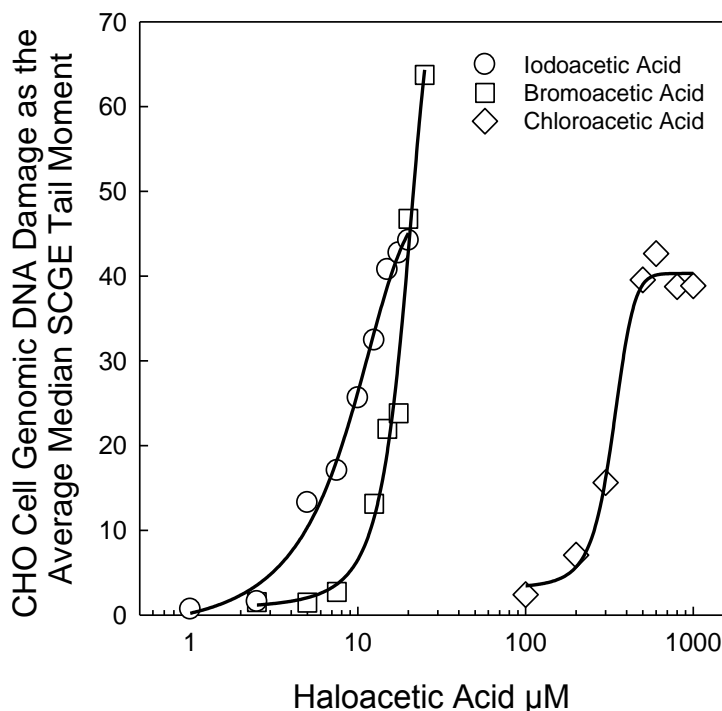
MONOHALOACETIC ACIDS

Of the three monohaloacetic acids (monoHAAs), bromoacetic acid (BAA) and chloroacetic acid (CAA) are regulated by the U.S. EPA, while iodoacetic acid (IAA) is a U.S. EPA priority unregulated DBP (U. S. Environmental Protection Agency 2006). IAA and BAA were demonstrated to be exceedingly cytotoxic and potent inducers of genomic DNA damage in mammalian and human cells (Plewa et al. 2010; Cemeli et al. 2006; Plewa et al. 2004; Zhang et al. 2010; Attene-Ramos, Wagner, and Plewa 2010). Figure 1.1 illustrates the comparative chronic cytotoxicity (72 h exposure) of IAA, BAA and CAA in Chinese hamster ovary (CHO) cells with LC_{50} (%C $\frac{1}{2}$) values of 2.9 μ M, 10 μ M and 840 μ M, respectively (Plewa et al. 2010). Figure 1.2 presents the comparative genomic DNA damaging activity (4 h exposure) of IAA, BAA and CAA in CHO cells using single cell gel electrophoresis (SCGE) with SCGE genotoxic potency values of 8.7 μ M, 17 μ M, and 410 μ M, respectively (Plewa et al. 2010). The SCGE genotoxic potency value is the molar concentration of the HAA that is at the midpoint of the genotoxicity concentration-response curve.



Source: Reprinted with permission from Plewa, M. J.; Wagner, E. D.; Richardson, S. D.; Thruston, A. D., Jr.; Woo, Y. T.; McKague, A. B., *Environ. Sci. Technol.* 2004, 38, (18), 4713-4722. Copyright 2004, American Chemical Society).

Figure 1.1 Log-linear plots illustrating the chronic cytotoxic capacity of IAA, BAA and CAA in CHO cells



Source: Reprinted with permission from Plewa, M. J.; Wagner, E. D.; Richardson, S. D.; Thruston, A. D., Jr.; Woo, Y. T.; McKague, A. B., *Environ. Sci. Technol.* 2004, 38, (18), 4713-4722. Copyright 2004, American Chemical Society.

Figure 1.2 Log-linear plots illustrating the genomic DNA damaging capacity of IAA, BAA and CAA in CHO cells

Comparative Mammalian Cell Toxicological Responses: Mechanisms of Action

A comparison of the interaction of the physicochemical measurements of the monoHAAs and their cytotoxic and genotoxic potencies was published (Plewa et al. 2004). The cytotoxicity and genotoxicity of the monoHAAs are related to the cellular uptake and transport of the chemicals and their subsequent chemical interaction with cellular macromolecules. Table 1.1 summarizes several relevant physicochemical properties and parameters of the monoHAAs.

Table 1.1
Physicochemical properties of monoHAAs

Physicochemical properties of monoHAAs ^a				Bond length, bond dissociation energy and relative S _N 2 reactivity of C–X bond ^b			
Compd	log <i>P</i>	pKa	ELUMO (AU)	C–X	Length (Å)	Dis. Energy (kcal/mol)	Relative S _N 2
CAA	0.38	2.82	0.126	C–Cl	1.77	78.5	1
BAA	0.52	2.90	0.111	C–Br	1.93	65.9	50
IAA	0.91	3.12	0.091	C–I	2.14	57.4	150-200

^a *Source:* Richard and Hunter 1996; Hansch, Leo, and Hoekman 1995.

^b *Source:* Loudon 1995.

The ability of the monoHAAs to cross cell membranes is dependent on their lipophilicity, the degree of ionization, and possible cellular transport mechanisms. The rank order of the monoHAA cytotoxicity and genotoxicity in CHO cells correlates with the log *P* of the un-ionized monoHAAs. The ranking follows the order of IAA > BAA > CAA. The lipophilicity of, and cell permeability to, monoHAAs can be substantially decreased by ionization, which is determined by their p*K*_a and the pH of the medium. The fraction (*f*) of un-ionized monoHAAs can be calculated by the formula presented below (Xu et al. 2002).

$$f = 1 / (1 + 10^{(pH - pK_a)})$$

Chemicals with higher p*K*_a values are less likely to be ionized. For the monoHAAs the ranking of p*K*_a follows the order of IAA > BAA > CAA that correlates well with CHO cell cytotoxicity (*r* = -0.71) and genotoxicity (*r* = -0.72) (Plewa et al. 2004). There is some evidence of active transport of CAA and BAA across synthetic membranes (Yoshikawa et al. 1986), although the relevance of these synthetic membranes to biological membranes remains unstudied. Tissue distribution studies in rats (Hayes, Short, and Gibson 1973) showed significant accumulation of CAA and IAA in the kidney and liver. Yet percutaneous absorption using human skin sections demonstrated poor permeability to CAA and BAA around neutral pH (Xu et al. 2002).

TOXICOGENOMICS

With the advent of microarray technology, a global analysis of cellular toxicological response is possible to identify the mechanisms of actions by DBPs and the functional gene assemblies and metabolic pathways involved (Waters, Jackson, and Lea 2010). Toxicogenomics is the combination of genetic microarray technology and toxicological methods and is the study of the relationship between the structure and activity of the genome and the adverse biological effects of toxic agents (Waters, Jackson, and Lea 2010; Thybaud, Le Fevre, and Boitier 2007; Aardema and MacGregor 2002). The goal of toxicogenomics is to better understand mechanisms of toxicity and to identify gene expression patterns that lead to a deleterious disease outcome. In this study we conducted a toxicogenomic analysis of the monoHAA DBPs using normal, non-transformed human cells. Several evaluations of DBP toxicity were recently published using high levels of exposure in rodent models. The DBPs evaluated were dichloroacetic acid (Thai et al. 2003), bromochloroacetic acid (Tully et al. 2005) and potassium bromate (Delker et al. 2006). In general for all three studies, the largest number of genes with differential expression was involved with cancer induction, cell death, and oxidative stress. Unfortunately, most of the responsive genes identified were not confirmed by quantitative real-time polymerase chain reaction analysis (qRT-PCR).

The monoHAAs provide an excellent model to evaluate the impact of the halogen species on the human transcriptome profiles of toxic response genes and genes involved in human DNA damage/DNA repair. These three monoHAAs differ only by the species of their single halogen and their chronic cytotoxic and genotoxic potencies were directly compared using *in vitro* mammalian cell assays (Plewa et al. 2002; Plewa et al. 2010; Plewa et al. 2004; Zhang et al. 2010). With toxicogenomic analysis we significantly increased the resolving power of the *in vitro* bioassays used to study DBPs. Most studies use relatively high concentrations of DBPs as compared to those experienced by the public consuming disinfected water. Being able to

determine mechanisms of responses at lower concentrations provide data that is more applicable to real world conditions. In addition, this work highlighted mechanisms of toxic responses and introduced a more rational approach in identifying those DBPs that are the most likely to be involved in inducing adverse health effects.

HYPOTHESIS

Our general hypothesis was to determine if the halogen species (I, Br, Cl) of the monoHAAs differentially modulate the expression of human DNA damage/repair genes and human toxic response genes. These data established the molecular role of the halogen species on the toxicology of DBPs and may be useful in defining molecular human biomarkers that could be employed in enhancing the resolution of epidemiological studies on the health effects of disinfected water.

OBJECTIVES

The objectives of this study included the following.

1. Determine the DNA repair kinetics for iodoacetic, bromoacetic and chloroacetic acids in CHO cells.
2. Determine the chronic cytotoxicity of IAA, BAA and CAA to non-transformed normal human embryonic cells.
3. Compare the cytotoxic sensitivity of human cells with that of CHO cells.
4. Determine the acute genomic DNA damaging capacity of IAA, BAA and CAA to non-transformed, normal human embryonic cells.
5. Compare the genotoxic sensitivity of human cells with that of CHO cells.
6. Using gene array technologies, determine if nontoxic concentrations of each monoHAA differentially alters the expression of human genes involved in DNA damage/repair and human toxic responses.
7. Determine the human functional gene assemblies and metabolic pathways that are altered after exposure to monoHAAs.
8. Explore if these gene expression changes may ultimately result in human disease and if specific gene functional groups could be used as human biomarkers.

CHAPTER 2 MATERIALS AND METHODS

INTRODUCTION

This research is involved in the quantitative comparison of the cytotoxic, genotoxic, DNA repair and toxicogenomic impact of the monoHAAs, IAA, BAA and CAA.

REAGENTS

General laboratory reagents were purchased from Fisher Scientific Co. (Itasca, IL) and Sigma Chemical Co. (St. Louis, MO). Media supplies and fetal bovine serum (FBS) were purchased from Hyclone Laboratories (Logan, UT); human epidermal growth factor (EGF) was obtained from Sigma Chemical Co. (St. Louis, MO). The source and purity of the monoHAAs are listed in Table 2.1. Stock solutions were prepared in dimethylsulfoxide (DMSO) and stored at -22°C .

All laboratory chemicals were reagent grade or higher. All laboratory glassware and plasticware were purchased from reputable vendors. RNase-free and DNase-free reagents, pipet tips, plasticware and glassware were kept separated from the general laboratory supply. The single channel pipetmen and the multichannel pipetmen used to load the PCR gene arrays were calibrated and were reserved only for use in genomic experiments.

BAA is a regulated DBP that is a colorless solid and a relatively strong alkylating agent. CAA is an organochlorine compound that is a regulated DBP by the U.S. EPA. IAA is an unregulated DBP. These agents are toxic because, like many alkyl halides, they are alkylating agents that can react with cysteine residues in proteins. Table 2.1 characterizes the monoHAAs used in this study, their sources and purities.

Table 2.1
Description of the mono-haloacetic acids

monoHAA and Abbreviation	CASN	Molecular Formula	MW	Source and Purity
Bromoacetic Acid (BAA)	79-08-3	$\text{BrCH}_2\text{CO}_2\text{H}$	138.95	Fluka Chem. Co., >99%
Chloroacetic Acid (CAA)	79-11-8	$\text{ClCH}_2\text{CO}_2\text{H}$	94.50	Fluka Chem. Co., >99%
Iodoacetic Acid (IAA)	64-69-7	$\text{ICH}_2\text{CO}_2\text{H}$	185.95	Aldrich Chem. Co., >98%

CULTURED CELLS

Chinese Hamster Ovary Cells

CHO cells are widely used in toxicology. The transgenic CHO cell line AS52 (Tindall et al. 1984; Tindall and Stankowski 1989) was derived from the parental CHO line K1-BH4 (Hsie et al. 1975, 1975). Clone 11-4-8 was isolated from AS52 by Dr. E. Wagner and it expresses a stable chromosome complement, a consistent cell doubling time as well as functional p53 protein (Wagner et al. 1998, 1998; Tzang et al. 1999). Stock cultures of the CHO cells were frozen in a solution of 90% FBS:10% DMSO (v/v) and stored at -80°C . Cells were grown on glass culture

plates in Hams F12 medium plus 5% FBS at 37°C in a humidified atmosphere of 5% CO₂. The cells exhibit normal morphology, express cell contact inhibition and grow as a monolayer without expression of neoplastic foci. CHO cells were transferred when the culture became confluent. A photomicrograph of clone 11-4-8 CHO cells is presented in Figure 2.1.



Figure 2.1 Microphotograph of CHO cells clone 11-4-8.

Human Small Intestine Epithelial Cells

Human small intestine cell line FHs 74int was used for the transcriptome profile experiments (Figure 2.2). These cells were obtained from the American Type Culture Collection (ATCC, Manassas, VA). The cell line originated from a female fetus 3-4 months into gestation (Smith 1979). The cell culture was prepared from isolate CCL241. Culture medium with epidermal growth factor (EGF) at 30 ng/mL expressed a cell doubling time of approximately 65 hr. The cell culture doubling time without EGF was 168 hr. Cells of passage 20 can undergo 15 additional population doublings. The cells are non-neoplastic, diploid cells that are reverse transcriptase negative, adherent, and exhibit cell contact inhibition. FHs cells were maintained in modified Dulbecco's Hybr-Care™ medium (ATCC) with 2 mM L-glutamine plus 10% FBS, 1% antibiotic (10 units/mL penicillin G sodium, 10 µg/mL streptomycin sulfate, 25 µg/mL amphotericin B, 0.85% saline), 30 ng/mL human EGF at 37°C in a humidified atmosphere of 5% CO₂.

Cell Viability

Concurrent with the genotoxicity analysis, the acute cytotoxicity of the cells was evaluated from a 1:1 (v/v) mixture of cell suspension and 0.05% trypan blue vital dye in phosphate-buffered saline (PBS) (Phillips 1973). As in our past work, genotoxicity data were not used if acute cytotoxicity exceeded 30% (Wagner and Plewa 2009).

For the toxicogenomic experiments, cell viability was determined immediately after exposure or 24 h after exposure. FHs cells were exposed to the monoHAAs in microplates at a titer of 1×10^4 cells/well. The microplates were covered with sterile AlumnaSeal (RPI Corporation, Mt Prospect, IL) and incubated for 30 min or 4 h at 37°C. The cells were washed 3× with PBS and cell viability was determined immediately after exposure with trypan blue. With parallel microplates, 200 µL of complete Hybri-Care™ medium were added to each well; these microplates were incubated for 24 h at 37°C, 5% CO₂. The microplates were stained with the histological dye crystal violet and analyzed as previously published (Muellner et al. 2010). Cell density was calculated as the percentage of the concurrent negative control. The positive control was 25% DMSO.

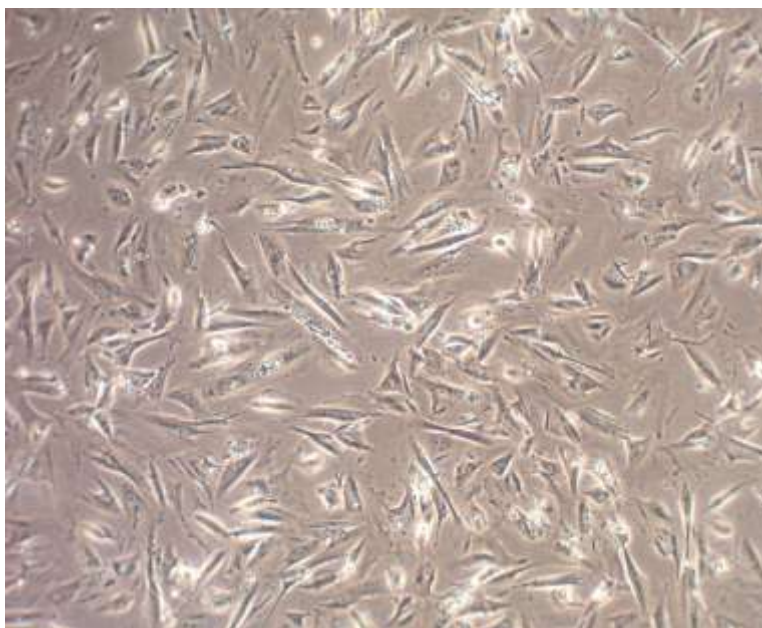


Figure 2.2 Microphotograph of human embryonic FHs 74int cells.

SINGLE CELL GEL ELECTROPHORESIS (SCGE) ASSAY

The SCGE assay was performed as described previously with minor modifications (Wagner and Plewa 2009). The day before treatment, 4×10^4 mammalian or human cells were added to each microplate well in 200 µL of complete medium (F12 +5% FBS for CHO cells or Hybri-Care™ medium + 10% FBS + 30 ng/mL EGF for human FHs cells) and incubated overnight. The next day the cells were washed with Hank's balanced salt solution (HBSS) and treated with the monoHAA in cell culture medium without FBS or EGF. The wells were covered with sterile AlumnaSeal. After the treatment time (30 min or 4 h incubation), the cells were washed twice with HBSS and harvested with 50 µL of 0.01% trypsin + 53 µM EDTA. The trypsin was inactivated with 70 µL of complete medium with FBS. A 10 µL aliquot of the cell suspension was removed to measure acute cytotoxicity using the vital dye trypan blue. The remaining suspension from each well was embedded in a layer of low-melting point agarose prepared with phosphate-buffered saline (PBS) on clear microscope slides that were previously

coated with a layer of 1% normal melting point agarose prepared with deionized water and dried overnight. Detailed methods for preparing and electrophoresing the SCGE microgels were published previously (Plewa et al. 2002; Wagner and Plewa 2009). Cellular membranes were removed by an overnight immersion in lysing solution at 4°C. The microgels were placed in an alkaline buffer (pH 13.5) in an electrophoresis tank, and the DNA was denatured for 20 min. The microgels were electrophoresed at 25 V, 300 mA (0.72 V/cm) for 40 min at 4°C. The microgels were removed, neutralized with Tris buffer (pH 7.5), rinsed in cold water, dehydrated in cold methanol, dried at 50°C, and stored at room temperature in a covered slide box. For analysis, the microgels were hydrated in cold water for 20 min and stained with 65 µL of 20 µg/mL ethidium bromide for 3 min. The microgels were rinsed in cold water and analyzed with a Zeiss fluorescence microscope with an excitation filter of BP 546/10 nm and a barrier filter of 590 nm. For each experiment, two microgels were prepared per treatment group. Concurrent negative (medium only) and positive controls (ethyl methanesulfonate 3.8 mM) were conducted with each experiment. The microgels were coded and 25 randomly chosen nuclei were analyzed for each microgel using a charge coupled device camera. A computerized image analysis system (Komet version 3.1, Kinetic Imaging Ltd., Liverpool, U.K.) was employed to determine the % tail DNA (the amount of DNA that migrated from the nucleus into the agarose gel) as an index of DNA damage. The digitalized data were automatically transferred to a computer-based spreadsheet for subsequent statistical analysis.

DNA REPAIR EXPERIMENT TREATMENT CONDITIONS

Although there are many studies on the induction of DNA damage by DBPs, little information exists on the repair of DBP-induced DNA lesions (Komaki et al. 2009; Liviac, Creus, and Marcos 2009, 2009). Currently in the literature there is no systematic analysis of the DNA repair kinetics of regulated DBPs nor is there an example of correlating chemical structure activity relationships and repair. One aim of this research was to characterize the genotoxicity induced by these related monoHAAs in mammalian cells and determine the kinetics of DNA repair. The day before treatment, CHO cells were plated at a titer of 2×10^4 cells in 200 µL of F12 + 5% FBS medium per well in a sterile flat-bottom 96-well microplate. On the next day, the cells were washed with HBSS and treated with the monoHAAs in F12 medium without FBS in a total volume of 25 µL for 4 h at 37°C, 5% CO₂. The wells were covered with AlumnaSeal™. The concentrations of the monoHAAs for the DNA repair studies were first determined so that the same level of genomic DNA damage was induced. The treatment concentrations were 6 mM, 60 µM, and 25 µM for CAA, BAA and IAA, respectively. After treatment, the solution was aspirated from the wells and the cells were washed 2× with HBSS. The cells from one well were immediately harvested and microgels were prepared for the determination of DNA damage with no time for repair. F12 medium without FBS (100 µL) was added to the other wells, and the microplate was returned to the incubator for designated times. This recovery period (liquid holding time) allowed for DNA repair. The microgels were analyzed as described in the SCGE assay section.

MONOHAA TOXICOGENOMIC ANALYSIS

MonoHAA Treatment of Human FHs Cells and RNA Isolation and Purification

Non-transformed human FHs cells were employed for all of the toxicogenomic experiments. Four days prior to treatment, 4×10^5 FHs 74 Int cells were seeded in each well in six-well plates. After a 30 min or 4 h exposure to the monoHAAs, cells were washed twice with HBSS, harvested, transferred to RNase-free 1.5 mL centrifuge tubes and centrifuged at $300 \times g$ for 5 min. An aliquot of each cell suspension was retained prior to centrifugation for acute cytotoxicity and SCGE analyses. The supernatant was removed and RNA isolated using a Qiagen RNeasy Mini Kit (Valencia, CA) following the recommended protocol for animal cell isolation. To generate a high RNA yield, cell suspensions were pooled from 2 wells with identical treatments. DNase treatment of the RNA samples was conducted using Ambion DNA-free DNase (Austin, TX) according to manufacturer specifications. RNA concentrations were determined using the NanoDrop 1000 from Thermo Fisher Scientific (Wilmington, DE). The resulting genomic DNA-free RNA was concentrated by vacuum centrifugation for 15 min using the Speedvac system AE52010 from Savant (Halbrook, NY). RNA quantity was determined using the Agilent 2100 Bioanalyzer (Santa Clara, CA). RNA Integrity Numbers (RIN) were in the range from 8.2 to 9.9 (RNA quality for microarray analysis must have RIN values greater than 7) (Schroeder et al. 2006). High quality RNA is essential for qRT-PCR arrays.

cDNA Synthesis

cDNAs were synthesized using the SuperArray RT² PCR Array First Strand Kit (Frederick, MD). RNA samples were diluted to a constant concentration for each monoHAA exposure. One μL of the P2 enzyme, from the SuperArray RT² PCR Array First Strand Kit, was added to the nuclease-free PCR tube containing the diluted RNA. A MJ Research (Waltham, MA) PTC-100 programmable thermocycler was used to conduct the reactions. The annealing reaction was conducted at 70°C for 3 min and held on ice. The RT cocktail was prepared by mixing 10 μL of the annealing mixture with 10 μL of the RT cocktail. This mixture was incubated at 37°C for 60 min and heated to 95°C for 5 min to hydrolyze the RNA and inactivate the reverse transcriptase. The finished reaction was held on ice. After cDNA synthesis, the samples were diluted with 91 μL of nuclease free water and stored at -20°C .

Real Time PCR Analyses

A new quantitative method for analyzing modulation in gene expression is the PCR array. Human PCR arrays are less expensive than typical human gene chip microarrays (e.g. Affymetrix) and combine qRT-PCR with multiple gene profiling abilities of a microarray. The gene array can be focused to evaluate functional gene groups for specific pathways or disease states. Although PCR arrays cannot encompass the high number of genes assayed as gene chip microarrays, PCR arrays are more focused to specific genetic functional assemblies and automatically confirm a response to specific toxic response genes and pathways.

A DNA damage signaling focused pathway specific qRT-PCR array (APHS-029B) was employed (Quellhorst et al. 2006). A flow diagram of the qRT-PCR methodology that we applied is presented in Figure 2.3. The genes evaluated for their expression are listed in Table

2.2. An aliquot of the diluted first strand synthesis reaction (102 μL) was added to the SuperArray RT² Real-Time SYBR Green/ROX PCR master mix (Frederick, MD) and nuclease-free H₂O according to the RT² Profiler PCR Array System user manual. The cDNA/master mix cocktail was placed into a 25 mL sterile, nuclease free reservoir and 25 μL were placed into each well of a pathway specific qRT-PCR array (SuperArray) using an eight channel multi-pipettor and changing tips after each addition. Optical cap strips were tightly placed onto each column of the microplate. The microplate was centrifuged to collect the liquid to the bottom of the wells. Real-time PCR analysis was conducted using a two-step cycling program on a Stratagene Mx3000p thermocycler (Stratagene, La Jolla, CA). Concurrent quality controls measuring genomic DNA contamination, reverse transcription efficiency, and PCR amplification efficiencies were analyzed and were within satisfactory limits. We have developed a history of using these qRT-PCR gene arrays and are pleased with the quality and robustness of the data that the technology provides to toxicogenomic analyses (Attene-Ramos et al. 2010; Muellner et al. 2010).

The raw and normalized data are available in the Gene Expression Omnibus (GEO) database (Edgar, Domrachev, and Lash 2002; Barrett et al. 2007) under the NCBI tracking system #15759010 series accession number.

Human DNA Damage/Repair Genes and Human Toxic Response Genes

We investigated the ability of the monoHAAs to modulate the expression of genes involved in DNA damage/repair pathways by employing a SuperArray PCR gene array. A description of the genes analyzed in the array is presented in Table 2.2 (Arikawa et al. 2006). The house-keeping genes used for normalization of the arrays are listed at the end of Table 2.2 (H01-H05).

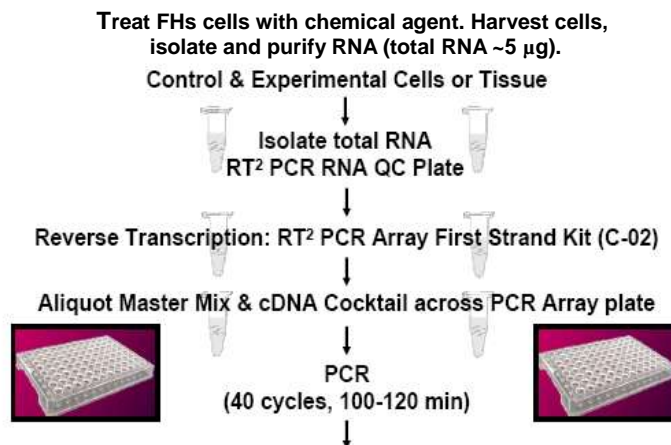


Figure 2.3 PCR Gene Array™ Experimental Design with Human FHs Cells.

Table 2.2
DNA damage and repair related genes analyzed in this study

Array Position	Unigene	GeneBank	Symbol	Description
A01	Hs.431048	NM_005157	<i>ABL1</i>	V-abl Abelson murine leukemia viral oncogenes homolog 1
A02	Hs.601206	NM_198889	<i>ANKRD17</i>	Ankyrin repeat domain 17
A03	Hs.73722	NM_080649	<i>APEX1</i>	APEX nuclease (multifunctional DNA repair enzyme) 1
A04	Hs.367437	NM_000051	<i>ATM</i>	Ataxia telangiectasia mutated (includes complementation groups A, C and D)
A05	Hs.271791	NM_001184	<i>ATR</i>	Ataxia telangiectasia and Rad3 related
A06	Hs.533526	NM_000489	<i>ATRX</i>	Alpha thalassemia/mental retardation syndrome X-linked (RAD54 homolog, <i>S. cerevisiae</i>)
A07	Hs.194143	NM_007294	<i>BRCA1</i>	Breast cancer 1, early onset, dsDNA repair
A08	Hs.519162	NM_006763	<i>BTG2</i>	BTG family, member 2
A09	Hs.292524	NM_001239	<i>CCNH</i>	Cyclin H
A10	Hs.184298	NM_001799	<i>CDK7</i>	Cyclin-dependent kinase 7 (MO15 homolog, <i>Xenopus laevis</i> , cdk-activating kinase)
A11	Hs.24529	NM_001274	<i>CHEK1</i>	CHK1 checkpoint homolog (<i>S. pombe</i>)
A12	Hs.291363	NM_007194	<i>CHEK2</i>	CHK2 checkpoint homolog (<i>S. pombe</i>)
B01	Hs.135471	NM_006384	<i>CIB1</i>	Calcium and integrin binding 1 (calmyrin)
B02	Hs.249129	NM_001279	<i>CIDEA</i>	Cell death-inducing DFFA-like effector a
B03	Hs.151573	NM_004075	<i>CRY1</i>	Cryptochrome 1 (photolyase-like)
B04	Hs.290758	NM_001923	<i>DDB1</i>	Damage-specific DNA binding protein 1, 127kDa
B05	Hs.505777	NM_004083	<i>DDIT3</i>	DNA-damage-inducible transcript 3
B06	Hs.339396	NM_007068	<i>DMC1</i>	DMC1 dosage suppressor of mck1 homolog, meiosis-specific homologous recombination (yeast)
B07	Hs.435981	NM_001983	<i>ERCC1</i>	Excision repair cross-complementing rodent repair deficiency, complementation group 1 (includes overlapping antisense sequence)
B08	Hs.487294	NM_000400	<i>ERCC2</i>	Excision repair cross-complementing rodent repair deficiency, complementation group 2 (xeroderma pigmentosum D)
B09	Hs.498248	NM_130398	<i>EXO1</i>	Exonuclease 1
B10	Hs.591084	NM_004629	<i>FANCG</i>	Fanconi anemia, complementation group G
B11	Hs.409065	NM_004111	<i>FEN1</i>	Flap structure-specific endonuclease 1
B12	Hs.292493	NM_001469	<i>XRCC6</i>	X-ray repair complementing defective repair in Chinese hamster cells 6 (Ku autoantigen, 70kDa)
C01	Hs.80409	NM_001924	<i>GADD45A</i>	Growth arrest and DNA-damage-inducible, alpha
C02	Hs.9701	NM_006705	<i>GADD45G</i>	Growth arrest and DNA-damage-inducible, gamma
C03	Hs.545196	NM_002066	<i>GML</i>	GPI anchored molecule like protein
C04	Hs.577202	NM_005316	<i>GTF2H1</i>	General transcription factor IIH, polypeptide 1, 62kDa

(continued)

Table 2.2 (Continued)

Array Position	Unigene	GeneBank	Symbol	Description
C05	Hs.191356	NM_001515	<i>GTF2H2</i>	General transcription factor IIIH, polypeptide 2, 44kDa
C06	Hs.386189	NM_016426	<i>GTSE1</i>	G-2 and S-phase expressed 1
C07	Hs.152983	NM_004507	<i>HUS1</i>	HUS1 checkpoint homolog (<i>S. pombe</i>)
C08	Hs.503048	NM_002180	<i>IGHMBP2</i>	Immunoglobulin mu binding protein 2
C09	Hs.17253	NM_054111	<i>IHPK3</i>	Inositol hexaphosphate kinase 3
C10	Hs.61188	NM_033276	<i>XRCC6BP1</i>	XRCC6 binding protein 1
C11	Hs.1770	NM_000234	<i>LIG1</i>	Ligase I, DNA, ATP-dependent
C12	Hs.463978	NM_002758	<i>MAP2K6</i>	Mitogen-activated protein kinase kinase 6
D01	Hs.432642	NM_002969	<i>MAPK12</i>	Mitogen-activated protein kinase 12
D02	Hs.35947	NM_003925	<i>MBD4</i>	Methyl-CpG binding domain protein 4
D03	Hs.195364	NM_000249	<i>MLH1</i>	MutL homolog 1, colon cancer, nonpolyposis type 2 (<i>E. coli</i>)
D04	Hs.436650	NM_014381	<i>MLH3</i>	MutL homolog 3 (<i>E. coli</i>)
D05	Hs.509523	NM_002431	<i>MNAT1</i>	Menage a trois homolog 1, cyclin H assembly factor (<i>Xenopus laevis</i>)
D06	Hs.459596	NM_002434	<i>MPG</i>	N-methylpurine-DNA glycosylase
D07	Hs.192649	NM_005590	<i>MRE11A</i>	MRE11 meiotic recombination 11 homolog A (<i>S. cerevisiae</i>)
D08	Hs.597656	NM_000251	<i>MSH2</i>	MutS homolog 2, colon cancer, nonpolyposis type 1 (<i>E. coli</i>)
D09	Hs.280987	NM_002439	<i>MSH3</i>	MutS homolog 3 (<i>E. coli</i>)
D10	Hs.271353	NM_012222	<i>MUTYH</i>	MutY homolog (<i>E. coli</i>)
D11	Hs.396494	NM_018177	<i>N4BP2</i>	Nedd4 binding protein 2
D12	Hs.492208	NM_002485	<i>NBN</i>	Nibrin
E01	Hs.66196	NM_002528	<i>NTHL1</i>	Nth endonuclease III-like 1 (<i>E. coli</i>)
E02	Hs.380271	NM_002542	<i>OGG1</i>	8-oxoguanine DNA glycosylase
E03	Hs.20930	NM_020418	<i>PCBP4</i>	Poly(rC) binding protein 4
E04	Hs.147433	NM_182649	<i>PCNA</i>	Proliferating cell nuclear antigen
E05	Hs.424932	NM_004208	<i>AIFM1</i>	Apoptosis-inducing factor, mitochondrion-associated, 1
E06	Hs.111749	NM_000534	<i>PMS1</i>	PMS1 postmeiotic segregation increased 1 (<i>S. cerevisiae</i>)
E07	Hs.632637	NM_000535	<i>PMS2</i>	PMS2 postmeiotic segregation increased 2 (<i>S. cerevisiae</i>)
E08	Hs.225784	NM_005395	<i>PMS2L3</i>	Postmeiotic segregation increased 2-like 3
E09	Hs.78016	NM_007254	<i>PNKP</i>	Polynucleotide kinase 3'-phosphatase
E10	Hs.631593	NM_014330	<i>PPP1R15A</i>	Protein phosphatase 1, regulatory (inhibitor) subunit 15A
E11	Hs.491682	NM_006904	<i>PRKDC</i>	Protein kinase, DNA-activated, catalytic polypeptide
E12	Hs.531879	NM_002853	<i>RAD1</i>	RAD1 homolog (<i>S. pombe</i>)
F01	Hs.16184	NM_002873	<i>RAD17</i>	RAD17 homolog (<i>S. pombe</i>)
F02	Hs.375684	NM_020165	<i>RAD18</i>	RAD18 homolog (<i>S. cerevisiae</i>)
F03	Hs.81848	NM_006265	<i>RAD21</i>	RAD21 homolog (<i>S. pombe</i>)

(continued)

Table 2.2 (Continued)

Array Position	Unigene	GeneBank	Symbol	Description
F04	Hs.128904	NM_005732	<i>RAD50</i>	RAD50 homolog (<i>S. cerevisiae</i>)
F05	Hs.631709	NM_002875	<i>RAD51</i>	RAD51 homolog (RecA homolog, <i>E. coli</i>) (<i>S. cerevisiae</i>)
F06	Hs.172587	NM_133509	<i>RAD51L1</i>	RAD51-like 1 (<i>S. cerevisiae</i>)
F07	Hs.240457	NM_004584	<i>RAD9A</i>	RAD9 homolog A (<i>S. pombe</i>)
F08	Hs.546282	NM_002894	<i>RBBP8</i>	Retinoblastoma binding protein 8
F09	Hs.443077	NM_016316	<i>REV1</i>	REV1 homolog (<i>S. cerevisiae</i>)
F10	Hs.461925	NM_002945	<i>RPA1</i>	Replication protein A1, 70kDa
F11	Hs.408846	NM_022367	<i>SEMA4A</i>	Sema domain, immunoglobulin domain (Ig), transmembrane domain (TM) and short cytoplasmic domain, (semaphorin) 4A
F12	Hs.591336	NM_014454	<i>SESN1</i>	Sestrin 1
G01	Hs.211602	NM_006306	<i>SMCIA</i>	Structural maintenance of chromosomes 1A
G02	Hs.81424	NM_003352	<i>SUMO1</i>	SMT3 suppressor of mif two 3 homolog 1 (<i>S. cerevisiae</i>)
G03	Hs.408312	NM_000546	<i>TP53</i>	Tumor protein p53 (Li-Fraumeni syndrome)
G04	Hs.192132	NM_005427	<i>TP73</i>	Tumor protein p73
G05	Hs.344812	NM_016381	<i>TREX1</i>	Three prime repair exonuclease 1
G06	Hs.191334	NM_003362	<i>UNG</i>	Uracil-DNA glycosylase
G07	Hs.591907	NM_000380	<i>XPA</i>	Xeroderma pigmentosum, complementation group A
G08	Hs.475538	NM_004628	<i>XPC</i>	Xeroderma pigmentosum, complementation group C
G09	Hs.98493	NM_006297	<i>XRCC1</i>	X-ray repair complementing defective repair in Chinese hamster cells 1
G10	Hs.647093	NM_005431	<i>XRCC2</i>	X-ray repair complementing defective repair in Chinese hamster cells 2
G11	Hs.592325	NM_005432	<i>XRCC3</i>	X-ray repair complementing defective repair in Chinese hamster cells 3
G12	Hs.444451	NM_016653	<i>ZAK</i>	Sterile alpha motif and leucine zipper containing kinase AZK
H01	Hs.534255	NM_004048	<i>B2M</i>	Beta-2-microglobulin
H02	Hs.412707	NM_000194	<i>HPRT1</i>	Hypoxanthine phosphoribosyltransferase 1 (Lesch-Nyhan syndrome)
H03	Hs.546356	NM_012423	<i>RPL13A</i>	Ribosomal protein L13a
H04	Hs.544577	NM_002046	<i>GAPDH</i>	Glyceraldehyde-3-phosphate dehydrogenase
H05	Hs.520640	NM_001101	<i>ACTB</i>	Actin, beta

QUALITY ASSURANCE/QUALITY CONTROL

Data Analysis

We have established a reputation for high quality work on the toxicity and genotoxicity of drinking water disinfection by-products employing comparative biological assays. In addition we have worked closely with colleagues who are analytical chemists who have conducted DBP research. Quality assurance/quality control is a priority of our laboratory. We have an annual

calibration of our Rainin pipettes by a factory technician who is certified by the manufacturer. We calibrate our balances and have our three biological/chemical safety hoods certified each year. The chronic cell cytotoxicity assay and the SCGE assay are conducted according to published procedures and we include positive controls with our assays. We also employ statistical methods that have been approved in peer-reviewed scientific journals. Our tissue culture facility is maintained to the highest levels of quality. We retain the biohazard safety license for our media room. Our autoclaves and laboratory glassware washing facility are maintained by technicians from the University of Illinois. We conform to all of the regulations of the Division of Research Safety of the University of Illinois at Urbana-Champaign.

Data from the experiments were transferred to Excel spreadsheets and analyzed using standard statistical and graphical functions of well-known scientific software packages (e.g. SigmaPlot, SigmaStat and Table Curve). All data were maintained in data books and in electronic files for sharing amongst the research group. The FHs cell cytotoxicity data were analyzed using parametric statistical approaches that we have published. For the SCGE assay the % tail DNA values are not normally distributed and violate the requirements for analysis by parametric statistics. The average % tail DNA values for each slide were determined and the data averaged amongst all of the microgels for a specific concentration. Averaged mean values express a normal distribution according to the central limit theorem (Box, Hunter, and Hunter 1978). The averaged mean % tail DNA values obtained from repeated experiments were used with a one-way analysis of variance test (Lovell and Omori 2008). If a significant F value of $P \leq 0.05$ was obtained, a Holm-Sidak multiple comparison versus the control group analysis was conducted. The power of the test statistic ($1-\beta$) was maintained as ≥ 0.8 at $\alpha = 0.05$. For the PCR gene array studies, we used the Stratagene software package with the qRT-PCR instrument and software to provide the threshold cycle (C_t) values for the genes on the PCR arrays. Finally the normalized C_t values were used in the calculation of fold-changes in gene expression for a pair-wise comparison using the $\Delta\Delta C_t$ method (Quellhorst et al. 2006). All calculations were kept on electronic spreadsheets and archived for the project.

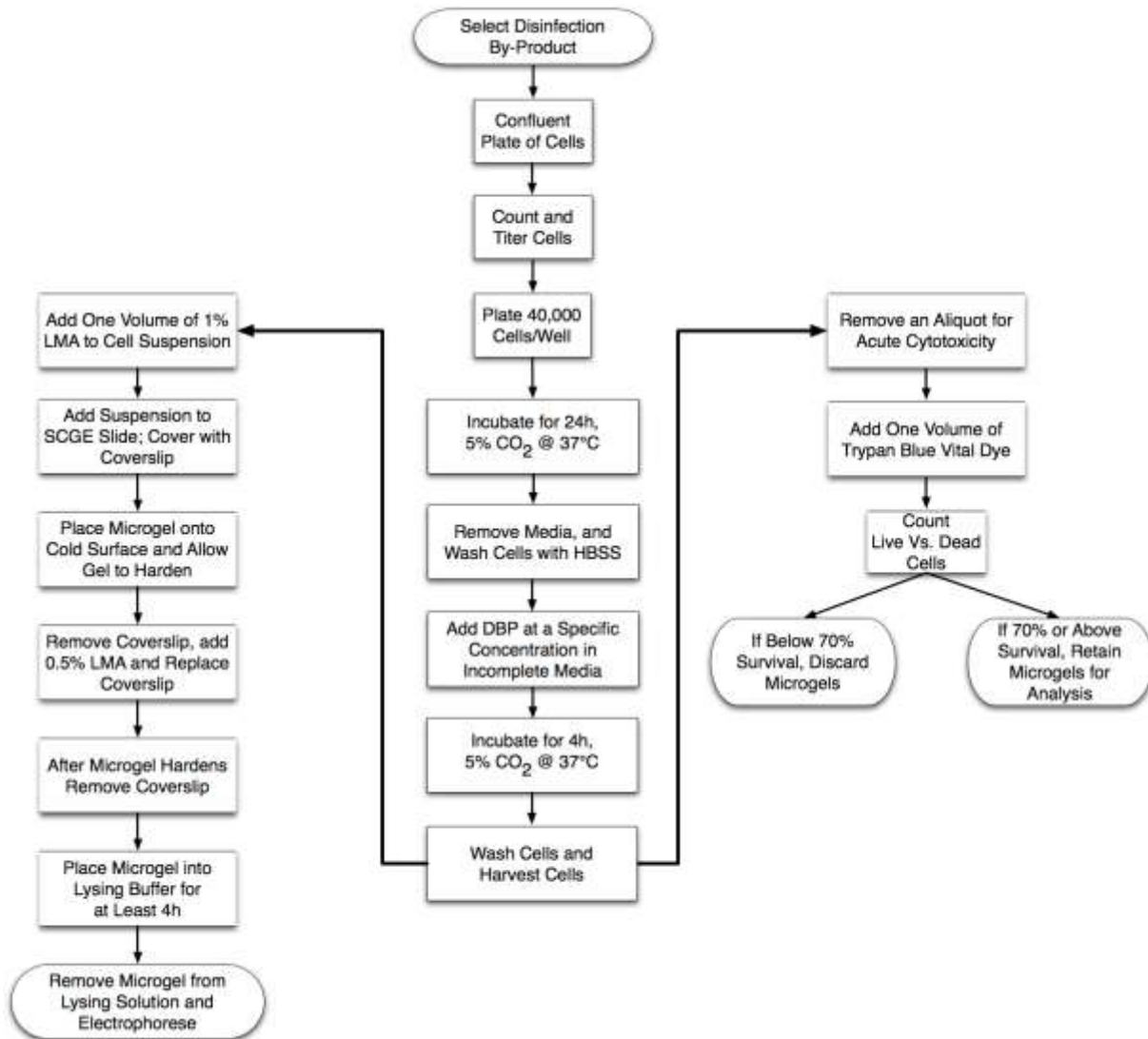
Safety

Safety is a principal concern in our laboratory. Manipulations of toxic and mutagenic and or carcinogenic chemicals were conducted using disposable papers and gloves in a certified biological/chemical safety hood. The regulations of the Division of Research Safety at the University of Illinois were strictly implemented throughout this project.

CHAPTER 3 HUMAN FHS CELLS AND TOXICOGENOMIC ANALYSES

SCGE ANALYSIS OF IAA, BAA, AND CAA USING HUMAN FHS CELLS

One of the objectives of this research was to conduct SCGE analyses of the three monoHAAs using nontransformed human FHs cells (Figure 3.1). These concentration-response data are essential in order to calculate the equivalent biological response as well as the acute cytotoxicity response for each monoHAA. For this report we used the % Tail DNA as our metric of DNA damage (Wagner and Plewa 2009).



Source: Reprinted with permission from Plewa, M.J.; Wagner, E.D. Mammalian Cell Cytotoxicity and Genotoxicity of Disinfection By-Products. Copyright 2009, Water Research Foundation.

Figure 3.1 Flow chart of the SCGE assay

Iodoacetic Acid

IAA is an emerging DBP (Zhang et al. 2010; Plewa et al. 2004; Plewa et al. 2010) and it was evaluated for acute cytotoxicity and genomic DNA damaging activity with human FHs cells in a concentration range from 0 to 35 μM . Throughout this range there was no reduction in cell viability (Figure 3.2, top panel) and the induction of DNA damage was directly related to increased IAA concentration (Figure 3.2, lower panel).

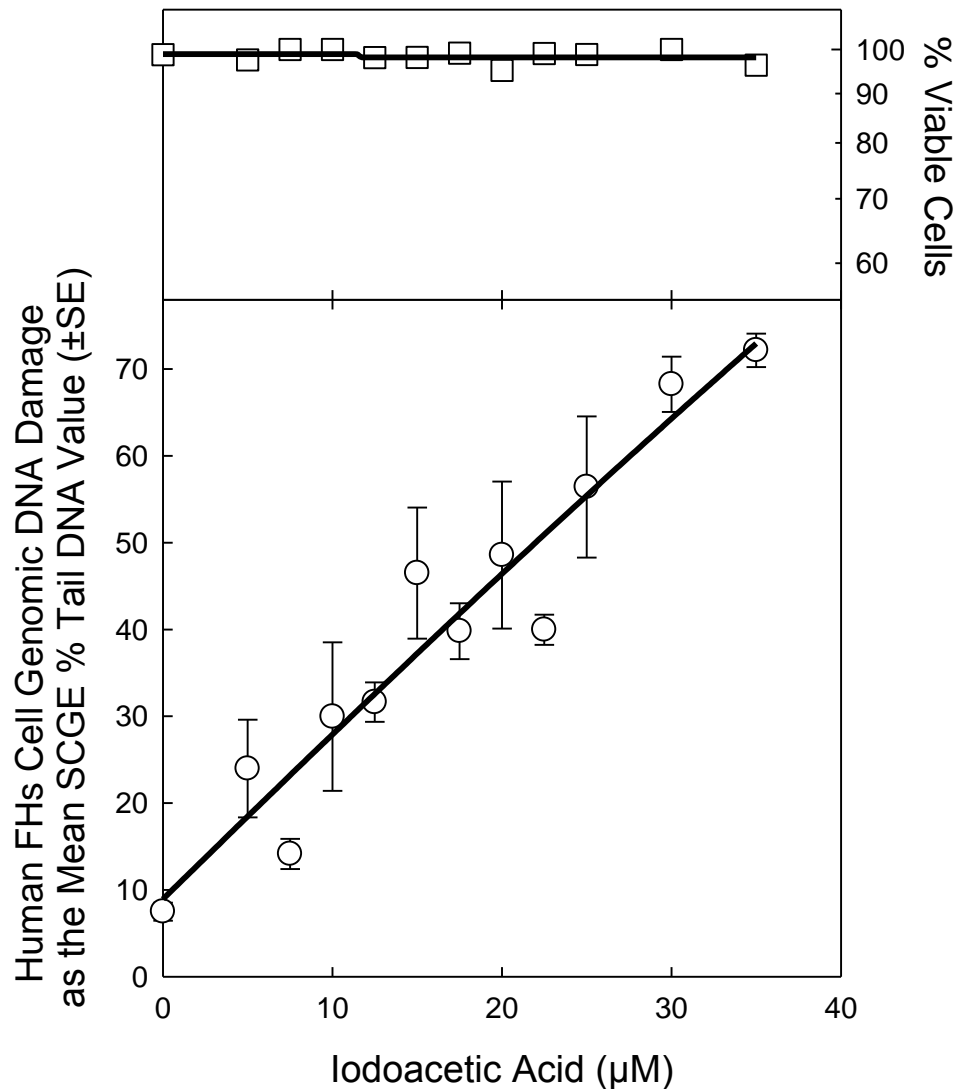


Figure 3.2 Acute cytotoxicity and genotoxicity induced by iodoacetic acid in human FHs cells.

Bromoacetic Acid

BAA is a regulated DBP (U. S. Environmental Protection Agency 2006). The concentration range for BAA was 0 to 150 μM . Within this range the response of the human FHs cells to BAA expressed increased genomic DNA damage that leveled out with higher BAA concentrations (Figure 3.3, lower panel). At the highest BAA concentration analyzed the acute cell viability was reduced to 77% (Figure 3.3, top panel).

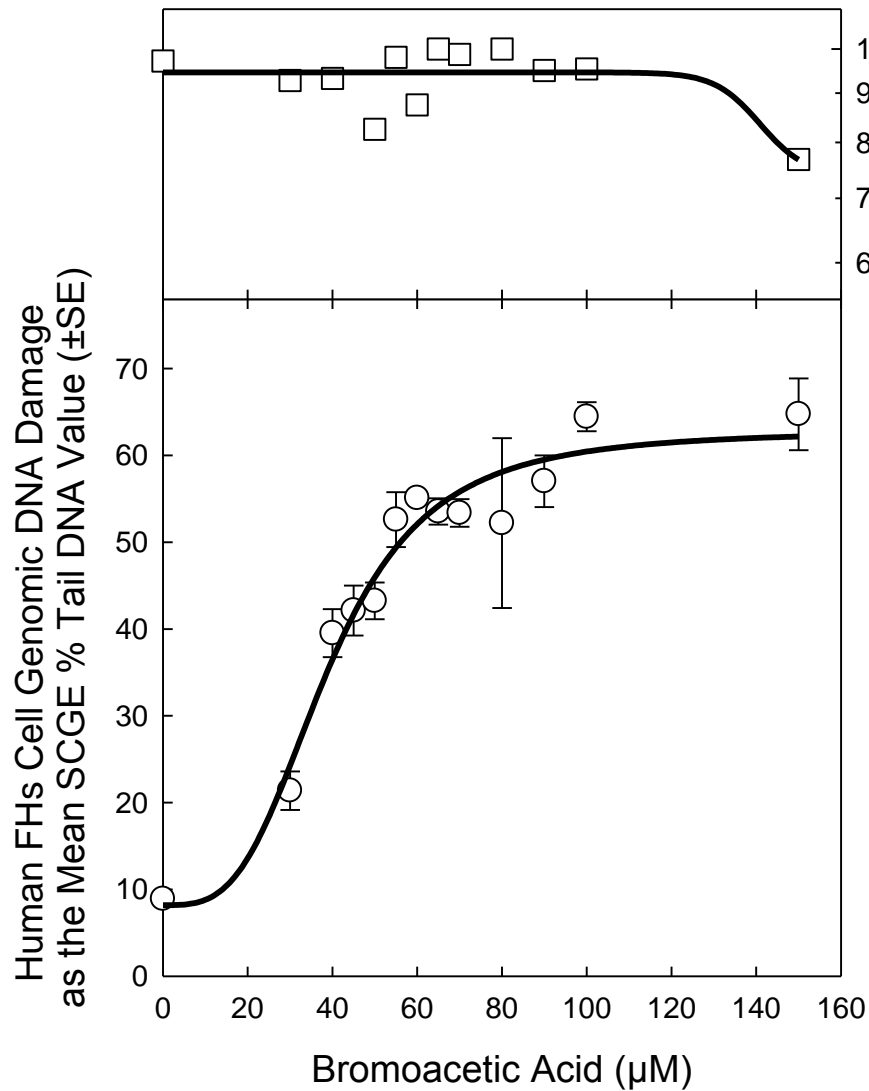


Figure 3.3 Acute cytotoxicity and genotoxicity induced by bromoacetic acid in human FHs cells.

Chloroacetic Acid

CAA is a regulated DBP (U. S. Environmental Protection Agency 2006) and it was evaluated with human FHs cells for acute cytotoxicity and genomic DNA damaging activity in a concentration range from 0 to 8 mM. Substantial cytotoxicity was observed at concentrations above 6 mM (Figure 3.4, top panel). Because of the high level of cell killing we limited the SCGE analysis to a concentration range of 0 to 6 mM. Within this concentration range the induction of DNA damage was directly related to increased CAA concentration (Figure 3.4, lower panel).

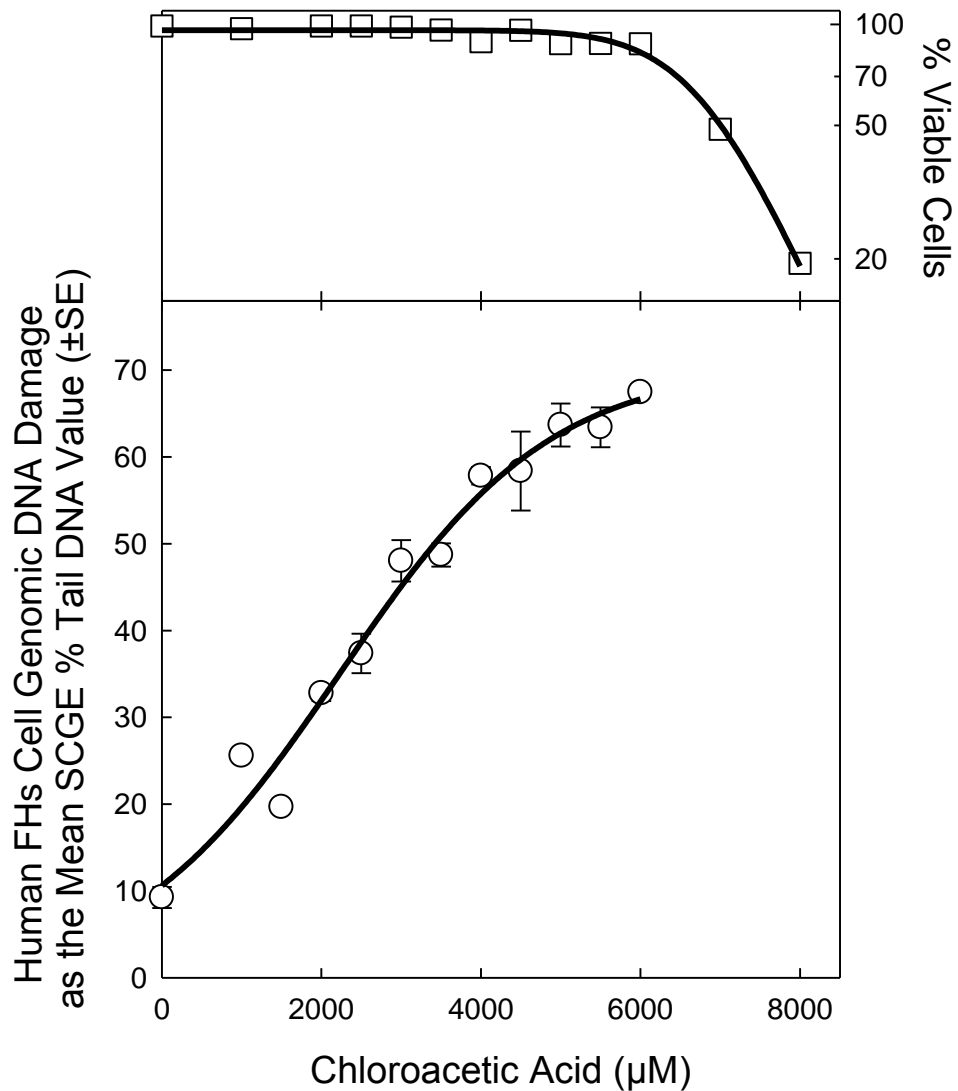


Figure 3.4 Acute cytotoxicity and genotoxicity induced by chloroacetic acid in human FHs cells.

EQUIVALENT GENOTOXIC EFFECTS AMONG THE MONOHALOACETIC ACIDS

In order to generate equivalent biological responses amongst the monoHAAs we conducted regression analysis on the concentration-response curves for the three monoHAAs. The concentration for each monoHAA that would induce a genotoxic impact of 20%, 40% and 50% SCGE Tail DNA was calculated. These concentrations that generated equivalent biological responses in human FHs cells were then used for the comparative toxicogenomic experimental designs. Using regression analyses (TableCurve v2.0) we determined the corresponding concentrations for each monoHAA. The r^2 values from the regression analyses for IAA, BAA and CAA were 0.89, 0.95, and 0.98, respectively (Table 3.1).

Table 3.1
Concentration of monoHAAs that induce equivalent levels of genomic DNA damage in non-transformed human FHs cells

MonoHAA	R^2 ^a	SCGE ^b 20%Tail DNA (HAA Molar Conc.)	SCGE 40%Tail DNA (HAA Molar Conc.)	SCGE 50%Tail DNA (HAA Molar Conc.)	ANOVA Test ^c
IAA	0.89	5.90×10^{-6}	16.6×10^{-6}	21.9×10^{-6}	$F_{11,24} = 7.26; P < 0.001$
BAA	0.95	23.8×10^{-6}	43.4×10^{-6}	56.5×10^{-6}	$F_{12,25} = 38.5; P < 0.001$
CAA	0.98	1.04×10^{-3}	2.60×10^{-3}	3.42×10^{-3}	$F_{11,22} = 96.4; P < 0.001$

Source: Reprinted with permission from Attene-Ramos, M. S.; Wagner, E. D.; Plewa, M. J., *Envion. Sci. Technol.* 2010, 44, (19), 7206-7212. Copyright 2010, American Chemical Society.

^a R^2 is the coefficient of determination for the regression analysis upon which HAA concentration was calculated for each level of genomic DNA damage. ^b Genotoxicity metric as the percentage of DNA that migrated into the microgel from the nucleus under SCGE conditions. At all monoHAA concentrations, no acute cytotoxicity was observed. ^c Degrees of freedom for the between groups and residual associated with the calculated F -test result and the resulting probability value.

Comparison of DNA Damage Induction by MonoHAAs in CHO and FHs Cells

We published the first systematic *in vitro* mammalian cell toxicological analysis of the monoHAAs (Plewa et al. 2004). Recently the induction of chronic cytotoxicity, genomic DNA damage, and point mutation in CHO cells were published for the entire class of haloacetic acids (Zhang et al. 2010; Plewa et al. 2010). With point mutation in CHO cells the descending rank order was IAA > BAA > CAA (Zhang et al. 2010). Similarly, the descending rank order of SCGE genotoxicity in CHO cells was IAA > BAA > CAA (Figure 3.5, panel A). This same rank order is observed for human FHs cells although the human cells are somewhat less sensitive (Figure 3.5, panel B). These data demonstrate that the CHO cell data were predictive of biological responses in human cells.

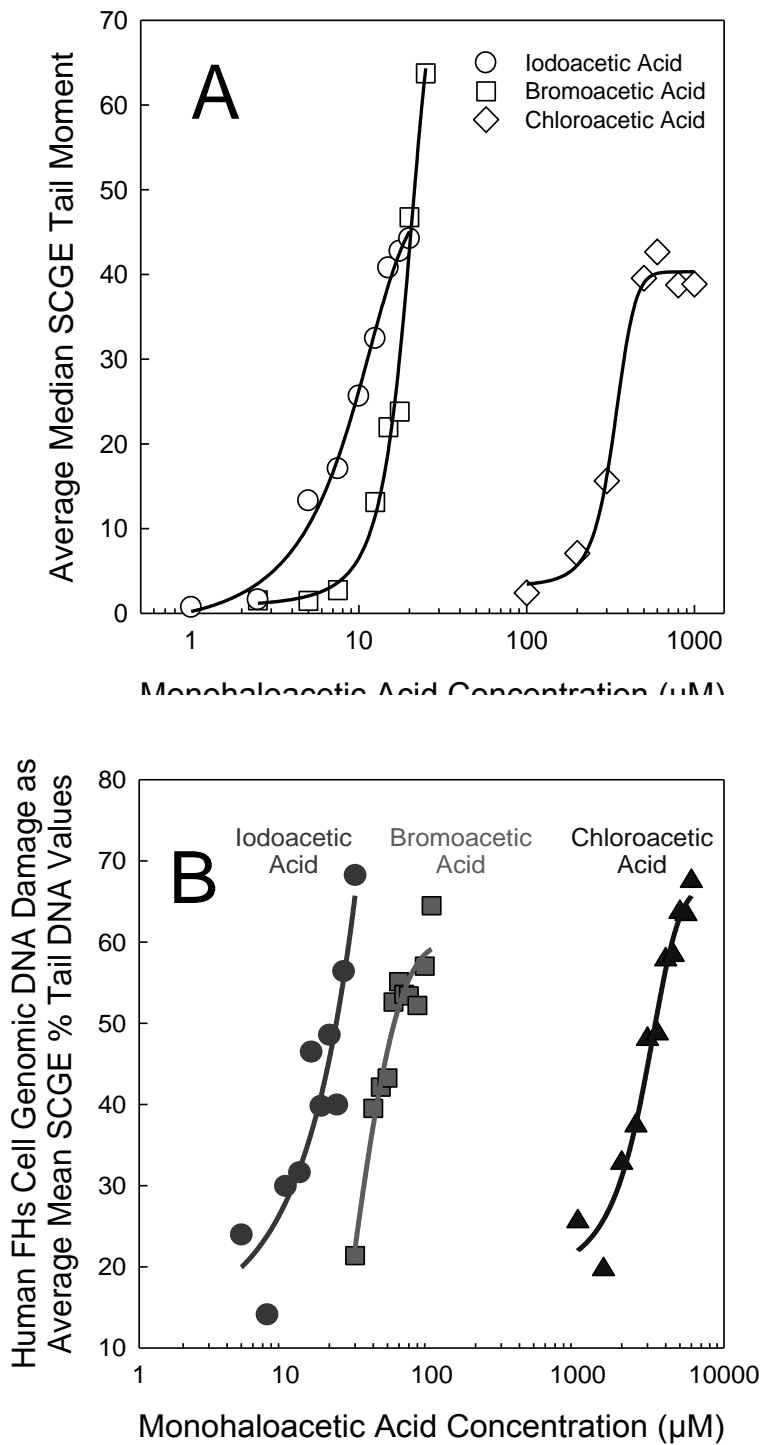


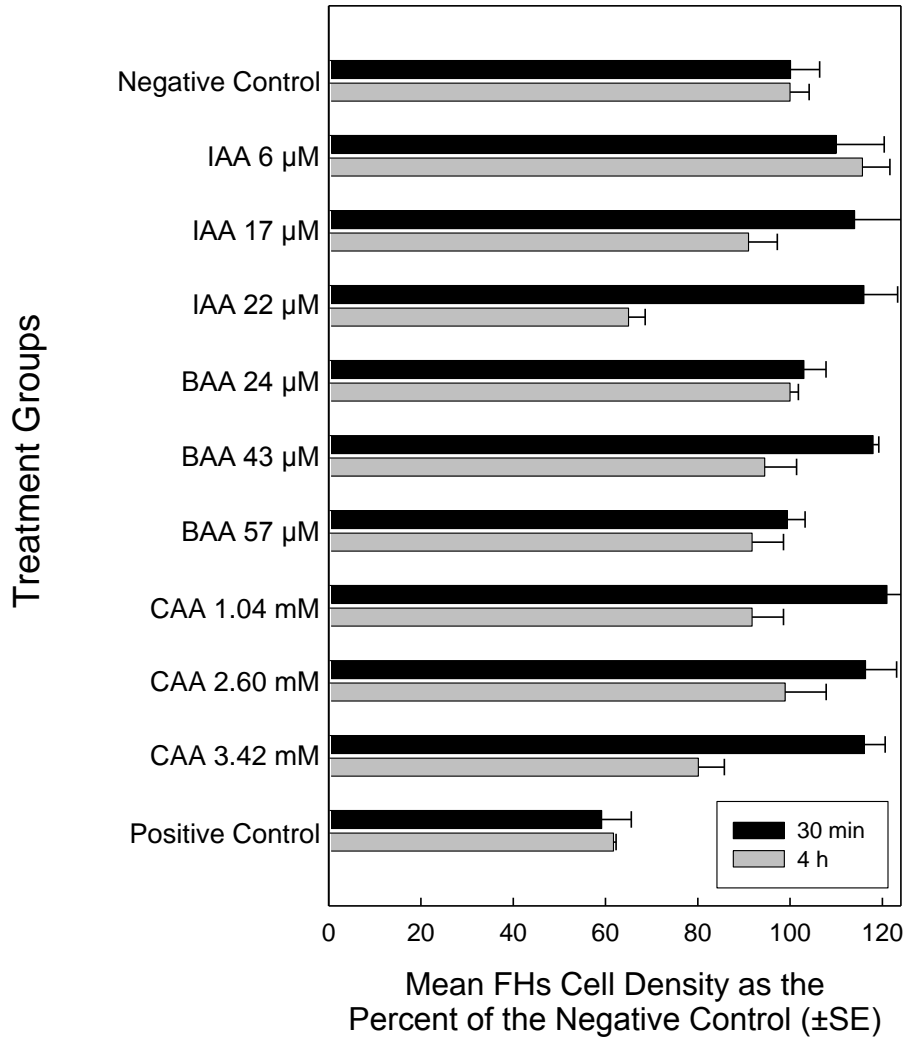
Figure 3.5 Log-linear plots illustrating the genomic DNA damaging capacity of iodoacetic acid, bromoacetic acid and chloroacetic acid in CHO cells (Panel A) and FHs cells (Panel B).

COMPARISON OF THE HUMAN FHS CELL DENSITIES AFTER EXPOSURE TO MONOHALOACETIC ACIDS

For the toxicogenomic experiments, cell viability was determined by trypan blue vital dye analysis immediately after exposure and also by a modified plating efficiency procedure. Human FHs cells were exposed to a series of concentrations of IAA, BAA or CAA that induced equivalent biological responses in flat bottom microplates at a titer of 1×10^4 cells/well (Table 3.1). The microplate wells were covered with sterile AlumnaSeal and incubated for 30 min or 4 h at 37°C. The cells were then washed 3× with PBS and 200 µL of complete Hybri-Care™ medium was added to each well. Microplates were incubated for 24 h at 37°C in a humidified atmosphere of 5% CO₂.

The microplates were stained with the histological dye crystal violet and analyzed as previously published (Plewa and Wagner 2009). The modified plating efficiency value for each monoHAA was calculated as the percentage of the cell density as compared to the negative control; the values for each concentration for each monoHAA are presented in Figure 3.6. The primary metric of plating efficiency is to determine the frequency of cells able to survive and divide after a treatment. In this evaluation which has a limited time frame, a reduction in the relative cell density after the 24 h growth period may not necessarily be due to cell killing. Past experiments demonstrated that each monoHAA concentration used in this study did not induce any acute cell killing (Figures 3.2, 3.3 and 3.4). If a concentration of a monoHAA caused cell cycle arrest there would be a reduction in the cell density. A reduction in cell density was observed only after a 4-h exposure to higher concentrations of IAA or CAA (Figure 3.6).

The conclusions from the data presented in Figures 3.2, 3.3, 3.4 and 3.6 were that under the selected monoHAA concentrations and exposure conditions, the viability of the treated FHs cells was not compromised. These concentrations and exposure conditions would ensure that for the toxicogenomic experiments, RNA would be extracted from viable cells.



Source: Reprinted with permission from Attene-Ramos, M. S.; Wagner, E. D.; Plewa, M. J., Environ. Sci. Technol. 2010, 44, (19), 7206-7212. Copyright 2010, American Chemical Society.

Figure 3.6 Cell density analyses of FHs cells exposed to monoHAAs for 30 min or 4 h and incubated for 24 h. The positive control was 25% dimethylsulfoxide

CHAPTER 4

BROMOACETIC ACID TOXICOGENOMICS

INTRODUCTION

One objective of this research was to integrate *in vitro* toxicology with focused toxicogenomic analysis of BAA and to evaluate the modulation of gene expression involved in DNA damage/repair and toxic responses, in normal non-transformed human cells. This work was to test the concept that directed, quantitative qRT-PCR gene arrays that were directly reflective of specific toxicological responses in human cells could reveal biological mechanisms for the observed toxicity. This work was a proof-of-concept project of the toxicogenomic program (Muellner et al. 2010).

We generated transcriptome profiles from human FHs cells treated with BAA at a concentration that was not acutely cytotoxic and that induced genomic DNA damage as measured by SCGE. FHs cells were treated with BAA with two different exposure times that captured the modulation of early and later gene expression. These data aid in defining the biological impact and toxicity mechanisms of BAA at concentrations within the resolving power of *in vitro* cytotoxicity and genotoxicity assays. This allows the integration of cytotoxicity, genotoxicity and toxicogenomic data for this regulated DBP.

GENERAL REQUIREMENTS AND LIMITS FOR TOXICOGENOMIC EXPERIMENTAL DESIGNS

Toxicogenomics is the combination of genetic microarray technology and toxicological methods and is the study of the relationship between the structure and activity of the genome and the adverse biological effects of toxic agents. Stringent conditions were established for the toxicogenomic experimental designs. These conditions included the following items.

1. The approach of using non-transformed human FHs cells was more expensive and labor intensive than using humor tumor cell lines, but the data may be more representative to real world experience.
2. Prior to conducting the gene array analyses the experimental design was devised for the monoHAA comparative study which included the decision of the type of gene array, the number of array replicates, the exposure times, and the statistical analysis to be applied to the toxicogenomic data.
3. Our design required that we conducted paired concurrent controls for each treatment group and time period.
4. All of the experiments were conducted at monoHAA concentrations that did not induce acute cytotoxic responses. This was to ensure that the isolated RNA came from viable cells rather from dead or dying cells.
5. For the comparative toxicogenomics of the monoHAAs, the concentrations that were used to treat the FHs cells generated equivalent biological responses.
6. After RNA isolation, the amount and quality of RNA extracts was carefully evaluated. For the comparative monoHAA toxicogenomic analyses the RNA concentrations were equalized across control and treatment groups for each exposure time group.

7. It was important to interpret the gene array data with a focus on gene expression affecting functional gene groups and metabolic pathways.

TOXICOGENOMIC ANALYSIS OF BROMOACETIC ACID

Treatment of FHs cells

The human FHs cells were treated for either 30 min or 4 h with 60 μ M BAA in a series of 6-well plates as described in Chapter 2.

RNA Isolation and DNase Treatment

After treatment the FHs cells were washed 3 \times in PBS and the cell suspensions were harvested and transferred to RNase-free microfuge tubes and centrifuged at 300 \times g for 5 min. An aliquot of each cell suspension was reserved, prior to centrifugation, for acute cytotoxicity and SCGE analysis. The supernatant was removed and RNA isolation was conducted using a Qiagen RNeasy Mini Kit. The cell suspensions were pooled from 2 wells generating a total of 6 RNA isolations (3 control and 3 treated) for each gene array and each time period. After cell lysing, Qiagen Qias shredder columns homogenized the samples and the RNA was eluted with nuclease free water (65°C) into a total volume of 100 μ L. DNase treatment of the RNA samples (Ambion DNA-free DNase) was conducted with 10 μ L of DNase I Buffer and 2 μ L rDNase I. Each sample was incubated at 37°C for 60 min. DNase Inactivation Reagent was added to each sample and incubated at room temperature for 4 min. All samples were centrifuged at 10,000 \times g for 1.5 min to pellet the Inactivation Reagent. The resulting genomic DNA-free RNA was transferred to RNA-free storage tubes. Samples yielded between 9-18 μ g of total RNA after DNase treatment. Aliquots from each sample were removed for RNA quantity and quality evaluations and the remainder was stored at -80°C.

RNA Quantity and Quality Assessment

A 50 mL, 1.2% agarose gel in 10 \times formaldehyde agarose (FA) gel buffer (200 mM MOPS, 50 mM sodium acetate, 10 mM EDTA, pH 7.0) with ethidium bromide in 250 mL of 1 \times FA running buffer (25 mL 10 \times FA gel buffer, 6.25 mL 37% formaldehyde, 220 mL nuclease-free H₂O) and 5 \times RNA loading buffer (16 μ L saturated bromophenol blue solution, 80 μ L 500 mM EDTA pH 8.0, 720 μ L 37% formaldehyde, 2 mL 100% glycerol, 3.084 mL formamide, 4 mL 10 \times FA gel buffer, 100 mL nuclease-free H₂O) was prepared. The denaturing gel equilibrated in the running buffer for 30 min. One volume of 5 \times RNA loading buffer was added to 4 volumes of RNA sample, mixed, and incubated for 5 min at 65°C. After heating, the samples were transferred to ice, loaded onto the gel and electrophoresed at 5-7 V/cm until the indicator dye ran approximately two-thirds of the length of the gel. Images of the gels were generated and the presence and intensity of the 28S and 18S bands were determined (Figure 4.1)

Spectrophotometric quantification of the RNA samples was conducted with all RNA samples using a Shimadzu BioSpec-mini DNA/RNA/Protein Analyzer (Columbia, MD). Aliquots of the RNA samples were diluted in 10 mM Tris·Cl, pH 7.0 and a full absorbance spectrum was obtained. RNA purity was determined by the A₂₆₀/A₂₈₀ ratio.

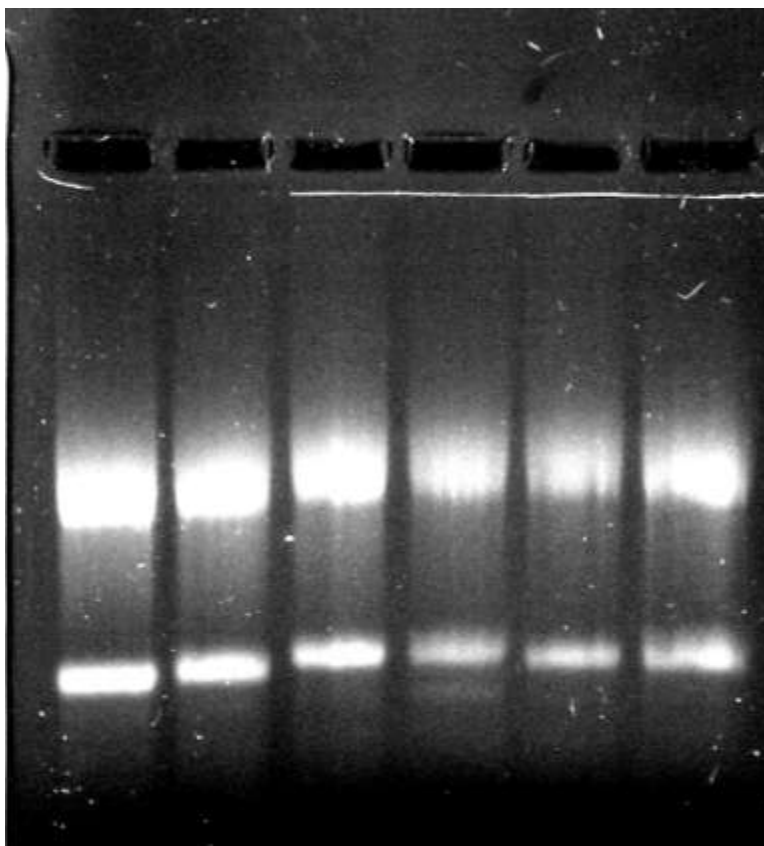


Figure 4.1 RNA gel from BAA treated FHs cells demonstrating the 28S and 18S bands with a 2:1 ratio.

cDNA Synthesis

A concentration of 0.7-0.8 μg of DNase-treated RNA was removed and cDNAs were synthesized using the SuperArray RT² PCR Array First Strand Kit (Frederick, MD). RNA samples were diluted to a constant concentration for each BAA exposure time (0.7 μg for the 4 h treatment and 0.8 μg for the 30 min treatment). One μL of the P2 enzyme, from the SuperArray RT² PCR Array First Strand Kit, was added to the nuclease-free PCR tube containing the diluted RNA. A MJ Research (Waltham, MA) PTC-100 programmable thermocycler was used to conduct the reactions. The annealing reaction was conducted at 70°C for 3 min and held on ice. The RT cocktail was prepared by mixing 10 μL of the annealing mixture with 10 μL of the RT cocktail. This mixture was incubated at 37°C for 60 min and heated to 95°C for 5 min to hydrolyze the RNA and inactivate the reverse transcriptase. The finished reaction was held on ice. After cDNA synthesis, the samples were diluted with 91 μL of nuclease free water and stored at -20°C.

Real Time PCR Analysis

An aliquot of the diluted first strand synthesis reaction (102 μ L) was added to the Super Array RT² Real-Time SYBR Green/ROX PCR master mix (Frederick, MD) and nuclease-free H₂O according to the RT² Profiler PCR Array System user manual. The cDNA/master mix cocktail was placed into a 25 mL sterile, nuclease free reservoir and 25 μ L was placed into each well of a SuperArray RT² Profiler PCR Array Human DNA Damage and Signaling Pathway array (Frederick, MD). This specific array contained primers for genes with functions involved in apoptosis, cell cycle arrest, cell cycle checkpoint, damaged DNA binding, base excision repair, double strand break repair, mismatch repair, and other genes related to DNA repair (Table 2.2). Optical cap strips were tightly placed onto each column of the microplate. The microplate was centrifuged to collect the liquid to the bottom of the wells. Using a two-step cycling program on a Stratagene Mx3000p (La Jolla, CA) (1 cycle for 10 min at 95°C, and 40 cycles of 15 s at 95 °C, 1 min at 60 °C) real-time PCR analysis was conducted. Data were collected using Stratagene MxPro (La Jolla, CA) software. Baseline thresholds were manually set to cycles 3-13 and the threshold fluorescence was set above the noise level and within the lower 1/3 of all the amplification plots (Figure 4.2). Data were transferred to Microsoft Excel (Redmond, WA) spreadsheets and analyzed using the SuperArray data analysis template (Frederick, MD). Built-in quality controls measuring genomic DNA contamination, reverse transcription efficiency, and poor PCR amplification efficiency were analyzed. Dissociation curves were also collected to ensure that the primers were functioning properly (Figure 4.3).

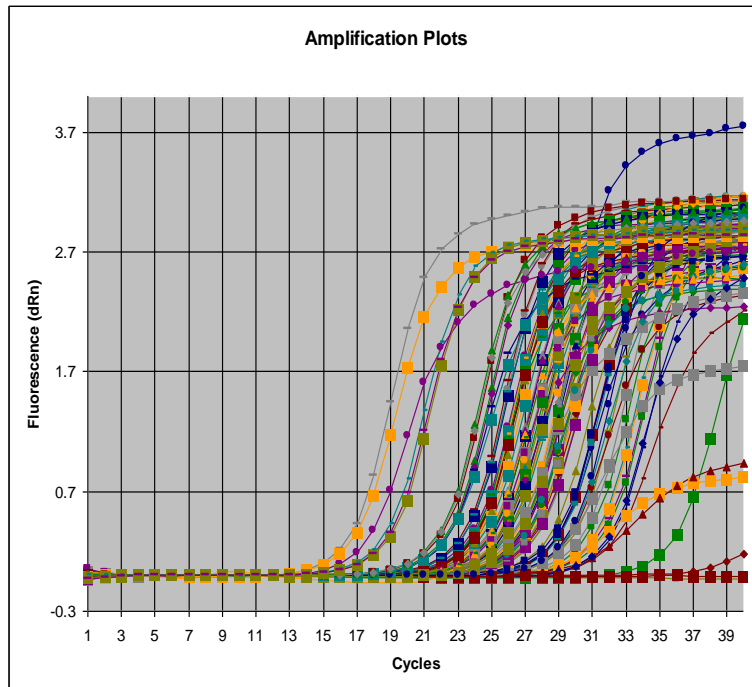


Figure 4.2 Example of an amplification plot generated by the Stratagene MxPro Software. The baseline is calculated between cycles 3-13 and the threshold value is set above the background and in the lower 1/3 of the plots. These settings were kept constant for all samples within each time group.

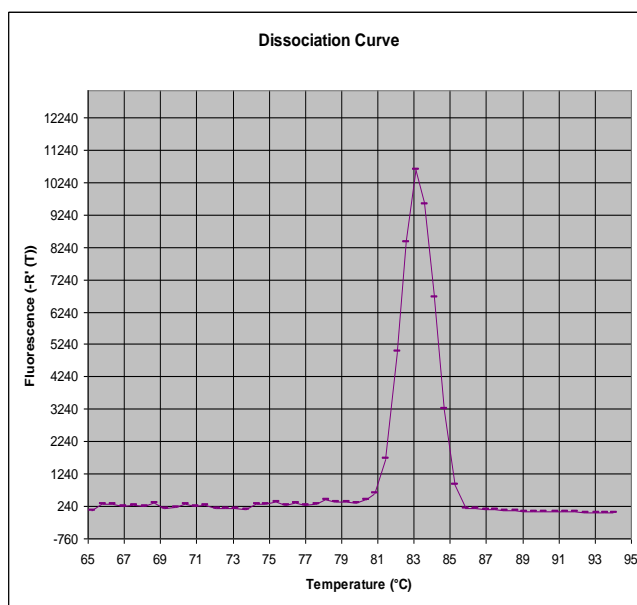


Figure 4.3 Example of a dissociation curve used to verify functioning primers.

Statistical Analysis

Quantitative real time PCR array data (three replicates per treatment and time point) were analyzed using the Rank Product method by means of the RankProd function of the Bioconductor package for R (Breitling et al. 2004; Hong et al. 2006) with $\alpha = 0.05$. We chose the direct test because the data are internally corrected by being derived from cells that express no acute cytotoxicity and the arrays focus on biologically relevant pathways that are directly connected to the toxicological endpoints.

FHs Cell Genotoxicity

In this initial study we found that the human FHs cells were slightly less sensitive to BAA than CHO cells (Plewa et al. 2010). We chose a treatment concentration of 60 μM that induced genomic DNA damage. With both exposure times (30 min and 4 h), there was no acute cytotoxicity.

Real-Time qRT-PCR Array Analysis

The experimental design provided two direct toxicological endpoints, genotoxicity and acute cytotoxicity. To integrate the toxicological endpoints with appropriate and focused toxicogenomic metrics, we used two arrays to evaluate the specific cellular response to BAA instead of a global transcriptome (gene chip) array. The SuperArray Human DNA Damage Signaling Pathway array and the Human Stress and Toxicity Pathway array focused on a series of metabolic pathways that complemented the toxicological effects of BAA. The RT² Profiler PCR Array system is a reliable and accurate method for analyzing the expression of groups of genes

within a functional category, by employing qRT-PCR. This approach combines the quantitative performance of qRT-PCR with the multiple gene-profiling capabilities of microarrays. Although fewer genes are represented with PCR arrays as compared to gene chip arrays, the quantitative nature of PCR is more precise and substantially limits the generation of false positive and negative responses, by focusing on a subset of genes of known importance and allowing much greater statistical power. The PCR array for DNA damage/repair and for human toxic response genes were used to profile the expression of 168 genes that were relevant to these specific pathways (Arikawa et al. 2006). A list of the genes analyzed for altered expression plus the raw and normalized data have been deposited at NCBI's Gene Expression Omnibus (Edgar, Domrachev, and Lash 2002) and can be accessed through GEO Series accession number GSE15488 (<http://www.ncbi.nlm.nih.gov/geo/query/acc.cgi?-acc=GSE15488>).

The level of 25 transcripts was modulated to a statistically significant degree in response to BAA treatment after 30 min (16 transcripts up-regulated and 9 down-regulated) (Table 4.1). The largest change in BAA-induced gene expression was observed for *RAD9A* ($2.9\times$ up-regulated) and *BRCA1* ($2.9\times$ down-regulated). The majority of the altered transcript profiles are those of genes involved in DNA repair and in cell cycle regulation (Figure 4.4). After 4 h of treatment the expression of 28 genes was modulated (12 up-regulated and 16 down-regulated) (Table 4.2 and Figure 4.4). Interestingly the largest fold changes in transcription as compared to the concurrent negative controls were in the expression of two genes encoding monooxygenase enzymes (*HMOX1* up-regulated $6.8\times$ and *FMO1* down-regulated $5.0\times$).

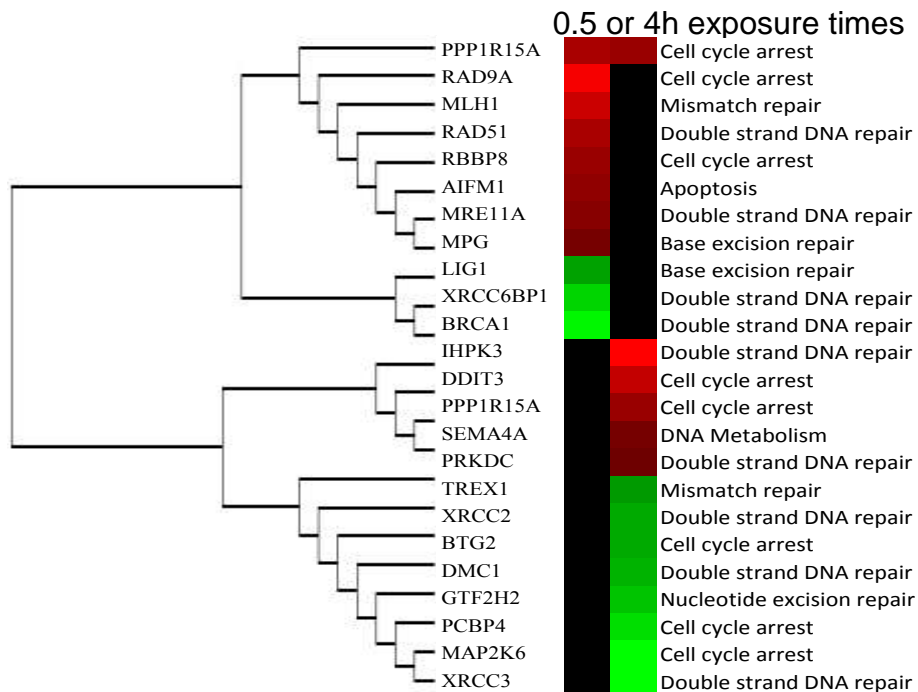


Figure 4.4 A dendrogram based on relative fold-change of genes after 30 min (left panel) and 4 hours (right panel) exposure of BAA in human FHs cells.

INTERPRETATION OF BROMOACETIC ACID TOXICOGENOMIC RESULTS

Many toxicogenomic *in vitro* studies use human tumor cell lines that are easy to grow and yield large amounts of RNA. However, such studies may be difficult to interpret. Tumor cell lines are genetically unstable and inherently exhibit aberrant gene expression. Comparing the modulation of gene expression in human tumor cell lines induced by a toxic agent questions the validity of the negative control. The use of the non-transformed human cell line FHs 74 Int with concurrent negative controls at each BAA treatment time avoids the difficulties that tumor cells present in toxicogenomic research. The concentration of the toxic agent also needs to be carefully considered. In toxicogenomic studies if a concentration of an agent induces significant levels of cell death (>30% lethality) the RNA extracted for microarray analysis is from dead or dying cells (Caba and Aubrecht 2006). It is highly probable that such transcript profiles will not reflect cellular responses to lower levels of the agent as experienced in human exposure. An additional concern is that much of the gene expression data reported in the literature is based on gene chip arrays without confirmation using qRT-PCR. It is prudent that transcriptome profile databases be founded on qRT-PCR confirmed individual gene expression for a competent toxicogenomic evaluation of specific toxicants. The use of PCR gene arrays addresses this concern (Arikawa et al. 2006).

After 30 min of BAA treatment we observed that 25 of the 168 genes analyzed exhibited modulated gene expression with a majority up-regulated (Figure 4.5, top panel). With 4 h of treatment the expression of 28 genes was modulated with 12 genes up-regulated and 16 down-regulated (Figure 4.5, bottom panel). The magnitude of the fold-changes in expression was greater with a 4-h treatment (Tables 4.1 and 4.2). With both exposure times the genes affected could be classified into three major categories, DNA damage/repair response, cell cycle and apoptosis regulation, and stress response and xenobiotic metabolism.

Functional analysis using the Database for Annotation, Visualization, and Integrated Discovery (DAVID) (Dennis et al. 2003; Huang, Sherman, and Lempicki 2009) suggested the involvement of members of two different signaling pathways, MAPK (*DDIT*) and TNF (*IL1A*, *IL1B*, *IL6*, *TNF*, *TNFSF10*) signaling pathways as a response to BAA toxicity. These two pathways play important roles in stopping cell proliferation and eventually decide the cellular fate. With both exposure times, the involvement of genes controlling the regulation of the cell cycle (*PPP1R15A*, *RAD9A*, *MAP2K6*, *PCBP4*, and *DDIT3*) indicate that DNA replication is likely prevented in order to allow time for the DNA repair processes to function (Harrison and Haber 2006).

Most of the DNA repair related genes that were modulated are involved at least in part in the cellular response to double strand DNA damage (Helleday et al. 2007; Brugmans, Kanaar, and Essers 2007; Harrison and Haber 2006; Su 2006; Bilsland and Downs 2005). This surprising result suggests that BAA may induce DNA double strand breaks, lesions similar to that of ionizing radiation. Double strand DNA breaks are considered to be one of the most toxic and mutagenic lesions (Helleday et al. 2007). Double strand DNA breaks must be repaired to restore the integrity, stability and reproducibility of the genome. In mammalian cells the repair of double strand breaks is mediated by two major systems, non-homologous DNA break end joining (error prone DNA repair) (Lieber et al. 2003) and homologous recombination repair (error free DNA repair) (Helleday et al. 2007; Karran 2000; Christmann et al. 2003). The altered expression of genes involved in double strand break repair with a 30 min BAA treatment were *BRCA1*, *MRE11A*, *ATM*, *XRCC6B*, and *RAD51* (Table 4.1); for the 4 h treatment the genes with altered

expression were *DMC1*, *XRCC2*, *XRCC3*, *PRKDC*, *RAD50*, and *IHPK3* (Table 4.2). The majority of these repair genes are involved in homologous recombination repair. BRCA1 protein is part of the BRCA1-associated genome surveillance complex (BASC) that detects double strand breaks (Christmann et al. 2003). BASC forms a complex with BRCA-2 and RAD51 proteins to generate the nucleoprotein filament that engages DNA homology and strand invasion required for recombination. RAD51 protein plays a central role in homology-directed DNA repair (Helleday et al. 2007). During the 30 min treatment the genes that have modulated expression are involved in the detection of DNA damage and the initiation of the RAD51 homology-directed DNA repair. With 4 h of exposure the alteration in gene expression shifted to those genes that are involved in the later stages of double strand DNA repair (including *XRCC2* and *XRCC3* binding and interaction at the recombination site).

By far the largest functional group of genes with altered expression was involved in the regulation of cell cycle. Cells under genotoxin-induced stress require time to suppress DNA replication and cell division, detect and repair damaged DNA and pass checkpoints controlling the commitment to programmed cell death. Figure 4.4 illustrates the temporal impact of BAA on the expression of genes affecting DNA damage detection and repair and cell cycle regulation. Such gene expression is markedly up-regulated with 30 min of exposure as compared to 4 h of exposure.

In order to better interpret the magnitude of the change in expression and the number of genes involved in the functional groups, we calculated a gene functional group expression index (Figure 4.6). We focused on three functional groups: (i) DNA damage/repair, (ii) cell cycle regulation and apoptosis, and (iii) stress response and xenobiotic metabolism. The index value for each group was the sum of the absolute fold change of expression (either up- or down-regulation) for genes within a selected functional group multiplied by the number of genes with altered expression. Although the metric within this index is in arbitrary units, it captures the magnitude of altered expression within a functional group at specific time periods of exposure. DNA damage/repair is generally up-regulated at the 30 min time period while at 4 h down-regulation is strongly evident. For expression of cell cycle regulation and apoptosis, a substantial increase in up-regulation is observed during the 30 min exposure; with 4 h exposure up-regulation is still high but is also accompanied by increased down-regulation in other genes. For genes involved in responses to toxic stress, the overall magnitude of change is less than the two previous functional groups; there is an increase in both up- and down-regulation with 4 h of exposure as compared to 30 min. The biological endpoint of DNA damage (SCGE) was linked with toxicogenomic analyses. BAA at a concentration and exposure time (30 min) that induced low levels of genotoxic insult without acute cytotoxicity, caused general up-regulation of genes associated with DNA damage/repair, cell cycle regulation and apoptosis. With a longer exposure to BAA (4 h), there was no detectable genotoxicity, while for the arrays there was a greater down-regulation of expression of genes associated with DNA damage/repair. With longer exposure there was increased modulation (both up- and down-regulation) in genes involved in cell cycle regulation and apoptosis and toxic response (Figure 4.6).

Toxicogenomic analysis of BAA provides enhanced sensitivity that complements traditional toxicity bioassays and indicates the cellular and molecular mechanisms involved in toxic responses to an agent. Assay of transcriptome profiles using qRT-PCR may provide biomarkers with greater sensitivity, specificity and faster turnaround time than traditional bioassays. The ultimate goal of this research is the generation of a comparative transcriptome

profile database that would potentially provide diagnostic information in epidemiological studies on the health effects of disinfected water.

Overall this work represents the first non-transformed human cell toxicogenomic study with a regulated drinking water disinfection by-product. We linked the biological endpoint of DNA damage (SCGE) with toxicogenomic arrays featuring primers for genes related to human DNA damage and repair, and general cellular responses to toxicity (Muellner et al. 2010).

Table 4.1
Gene expression changes in human FHs cells after 30 min BAA exposure

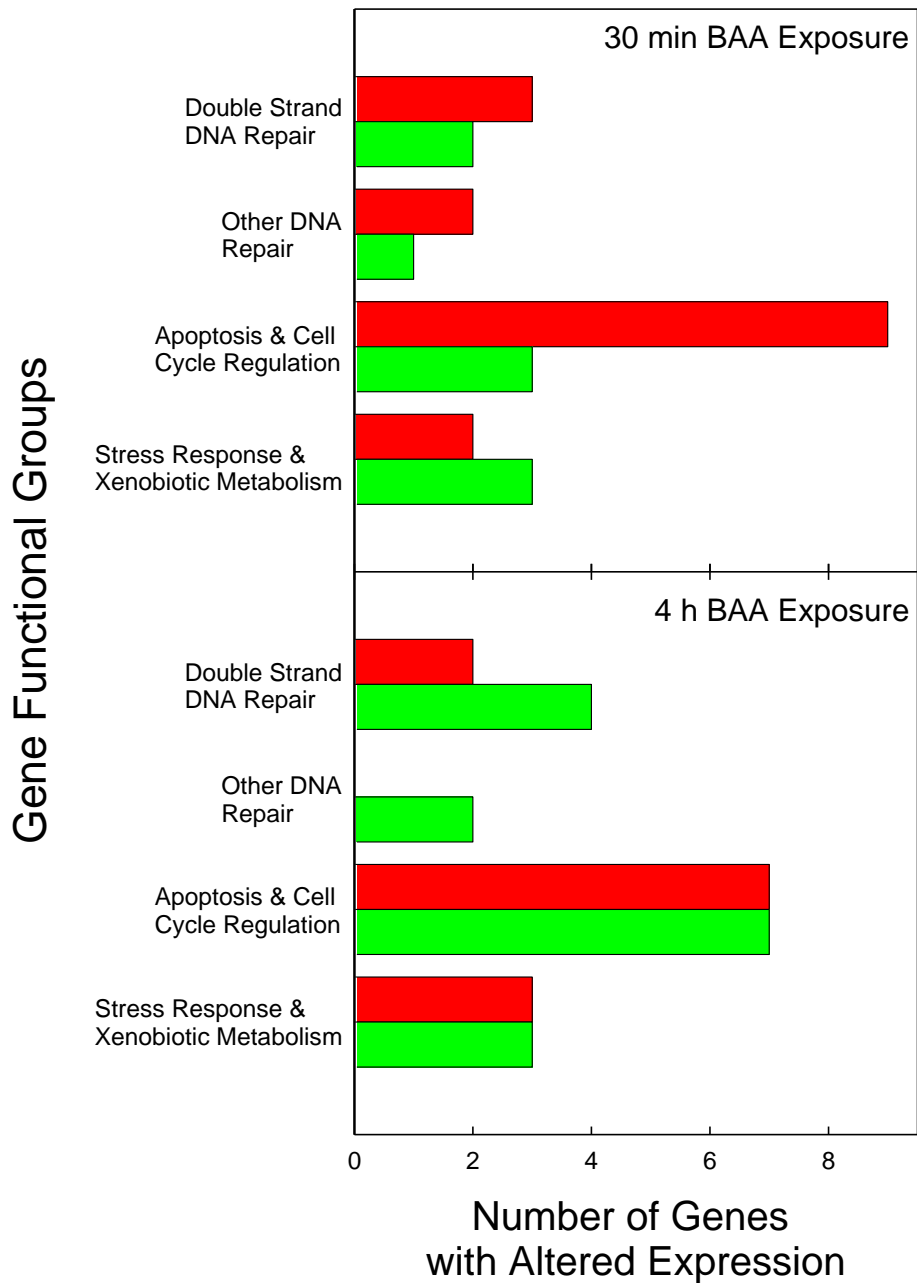
Gene Name	Fold Change	P Value	Reference
DNA Double Strand Break Repair			
<i>ATM</i>	1.26	0.03	(Riches, Lynch, and Gooderham 2008)
<i>BRCA1</i>	-2.90	0.003	(Zhao et al. 2007)
<i>MRE11A</i>	1.60	0.05	(Paul and Gellert 1998)
<i>RAD51</i>	2.00	0.01	(Lio et al. 2003)
<i>XRCC6BP1/KUB3</i>	-2.50	0.03	(Yang et al. 1999)
DNA Mismatch Repair			
<i>MLH1</i>	2.40	0.04	(Papadopoulos et al. 1994)
DNA Base Excision Repair			
<i>LIG1</i>	-1.90	0.04	(Tomkinson and Mackey 1998)
<i>MPG</i>	1.40	0.02	(Miao et al. 2000)
Cell Cycle Regulation and Apoptosis			
<i>AIFM1/PDCD8</i>	1.70	0.04	(Susin et al. 1999)
<i>CASP8</i>	1.39	0.01	(Boatright and Salvesen 2003)
<i>CASP10</i>	1.25	0.05	(Hengartner 2000)
<i>CSF2</i>	1.65	0.0006	(Scheuerer et al. 2000)
<i>PPP1R15A/GADD34</i>	2.00	0.02	(Hollander et al. 1997)
<i>RAD9A</i>	2.90	0.01	(Lieberman et al. 1996)
<i>RBBP8/CtIP</i>	1.80	0.04	(Yu and Baer 2000)
<i>IL1A</i>	1.29	0.03	(Nishida et al. 1987)
<i>IL1B</i>	1.55	0.004	(Nishida et al. 1987)
<i>LTA</i>	-1.83	0.01	(Gray et al. 1984)
<i>TNF</i>	-1.68	0.01	(Zhang and Wang 2006)
<i>TNFSF10</i>	-1.24	0.04	(Pitti et al. 1996)
Toxic Response and Xenobiotic Metabolism			
<i>CCL21</i>	-1.68	0.006	(Annunziato et al. 2000)
<i>EGR1</i>	1.46	0.005	(Davis et al. 2003)
<i>FM01</i>	-1.28	0.04	(Dolphin et al. 1991)
<i>GSR</i>	1.27	0.03	(Loos et al. 1976)
<i>NOS2a</i>	-2.01	0.001	(Moncada 1999)

Source: Reprinted with permission from Muellner, M.G.; Attene-Ramos, M.S.; Hudson, M.E.; Wagner, E.D.; Plewa, M.J., *Environ. Molec. Mutagen.* 2010, 51, 205-214. Copyright 2010 Wiley-Liss, Inc.

Table 4.2
Gene expression changes in human FHs cells after 4 h BAA exposure

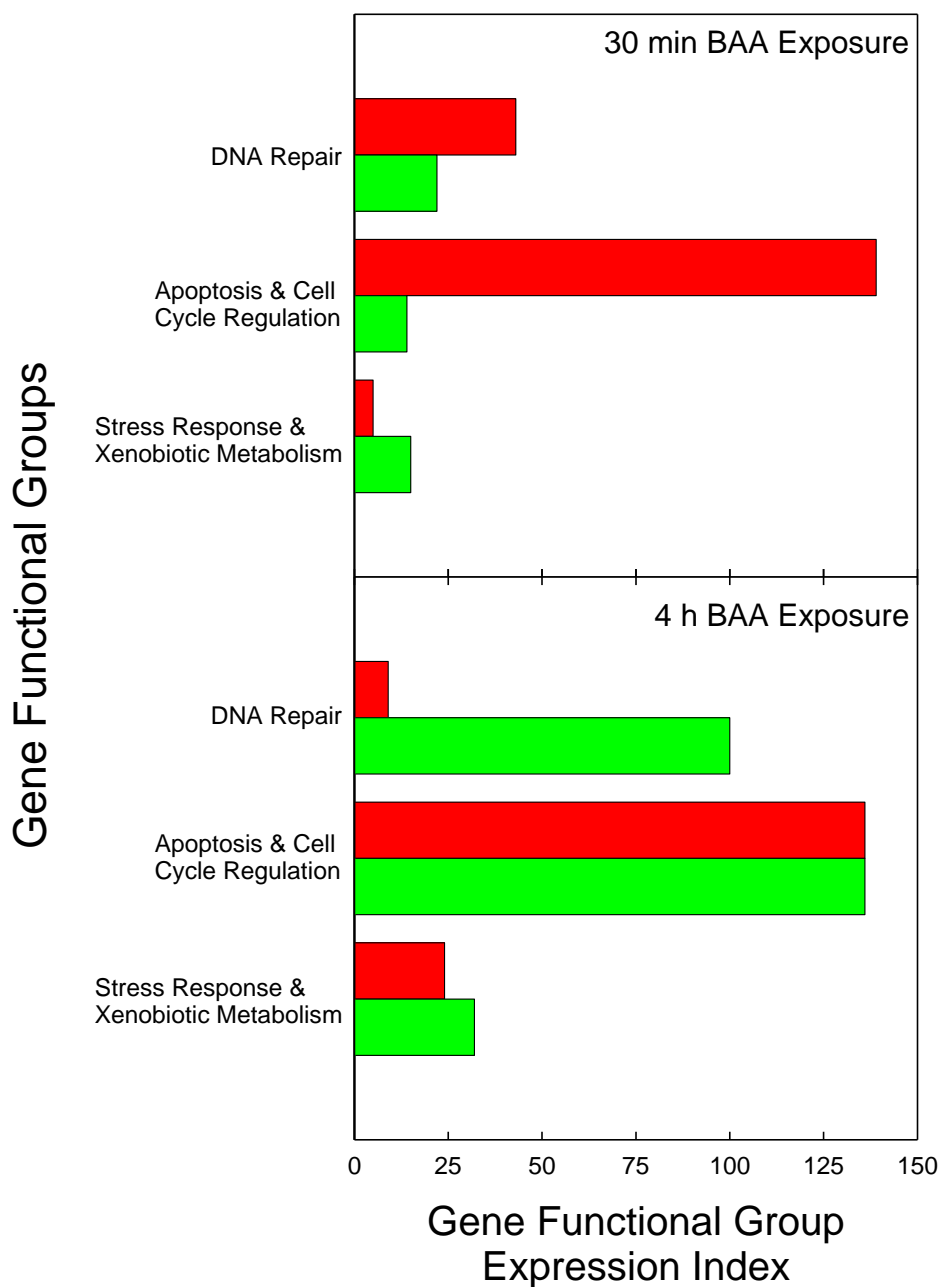
Gene Name	Fold Change	P Value	Reference
DNA Double Strand Break Repair			
<i>DMC1</i>	-2.10	0.01	(Habu et al. 1996)
<i>IHPK3</i>	3.10	0.0001	(Saiardi et al. 2001)
<i>PRKDC</i>	1.30	0.03	(Wang et al. 2004)
<i>RAD50</i>	-4.82	0.02	(Carney et al. 1998)
<i>XRCC2</i>	-2.00	0.02	(Cartwright et al. 1998)
<i>XRCC3</i>	-3.60	0.01	(Liu et al. 1998)
DNA Mismatch Repair			
<i>TREX1</i>	-1.80	0.01	(Mazur and Perrino 1999)
DNA Nucleotide Excision Repair			
<i>GTF2H2</i>	-2.30	0.01	(Lindahl and Wood 1999)
Cell Cycle Regulation and Apoptosis			
<i>BTG2</i>	-2.00	0.03	(Rouault et al. 1996)
<i>CASP8</i>	-2.08	0.02	(Boatright and Salvesen 2003)
<i>CRYAB</i>	2.25	0.01	(Mao et al. 2004)
<i>GDF15</i>	2.01	0.006	(Bootcov et al. 1997)
<i>HMOX1</i>	6.82	0.00001	(Malaguarnera et al. 2002)
<i>HSPA5</i>	1.72	0.02	(Reddy et al. 2003)
<i>IL1A</i>	-2.82	0.005	(Nishida et al. 1987)
<i>IL6</i>	-4.01	0.0008	(Zilberstein et al. 1986)
<i>LTA</i>	2.39	0.006	(Gray et al. 1984)
<i>MAP2K6</i>	-3.60	0.01	(Wang et al. 2000)
<i>NFKB1a</i>	2.41	0.002	(Cahir-McFarland et al. 2000)
<i>PCBP4/MCG10</i>	-2.60	0.02	(Makeyev and Liebhaber 2000)
<i>PPP1R15A/GADD34</i>	1.80	0.01	(Hollander et al. 1997)
<i>TNFSF10</i>	-2.37	0.02	(Pitti et al. 1996)
Toxic Response and Xenobiotic Metabolism			
<i>CSF2</i>	4.29	0.0002	(Scheuerer et al. 2000)
<i>DDIT3/CHOP</i>	2.30	0.002	(Park et al. 1992)
<i>EGR1</i>	-3.46	0.004	(Davis et al. 2003)
<i>FMO1</i>	-4.96	0.0001	(Dolphin et al. 1991)
<i>HSPAIL</i>	-2.11	0.02	(Ito et al. 1998)
<i>SEMA4A</i>	1.40	0.01	

Source: Reprinted with permission from Muellner, M.G.; Attene-Ramos, M.S.; Hudson, M.E.; Wagner, E.D.; Plewa, M.J., *Environ. Molec. Mutagen.* 2010, 51, 205-214. Copyright 2010 Wiley-Liss, Inc.



Source: Reprinted with permission from Muellner, M.G.; Attene-Ramos, M.S.; Hudson, M.E.; Wagner, E.D.; Plewa, M.J., Environ. Molec. Mutagen. 2010, 51, 205-214. Copyright 2010 Wiley-Liss, Inc.

Figure 4.5 Frequency distributions of BAA-induced modulation of gene transcript expression assorted by pathway related functional groups. Changes in gene expression for each exposure time (30 min and 4 h) is indicated by color (red = up-regulated; green = down-regulated).



Source: Reprinted with permission from Muellner, M.G.; Attene-Ramos, M.S.; Hudson, M.E.; Wagner, E.D.; Plewa, M.J., *Environ. Molec. Mutagen.* 2010, 51, 205-214. Copyright 2010 Wiley-Liss, Inc.

Figure 4.6 Frequency distribution of a gene functional group expression index for DNA damage/repair, cell cycle regulation and apoptosis, and stress response and xenobiotic metabolism groups. The index value for each group was the sum of the absolute fold change of expression (either up (red) or down (green) regulation) for genes within a selected functional group multiplied by the number of genes with altered expression.

CHAPTER 5

MONOHALOACETIC ACID COMPARATIVE TOXICOGENOMICS

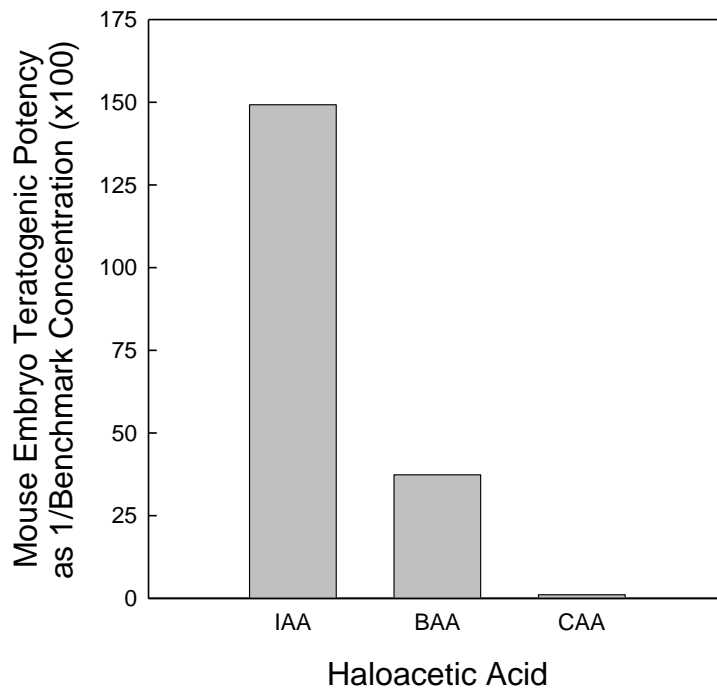
QUANTITATIVE COMPARATIVE TOXICOGENOMICS OF THE MONOHAAS

Toxicogenomics is a molecular tool to analyze the modulation of gene expression after exposure to a toxin. When compared to concurrent control transcriptome profiles, metabolic pathways involved in the cellular responses to toxic agents can be identified and provide insight on the biological mechanisms of toxicity (Hamadeh, Bushel et al. 2002; Hamadeh, Amin et al. 2002). Unfortunately much of the literature in toxicogenomics report the use of tumor cell lines that are exposed to cytotoxic concentrations of a genotoxin to observe effects on gene expression (Le Fevre et al. 2007). Tumor cell lines inherently exhibit aberrant gene expression and this fact calls into question the requirement of an adequate negative control. Control cells that exhibit “normal” gene expression are necessary to compare the transcriptome profiles of exposed cells. If tumor cell lines are used as controls, no true negative control is present within the experimental design. Likewise, with cytotoxic concentrations, transcript profiles will reflect those of dead or dying cells. In this project we avoided these experimental design shortcomings by using non-transformed human cells, concurrent negative controls with each treatment time and non-cytotoxic concentrations. An additional concern is that much of the gene expression data in the literature is based on gene chip arrays without qRT-PCR confirmation. Our experimental designs are based on the direct use of PCR gene arrays (Arikawa et al. 2006).

For this comparative human cell toxicogenomic analyses we chose three monoHAAs (Table 2.1) which represent a class of drinking water DBPs; BAA and CAA are regulated by the U.S. EPA (U. S. Environmental Protection Agency 2006). Since these monoHAAs differ only by a single halogen atom, it was possible to include structure activity relationship analyses and compare their physicochemical properties with transcriptome profiles.

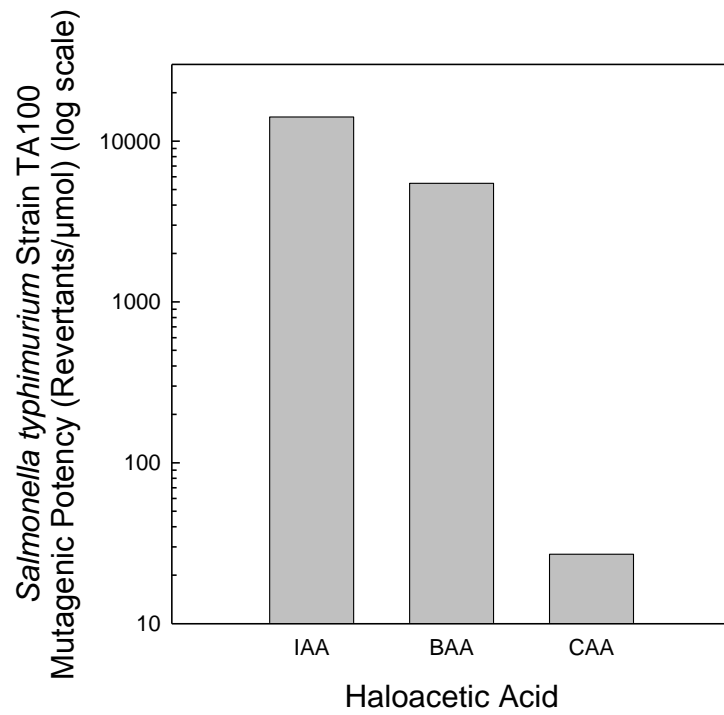
COMPARATIVE CYTOTOXICITY, GENOTOXICITY AND TERATOGENICITY OF THE MONOHALOACETIC ACIDS

From the published literature and results presented in this study, the commonality in biological response of the monoHAAs was observed; the rank order of adverse effects was iodo > bromo > chloro. This distribution of adverse biological activity was first noted by Hunter and colleagues measuring neural tube damage in mouse embryos (Richard and Hunter 1996; Hunter et al. 1996) (Figure 5.1). Our laboratory extended these studies to include cytotoxicity and genotoxicity in *S. typhimurium* (Plewa et al. 2002; Kargalioglu et al. 2002; Plewa et al. 2004) (Figure 5.2), mammalian cells (Plewa et al. 2004; Plewa et al. 2010) and human cells (Muellner et al. 2010; Attene-Ramos, Wagner, and Plewa 2010) (Figure 3.5). Recently point mutation in Chinese hamster cells by the monoHAAs was investigated (Zhang et al. 2010) (Figure 5.3). In all cases of cytotoxicity, genotoxicity, mutagenicity and teratogenicity, the rank order of induced, adverse biological responses remained iodo > bromo > chloro.



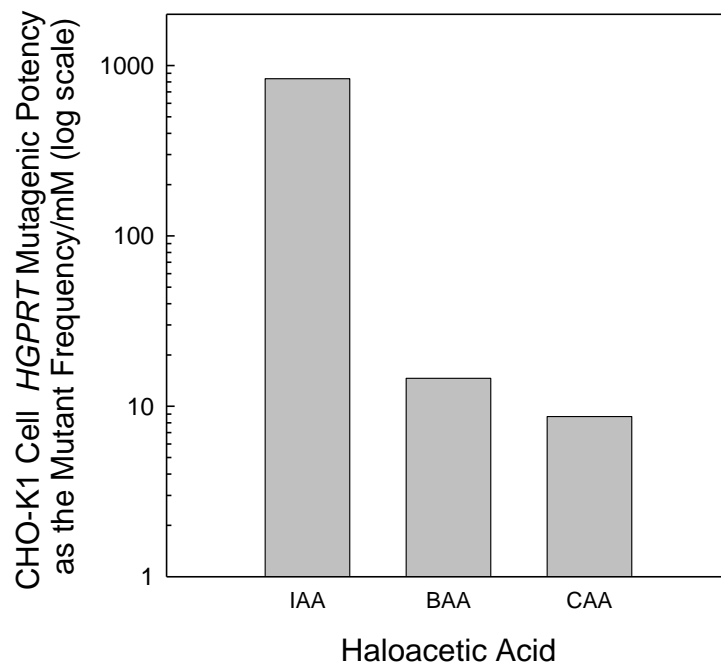
Source: Data from Richard and Hunter 1996.

Figure 5.1 MonoHAA induction of neural tube damage in mouse embryos. Benchmark concentration is the lower limit of the 95% confidence interval per M concentration of monoHAA required to produce 5% increase in number of embryos with neural tube defects.



Source: Data from Plewa et al. 2004.

Figure 5.2 MonoHAA induction of mutagenic potency in *S. typhimurium* strain TA100.



Source: Data from Zhang et al. 2010.

Figure 5.3 MonoHAA induction of mutagenic potency at the HGPRT locus in CHO-K1 cells.

CYTOTOXICITY AND GENOTOXICITY MEASUREMENTS ASSOCIATED WITH TOXICOGENOMIC EXPERIMENTS

We conducted a series of cytotoxicity studies using human FHs cells (Figure 2.2) with monoHAA concentrations that induced equivalent genotoxicity (20%, 40%, and 50% Tail DNA values) (Table 3.1) to ensure that the monoHAAs were not inducing excessively high levels of cell killing. Acute cell viability was determined with a vital dye method immediately after exposure; in parallel experiments the cell density was measured after removal of the monoHAA and an additional 24-h incubation in complete medium. For all monoHAA concentrations there was no increase in acute cytotoxicity (Figures 3.2-3.4). For the cells incubated 24 h after treatment, cell density was calculated as the percent of the concurrent negative control. In addition we microscopically investigated each well for floating (dead) cells. In all cases there was not an observable increase in detached cells as compared to the concurrent controls. The 24-h cell density data are presented in Figure 3.6. There was no decrease in relative cell density associated with a 30-min exposure to IAA, BAA or CAA followed by 24 h incubation in complete cell medium. There was a reduction in cell density in the 4-h treatments with higher concentrations of IAA and CAA; the lack of detached cells suggests this may be due to a reduction in cell cycle rather than cell killing. Based on equivalent genotoxic responses (SCGE 50% Tail DNA), lack of acute cytotoxicity, and 24-h cell density data, we chose IAA, BAA and CAA concentrations of 22 μ M, 57 μ M and 3.42 mM, respectively, for the toxicogenomic experiments (Table 3.1).

Concurrent SCGE analyses determined the genotoxicity induced in the FHs cells after exposure to each monoHAA. The data presented in Figure 5.4 demonstrates that the population of cells from which RNA was extracted expressed genomic DNA damage.

MONOHAA TREATMENT FOR TOXICOGENOMIC ANALYSES, RNA ISOLATION AND PURIFICATION

Four days prior to treatment, 4×10^5 FHs 74 Int cells were seeded in each well in six-well plates. After a 30 min or 4 h exposure to 22 μ M IAA, 57 μ M BAA or 3.42 mM CAA, cells were washed twice with HBSS, harvested, and centrifuged at $300 \times g$ for 5 min. An aliquot of each cell suspension was retained prior to centrifugation for acute cytotoxicity and SCGE analyses. The supernatant was removed and RNA isolated using a Qiagen RNeasy Mini Kit. DNase treatment of the RNA samples was conducted using Ambion DNA-free DNase and the RNA concentrations were determined using the NanoDrop 1000 from Thermo Fisher Scientific. The resulting genomic DNA-free RNA was concentrated by vacuum centrifugation for 15 min using the Speedvac system AE52010. RNA quantity was determined using the Agilent 2100 Bioanalyzer. RNA Integrity Numbers (RIN) were in the range from 8.2 to 9.9 (RNA quality for microarray analysis must have RIN values greater than 7) (Schroeder et al. 2006). High quality RNA is essential for qRT-PCR arrays. Figure 5.5 presents the nanodrop, electrophoresis of the RNA isolated from the control and IAA-treated FHs cells. The capillary electrophoresis analysis of the RNA isolated from each FHs cell sample in the IAA experiments is illustrated in Figure 5.6. The RNA concentration and purity (RIN values) for each monoHAA treatment group is presented in Table 5.1.

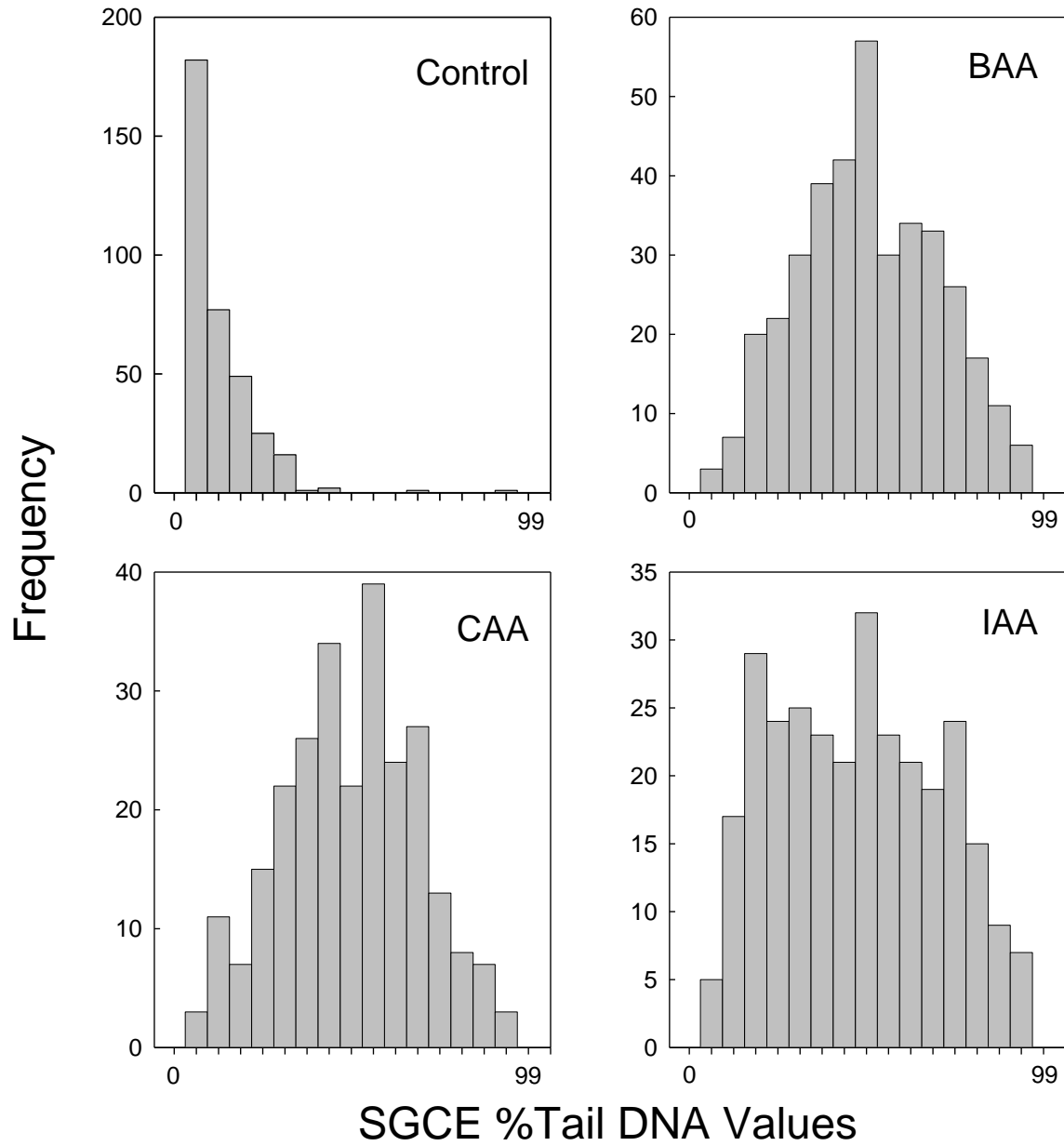


Table 5.1
RNA concentration and purity for each monoHAA treatment group

monoHAA Treatment Group	RNA Concentration Range (ng/ μ L)	RNA Integrity Number
30 min Control (IAA)	109 – 146	9.4 – 9.9
30 min IAA	214 – 287	9.7 – 9.9
4 h Control (IAA)	66 – 161	8.2 – 9.7
4 h IAA	190 – 214	9.7 – 9.8
30 min Control (BAA)	215 – 230	9.9 – 10.0
30 min BAA	280 – 343	9.9 – 10.0
4 h Control (BAA)	43 – 68	9.4 – 9.6
4 h BAA	28 – 259	8.4 – 9.9
30 min Control (CAA)	117 – 185	9.9 – 10.0
30 min CAA	138 – 235	9.8 – 10.0
4 h Control (CAA)	120 – 206	9.8 – 10.0
4 h CAA	94 – 232	9.8 – 10.0

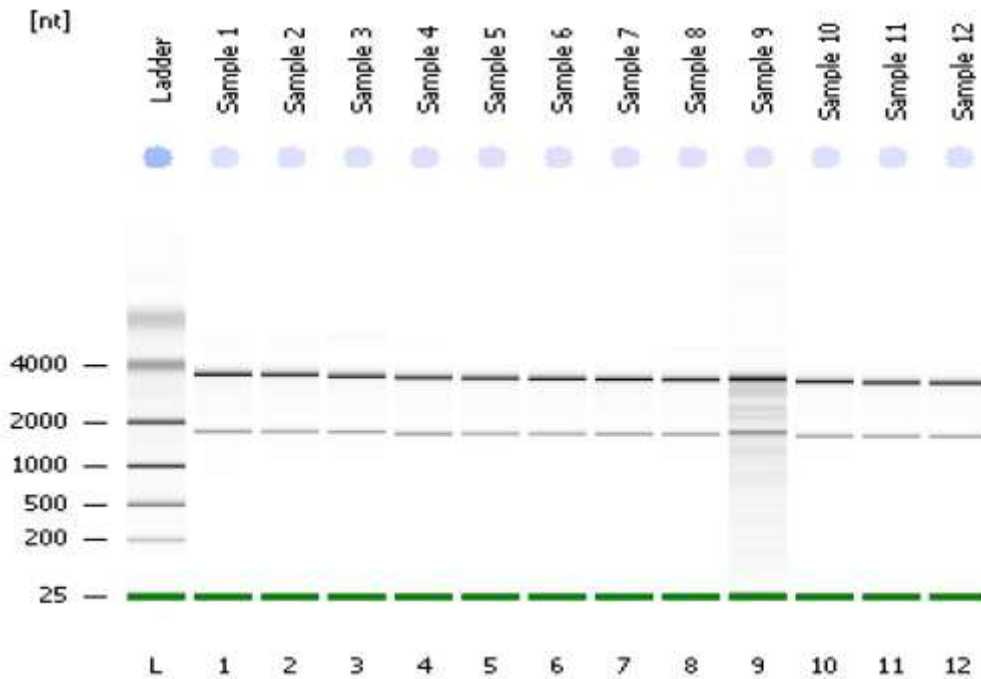


Figure 5.5 Electrophoresis of RNA samples isolated from control and FHs cells treated with IAA.

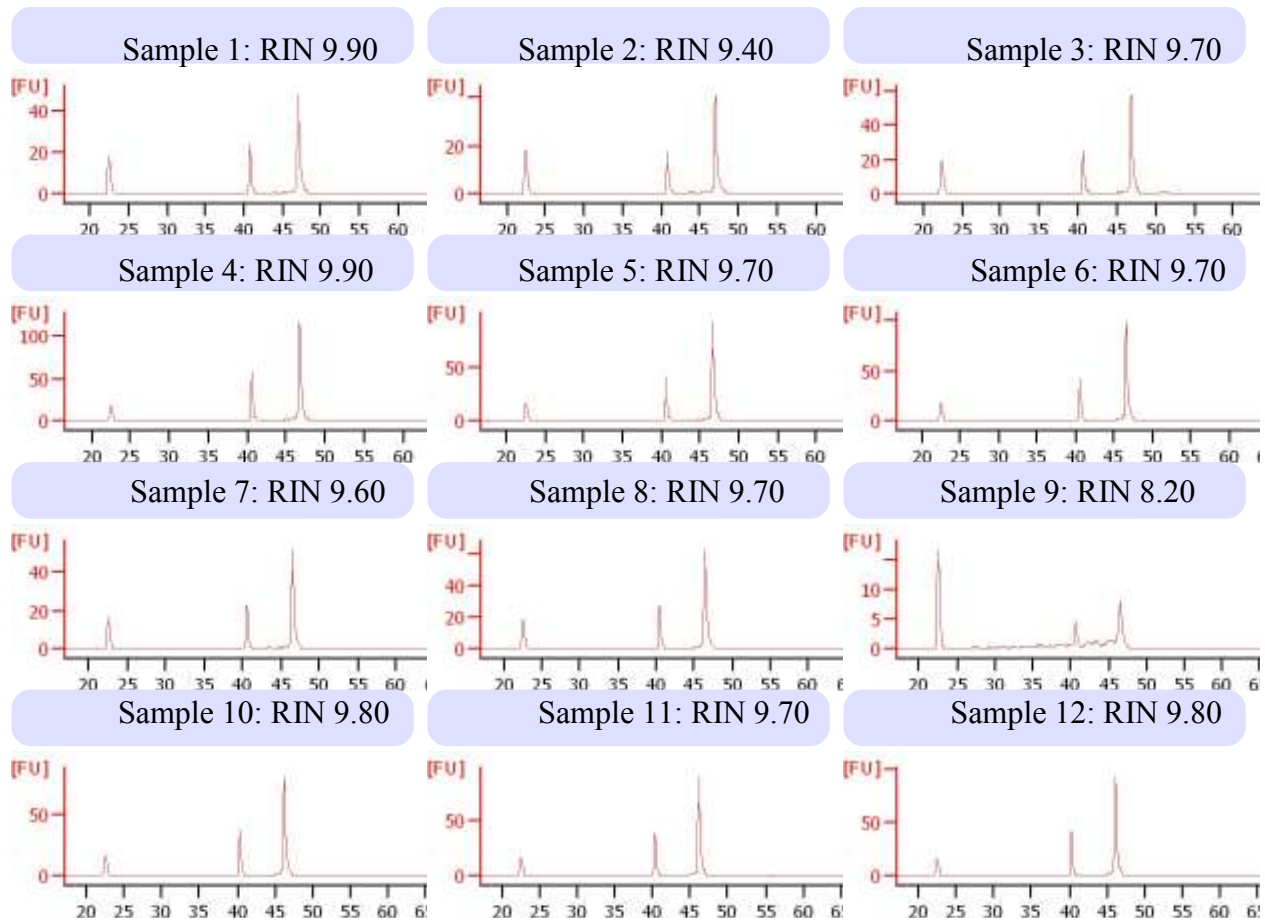


Figure 5.6 Capillary electrophoresis of RNA isolated from concurrent negative controls and IAA-treated human FHs cells. Note RIN values for RNA quality exceed the minimum value of 7.0.

cDNA SYNTHESIS

cDNAs were synthesized using the SuperArray RT² PCR Array First Strand Kit (Frederick, MD). RNA samples were diluted to a constant concentration for each monoHAA exposure. One μL of the P2 enzyme, from the SuperArray RT² PCR Array First Strand Kit, was added to the nuclease-free PCR tube containing the diluted RNA.

Using a MJ Research PTC-100 programmable thermocycler the annealing reaction was conducted at 70°C for 3 min and held on ice. The RT cocktail was prepared by mixing 10 μL of the annealing mixture with 10 μL of the RT cocktail. This mixture was incubated at 37°C for 60 min and heated to 95°C for 5 min to hydrolyze the RNA and inactivate the reverse transcriptase. The finished reaction was held on ice. After cDNA synthesis, the samples were diluted with 91 μL of nuclease free water and stored at -20°C.

QRT-PCR ARRAY

A DNA damage signaling focused pathway specific qRT-PCR array (APHS-029B) was employed for the quantitative comparison of the modulation of expression of human genes involved in DNA damage/DNA repair induced by the monoHAAs (Quellhorst et al. 2006). A flow diagram of the qRT-PCR methodology that we applied is presented in Figure 2.3. The human genes evaluated for their expression are listed in Table 2.2. An aliquot of the diluted first strand synthesis reaction was added to the SuperArray RT² Real-Time SYBR Green/ROX PCR master mix and nuclease-free H₂O. This cDNA/master mix cocktail was transferred to a sterile, nuclease free reservoir and 25 μ L were placed into each well of a pathway specific qRT-PCR array. Optical cap strips were tightly placed onto each column and the microplate was centrifuged. Quantitative real-time PCR analysis was conducted using a two-step cycling program on a Stratagene Mx3000p thermocycler. For each array we analyzed quality controls that measured genomic DNA contamination, reverse transcription efficiency, and PCR amplification efficiencies and these quality control parameters were within accepted limits.

COMPARATIVE ANALYSES OF HUMAN TRANSCRIPTOME PROFILES

Functional Grouping of Genes in the DNA Damage – DNA Repair qRT-PCR Array

The qRT-PCR gene array employed focused on gene function groups related to damaged DNA binding, DNA repair, cell cycle regulation and apoptosis (Table 2.2). Table 5.2 displays the gene in the qRT-PCR array according to functional group. The changes in gene expression induced by the monoHAAs as compared to their concurrent negative controls are listed in Table 5.3 (30 min exposure) and Table 5.4 (4 h exposure). The effects of CAA and BAA on gene modulation were greater at 4 h, both in terms of numbers of genes and in fold-changes from their controls. IAA affected approximately the same number of genes at both time points.

Human Transcriptome Profiles after MonoHAA Exposure

Figure 5.7 illustrates global gene expression changes for gene functional groups involving DNA damage/repair, cell cycle regulation and apoptosis for human FHs cells exposed to the monoHAAs. More genes exhibited altered expression after 4 h of exposure. Expression of 4 genes involved in the regulation of cell cycle and apoptosis were altered by all three monoHAAs (*MAP2K6* and *SESNI* (downregulated) and *DDIT3* and *IHPK3* (upregulated)). BAA and IAA expressed a similar pattern of gene expression changes when compared to CAA. Six genes were modulated by BAA and IAA; these genes are involved in DNA repair (*BTG2*, *XPA* and *DMC1*) and cell cycle regulation (*RBBP8*, *GADD45A* and *PPP1R15A*). *DMC1* encodes for a protein involved in dsDNA break repair. Both BAA and CAA downregulated the expression of *XRCC2*, while CAA and IAA downregulated the expression of *PCBP4*.

Transcriptome profiles impacted by the monoHAAs were predominantly with genes involved in dsDNA break repair, cell cycle arrest and apoptosis regulation (Figure 5.7). Genes modulated by structurally-related genotoxins may increase our understanding of the type of DNA damage generated and subsequent DNA repair. Figure 5.8 illustrates the distribution of altered gene expression for each monoHAA within gene functional groups. The similarity of altered gene expression is striking. All three monoHAAs modulated the expression of genes involved in

dsDNA break repair. Other types of DNA repair genes were impacted but with fewer numbers involved. The induction of oxidative stress may be one mechanism of HAA-associated genotoxicity (Cemeli et al. 2006); this is consistent with the altered expression of *PNKP* (Tables 5.3 and 5.4). Most oxidative stress-induced DNA lesions tend to be rapidly repaired except for dsDNA breaks (Shrivastav, De Haro, and Nickoloff 2008). These lesions are very toxic/mutagenic and require more time for repair (Helleday et al. 2007). Recently we determined the DNA repair kinetics for lesions induced by these monoHAAs (Komaki et al. 2009); they required extended times for DNA repair as compared to lesions induced by ethylmethanesulfonate, H₂O₂ or bulky-adducts (Rundell, Wagner, and Plewa 2003).

Table 5.2

SuperArray PAHS-029 gene array with genes assigned to functional groups	
Gene Functional Group	Genes in SuperArray DNA Damage/Repair Pathway (PAHS-029)
Apoptosis	<i>ABL1, BRCA1, CIDEA, GADD45A, GADD45G, GML, IHPK3, PCBP4, AIFM1 (PDCD8), PPP1R15A, RAD21, TP53, TP73</i>
Cell Cycle Arrest	<i>CHEK1, CHEK2, DDIT3 (CHOP), GADD45A, GML, GTSE1, HUS1, MAP2K6, MAPK12, PCBP4, PPP1R15A, RAD17, RAD9A, SESN1, ZAK</i>
Cell Cycle Checkpoint	<i>ATR, BRCA1, FANCG, NBN (NBS1), RAD1, RBBP8, SMC1A (SMC1L1), TP53</i>
Damaged DNA Binding	<i>ANKRD17, BRCA1, DDB1, DMC1, ERCC1, FANCG, FEN1, MPG, MSH2, MSH3, N4BP2, NBN (NBS1), OGG1, PMS2L3 (PMS2L9), PNKP, RAD1, RAD18, RAD51, RAD51L1, REV1 (REV1L), SEMA4A, XPA, XPC, XRCC1, XRCC2, XRCC3</i>
Base-excision Repair	<i>APEX1, MBD4, MPG, MUTYH, NTHL1, OGG1, UNG</i>
Double strand DNA Break Repair	<i>CIB1, FEN1, XRCC6 (G22P1), XRCC6BP1 (KUB3), MRE11A, NBN (NBS1), PRKDC, RAD21, RAD50</i>
Mismatch Repair	<i>ABL1, ANKRD17, EXO1, MLH1, MLH3, MSH2, MSH3, MUTYH, N4BP2, PMS1, PMS2, PMS2L3 (PMS2L9), TP73, TREX1</i>
Other DNA Repair Genes	<i>APEX2, ATM, ATRX, BTG2, CCNH, CDK7, CRY1, ERCC2 (XPD), GTF2H1, GTF2H2, IGHMBP2, LIG1, MNAT1, PCNA, RPA1, SUMO1</i>

Repressing cell division is critical to repair genomic DNA damage. A longer treatment time was associated with a reduction in cell density by 4 h treatments with CAA and IAA (Figure 3.6). A longer treatment time was also associated with increased numbers of genes with altered expression especially those involved in cell cycle regulation and apoptosis (Tables 5.3 and 5.4) (Figure 5.7). The reduction in cell density was not due to cytotoxicity because the mRNAs were isolated from viable cells. An increase in cell cycle arrest (Figures 5.8 and 5.9) was implicated as an explanation for this reduction.

We analyzed transcriptome profiles using the Database for Annotation, Visualization and Integrated Discovery (DAVID) (Huang, Sherman, and Lempicki 2009). The majority of the modulated genes were functionally categorized as genes responding to DNA damage or regulating cell cycle or apoptosis. Genes were assigned to different pathways as defined by

Biocarta or the Kyoto Encyclopedia of Genes and Genomes (KEGG) (Table 5.5). All of the treatments with one exception (CAA, 30 min) modulated genes involved in the ATM signaling pathway (Powers et al. 2004). Other modulated pathways include MAPK and p53 signaling (IAA 30 min and 4 h and BAA 4 h) and BRCA1, BRCA2 and ATR. These latter pathways highlight the involvement of dsDNA break repair to monoHAA-induced genomic insult. Similar to the gene functional annotations, all of these pathways are involved in stress response to DNA damage and regulate different stages in cell cycle progression or apoptosis.

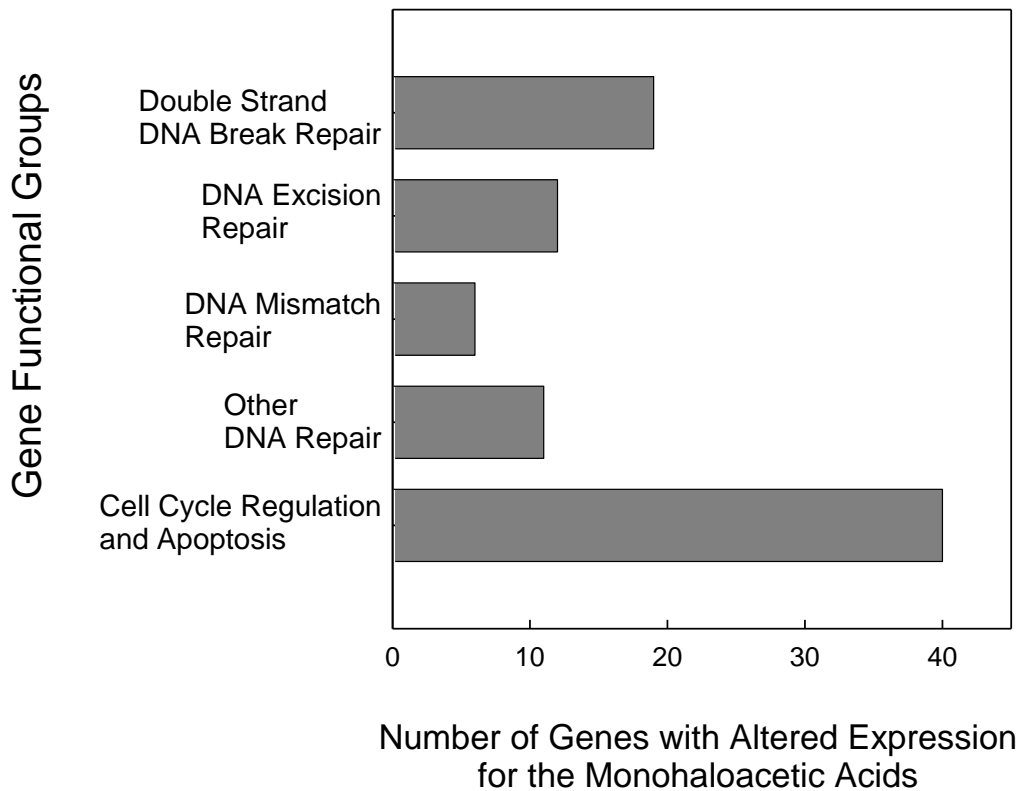


Figure 5.7 Global gene expression changes for gene functional groups involving DNA damage/repair, cell cycle regulation and apoptosis for human FHs cells exposed to the monoHAAs.

Table 5.3
Changes in gene expression from concurrent negative controls after 30 min of monoHAA exposure

Altered Gene Expression	Gene Function	BAA		CAA		IAA	
		×-Change	<i>P</i> Value	×-Change	<i>P</i> Value	×-Change	<i>P</i> Value
		BAA, CAA & IAA					
<i>PPP1R15A</i>	Apoptosis, cell cycle arrest	-1.71	0.0041	-1.25	0.0290	-3.67	0.0023
<i>XRCC3</i>	dsDNA break repair	-2.86	0.0001	-1.36	0.0077	-2.64	0.0125
		CAA & IAA					
<i>PNKP</i>	Damaged DNA binding, dsDNA break repair			-1.36	0.0023	3.79	0.0021
		Single monoHAA					
<i>HUS1</i>	Cell cycle arrest	-2.97	0.0001				
<i>SEMA4A</i>	Damaged DNA binding	-2.27	0.0004				
<i>MRE11A</i>	dsDNA break repair	-1.78	0.0168				
<i>ATM</i>	dsDNA break repair	-1.58	0.0298				
<i>PMS2L3</i>	Damaged DNA binding	-1.45	0.0367				
<i>RAD9A</i>	Cell cycle arrest, DNA excision repair	-1.44	0.0399				
<i>EXO1</i>	DNA mismatch repair	1.25	0.0004				
<i>XPC</i>	Damaged DNA binding, DNA excision repair			-1.35	0.0449		
<i>RAD50</i>	dsDNA break repair					-5.27	0.0001
<i>PCBP4</i>	Apoptosis, cell cycle arrest, damaged DNA binding					-4.44	0.0001
<i>IGHMBP2</i>	Damaged DNA binding					-3.53	0.0021
<i>ERCC1</i>	Damaged DNA binding					-3.09	0.0108
<i>FEN1</i>	Damaged DNA binding, DNA excision repair					-2.88	0.0224
<i>MAPK12</i>	Cell cycle arrest					-2.58	0.0339
<i>GADD45A</i>	Apoptosis, cell cycle arrest					-2.53	0.0243
<i>MUTYH</i>	Base excision DNA repair, mismatch repair					-2.52	0.0267
<i>SESN1</i>	Cell cycle arrest					1.33	0.0474
<i>DDIT3</i>	Cell cycle arrest					1.50	0.0363

(continued)

Table 5.3 (Continued)

Altered Gene Expression	Gene Function	×-Change BAA	<i>P</i> Value BAA	×-Change CAA	<i>P</i> Value CAA	×-Change IAA	<i>P</i> Value IAA
<i>TREX1</i>	DNA mismatch repair, dsDNA break repair					1.52	0.0394
<i>MBD4</i>	Base excision DNA repair, DNA mismatch repair					1.59	0.0144
<i>GTF2H1</i>	DNA excision repair					1.71	0.0155
<i>MLH1</i>	DNA mismatch repair					1.79	0.0051
<i>UNG</i>	DNA excision repair					1.89	0.0037

Source: Reprinted with permission from Attene-Ramos, M. S.; Wagner, E. D.; Plewa, M. J., *Environ. Sci. Technol.* 2010, 44, (19), 7206-7212. Copyright 2010, American Chemical Society.

Table 5.4
Changes in gene expression from concurrent negative controls after 4 h of monoHAA exposure

Altered Gene Expression	Gene Function	BAA		CAA		IAA	
		×-Change	P Value	×-Change	P Value	×-Change	P Value
		BAA, CAA & IAA					
<i>MAP2K6</i>	Cell cycle arrest	-5.98	0.0001	-6.22	0.0001	-4.55	0.0001
<i>SESN1</i>	Cell cycle arrest	-3.84	0.0006	-1.63	0.0211	-3.31	0.0005
<i>DDIT3</i>	Cell cycle arrest	1.53	0.0245	4.19	0.0001	2.60	0.0405
<i>IHPK3</i>	Apoptosis, cell cycle arrest	3.04	0.0001	5.05	0.0001	2.06	0.0001
		BAA & CAA					
<i>XRCC2</i>	Damaged DNA binding, dsDNA break repair	-3.59	0.0006	-1.61	0.0380		
		BAA & IAA					
<i>BTG2</i>	DNA damage repair, excision repair	-2.09	0.0148			-4.33	0.0001
<i>XPA</i>	Damaged DNA binding	-2.08	0.0087			-1.91	0.0280
<i>RBBP8</i>	Cell cycle checkpoint	1.60	0.0171			1.39	0.0186
<i>GADD45A</i>	Apoptosis, cell cycle arrest	2.28	0.0007			1.91	0.0004
<i>PPP1R15A</i>	Apoptosis, cell cycle arrest	2.79	0.0002			1.40	0.0163
<i>DMC1</i>	Damaged DNA binding, dsDNA break repair	2.79	0.0002			1.47	0.0161
		CAA & IAA					
<i>PCBP4</i>	Apoptosis, cell cycle arrest			-1.68	0.0424	-1.82	0.0374
		Single monoHAA					
<i>GTF2H2</i>	DNA excision repair	-2.02	0.0126				
<i>OGG1</i>	Damaged DNA binding, base excision repair	-1.91	0.0260				
<i>BRCA1</i>	Damaged DNA binding, dsDNA break repair	-1.83	0.0373				
<i>MRE11A</i>	dsDNA break repair	-1.83	0.0401				
<i>PMS1</i>	DNA mismatch repair	-1.82	0.0374				
<i>CHEK2</i>	Cell cycle checkpoint	1.63	0.0245				
<i>SEMA4A</i>	Damaged DNA binding	2.70	0.0002				
<i>XRCC3</i>	Damaged DNA binding, dsDNA break repair			-2.61	0.0006		
<i>MUTYH</i>	DNA excision repair, mismatch repair			-2.22	0.0010		

(continued)

Table 5.4 (Continued)

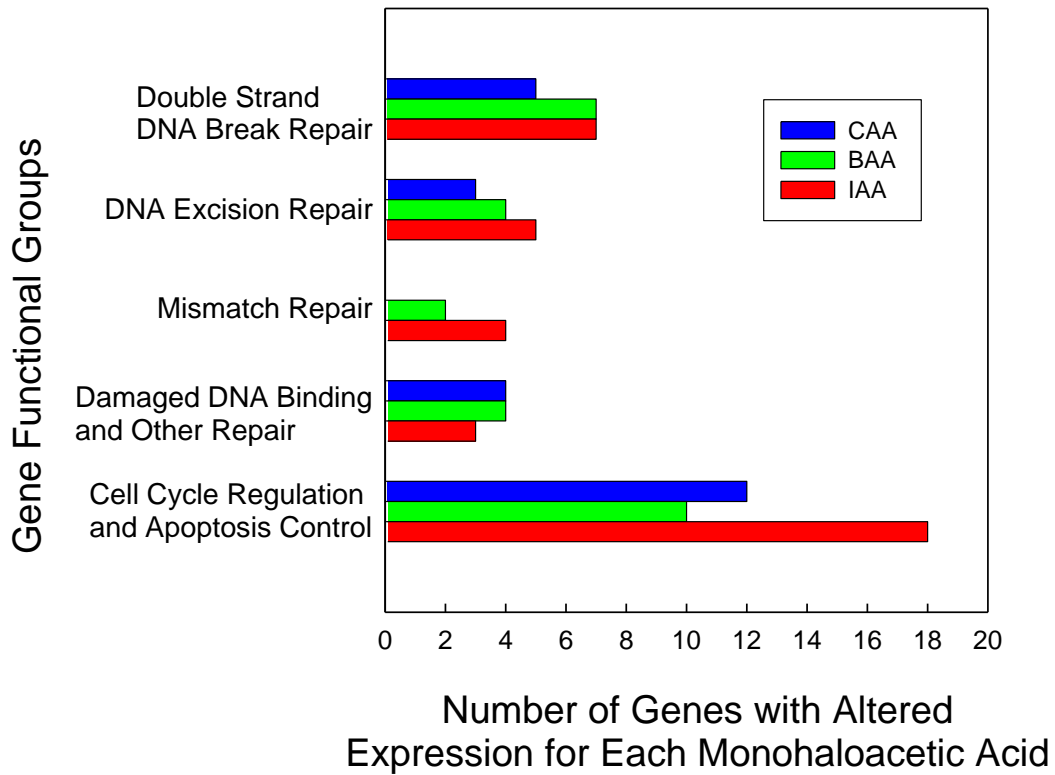
Altered Gene Expression	Gene Function	×-Change BAA	P Value BAA	×-Change CAA	P Value CAA	×-Change IAA	P Value IAA
<i>PNKP</i>	dsDNA break repair, cell cycle arrest			-2.09	0.0045		
<i>LIG1</i>	DNA damage repair			-1.78	0.0199		
<i>IGHMBP2</i>	Damaged DNA binding			-1.69	0.0439		
<i>FEN1</i>	Damaged DNA binding			-1.58	0.0477		
<i>ABL1</i>	Apoptosis, cell cycle arrest			1.26	0.0471		
<i>CDK7</i>	Cell cycle arrest, DNA damage repair			1.28	0.0443		
<i>RAD9A</i>	Cell cycle arrest, DNA excision repair			1.29	0.0311		
<i>TP73</i>	Apoptosis, cell cycle arrest			1.29	0.0404		
<i>CCNH</i>	Cell cycle arrest			1.34	0.0252		
<i>CRY1</i>	Cell cycle arrest			1.38	0.0146		
<i>ANKRD17</i>	Damaged DNA binding			1.51	0.0035		
<i>NBN</i>	Cell cycle checkpoint, dsDNA break repair					-3.13	0.0373
<i>N4BP2</i>	Damaged DNA binding, dsDNA break repair					-2.88	0.0012
<i>XPC</i>	Damaged DNA binding, excision repair					-2.10	0.0093
<i>MAPK12</i>	Cell cycle arrest					-1.81	0.0405
<i>GML</i>	Apoptosis, cell cycle arrest					1.30	0.0327
<i>EXO1</i>	DNA mismatch repair					1.69	0.0032
<i>GTSE1</i>	Cell cycle arrest					2.19	0.0001

Source: Reprinted with permission from Attene-Ramos, M. S.; Wagner, E. D.; Plewa, M. J., Environ. Sci. Technol. 2010, 44, (19), 7206-7212. Copyright 2010, American Chemical Society.

Table 5.5
MonoHAA-induced transcriptome profiles analyzed using the Database for
Annotation, Visualization and Integrated Discovery

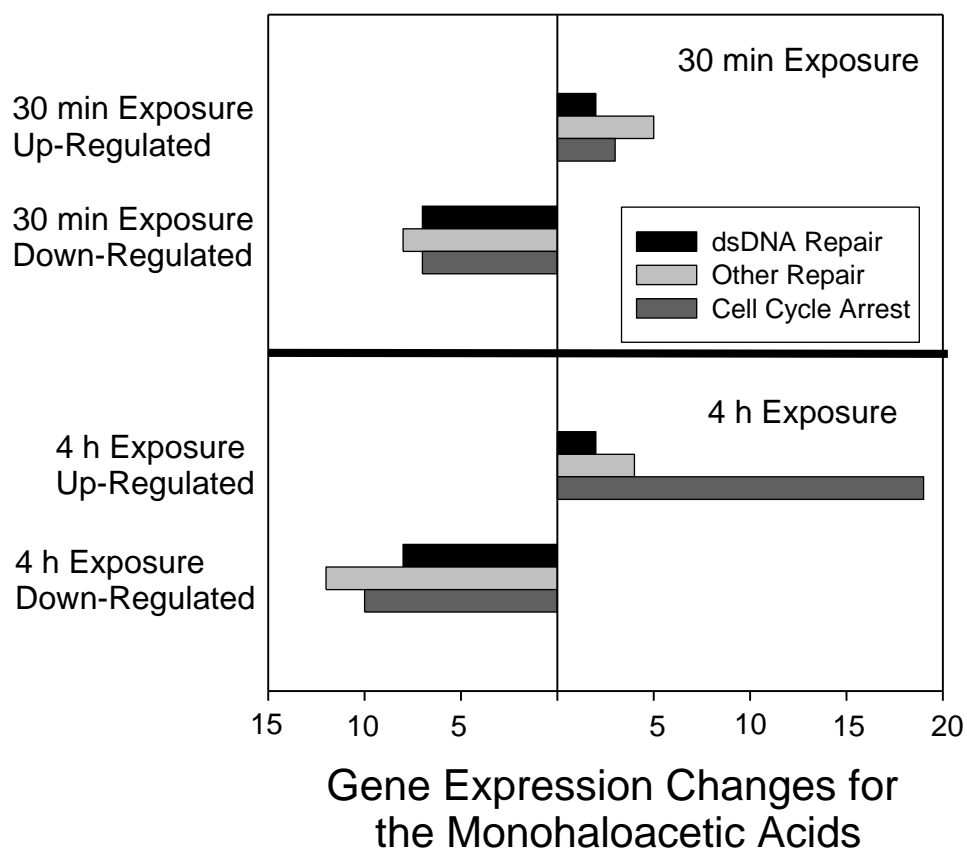
Pathway	BAA 30 min	CAA 30 min	IAA 30 min	BAA 4 h	CAA 4 h	IAA 4 h
ATM signaling pathway	X		X	X	X	X
Cell cycle control				X	X	
Cyclins and cell cycle regulation					X	
FC Epsilon RI signaling pathway						X
MAPK signaling pathway			X	X		X
p53 signaling pathway			X	X		X
Role of BRCA1, BRCA2 and ATR in cancer susceptibility and dsDNA repair pathways	X		X	X	X	

Source: Reprinted with permission from Attene-Ramos, M. S.; Wagner, E. D.; Plewa, M. J., *Environ. Sci. Technol.* 2010, 44, (19), 7206-7212. Copyright 2010, American Chemical Society.



Source: Reprinted with permission from Attene-Ramos, M. S.; Wagner, E. D.; Plewa, M. J., *Environ. Sci. Technol.* 2010, 44, (19), 7206-7212. Copyright 2010, American Chemical Society.

Figure 5.8 Changes in gene expression within gene functional groups in human FHs cells induced by BAA, CAA, or IAA



Source: Reprinted with permission from Attene-Ramos, M. S.; Wagner, E. D.; Plewa, M. J., *Environ. Sci. Technol.* 2010, 44, (19), 7206-7212. Copyright 2010, American Chemical Society.

Figure 5.9 Changes in gene expression in human FHs cells induced by the monoHAAs as a function of treatment time

In summary the monoHAAs, IAA, BAA and CAA are toxic disinfection byproducts. *In vitro* toxicological end points were integrated with DNA damage and repair pathway-focused toxicogenomic analyses to evaluate monoHAA-induced alterations of gene expression in normal, embryonic, nontransformed human cells. When compared to concurrent control transcriptome profiles, metabolic pathways involved in the cellular responses to toxic agents were identified and provided insight into the biological mechanisms of toxicity. Using the Database for Annotation, Visualization and Integrated Discovery to analyze the gene array data, the majority of the altered transcriptome profiles were associated with genes responding to DNA damage or those regulating cell cycle or apoptosis. The major pathways involved with altered gene expression were ATM, MAPK, p53, BRCA1, BRCA2, and ATR. These latter pathways highlight the involvement of DNA repair, especially the repair of double strand DNA breaks. All

of the resolved pathways are involved in human cell stress response to DNA damage and regulate different stages in cell cycle progression or apoptosis.

CHAPTER 6

REPAIR KINETICS OF DNA DAMAGE INDUCED BY THE MONOHALOACETIC ACIDS

INTRODUCTION

In order to reduce exposure to toxic DBPs, the U.S. EPA promulgated the Stage 1 Disinfectants and Disinfection Byproducts Rule (DBPR) in 1998 (U. S. Environmental Protection Agency 1998) and the Stage 2 DBPR in 2006 (U. S. Environmental Protection Agency 2006). In chlorinated water, haloacetic acids (HAAs) are the second most common class of DBPs (Krasner et al. 2006). The sum of five HAAs (monochloro-, dichloro-, trichloro-, monobromo- and dibromoacetic acid) is regulated by the U.S. EPA Stage 1 and Stage 2 DBPR at a permissible level of 60 µg/L (U. S. Environmental Protection Agency 1998, 2006).

The occurrence, genotoxicity and carcinogenicity of the HAAs were recently reviewed (Richardson et al. 2007). All five regulated HAAs were mutagenic in bacteria, induced genomic DNA damage in mammalian cells *in vitro* (Plewa et al. 2010) and induced point mutations in mammalian cells (Zhang et al. 2010). Among the three monoHAAs, IAA was the most cytotoxic and genotoxic followed by BAA and finally CAA (Plewa et al. 2002; Plewa et al. 2004; Zhang et al. 2010; Plewa et al. 2010). The rank order of the toxicity of these monoHAAs was correlated with their electrophilic reactivity and the carbon-halogen bond dissociation energy Table 1.1 (Plewa et al. 2004). The rank order of teratogenic potency (neural tube developmental defects in mouse embryos) was IAA > BAA > CAA (Richard and Hunter 1996; Hunter et al. 1996). Halogenated acetic acids containing bromine atoms were consistently more toxic and more genotoxic than the corresponding chlorine-substituted acids (Richardson et al. 2007).

Although there are many studies on the induction of DNA damage by DBPs, little information exists on the repair of DBP-induced DNA lesions (Liviak, Creus, and Marcos 2009, 2009). Currently in the literature there is no systematic analysis of the DNA repair kinetics of regulated DBPs nor is there an example of correlating chemical structure activity relationships and repair. One aim of this research was to characterize the genotoxicity induced by these related monoHAAs in mammalian cells and determine the kinetics of DNA repair. We employed monoHAA concentrations that induced approximately equivalent genotoxic effects. Our hypothesis was that if DNA lesions induced by these monoHAAs were similar, then no statistical difference would be observed in the kinetics of DNA repair. However, if the different halogen atoms (I, Br, Cl) induced different DNA lesions, then the DNA repair kinetics would be significantly different (Komaki et al. 2009).

COMPARATIVE ANALYSES OF DNA REPAIR KINETICS

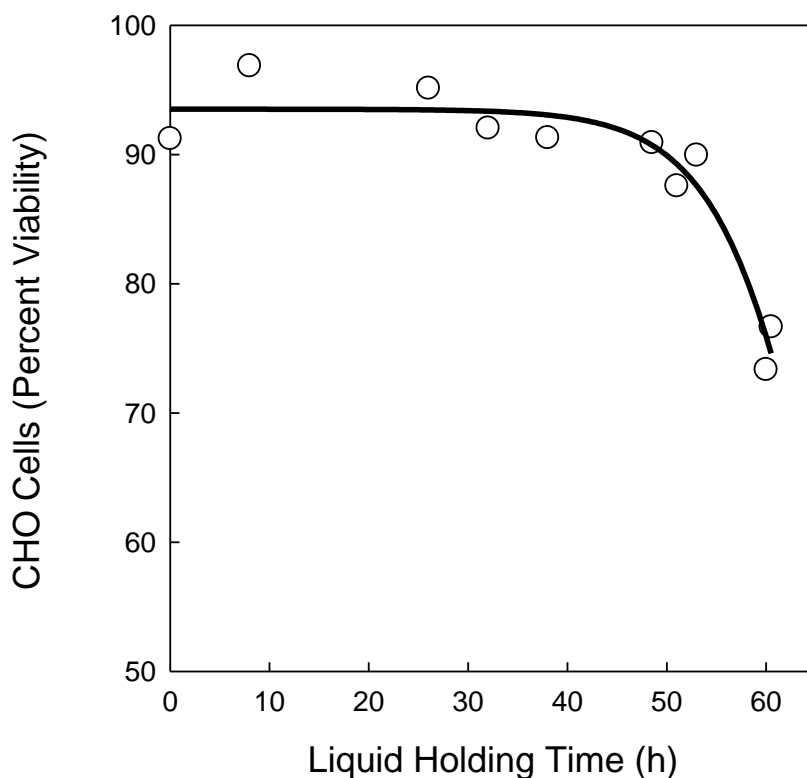
The day before treatment, CHO cells were plated at a titer of 2×10^4 cells in 200 µL of F12 + 5% FBS medium per well in a sterile flat-bottom 96-well microplate. On the next day, the cells were washed with HBSS and treated with the monoHAAs in F12 medium without FBS in a total volume of 25 µL for 4 h at 37°C, 5% CO₂. The wells were covered with AlumnaSeal™. The concentrations of the HAAs for the DNA repair studies were first determined so that the same level of genomic DNA damage was induced. The treatment concentrations were 25 µM IAA, 60 µM BAA, or 6 mM CAA. After treatment, the solution was aspirated from the wells and the cells were washed 2× with HBSS. The cells from one well were immediately harvested and

microgels were prepared for the determination of DNA damage with no time for repair. F12 medium without FBS (100 μ L) was added to the other wells, and the microplate was returned to the incubator for designated times. This recovery period (liquid holding time) allowed for DNA repair.

The monoHAAs used in this research induced genomic DNA damage in CHO cells. In this experimental design the concentration of each monoHAA was selected to induce approximately the same level of genotoxic damage. The % tail DNA for each monoHAA at 0-time liquid holding was normalized to a value of 100%. This allowed for a direct comparison of the rates of DNA repair among the three monoHAAs.

Liquid Holding Time and Cytotoxicity

We determined the cell viability throughout a 60 h time period with CHO cells maintained under liquid holding conditions (F12 medium without FBS). Over 50 h of liquid holding time was needed to cause a decline in CHO cell viability (Figure 6.1). There was no decrease in viability during the 24-h liquid holding timeframe for the DNA repair experiments.

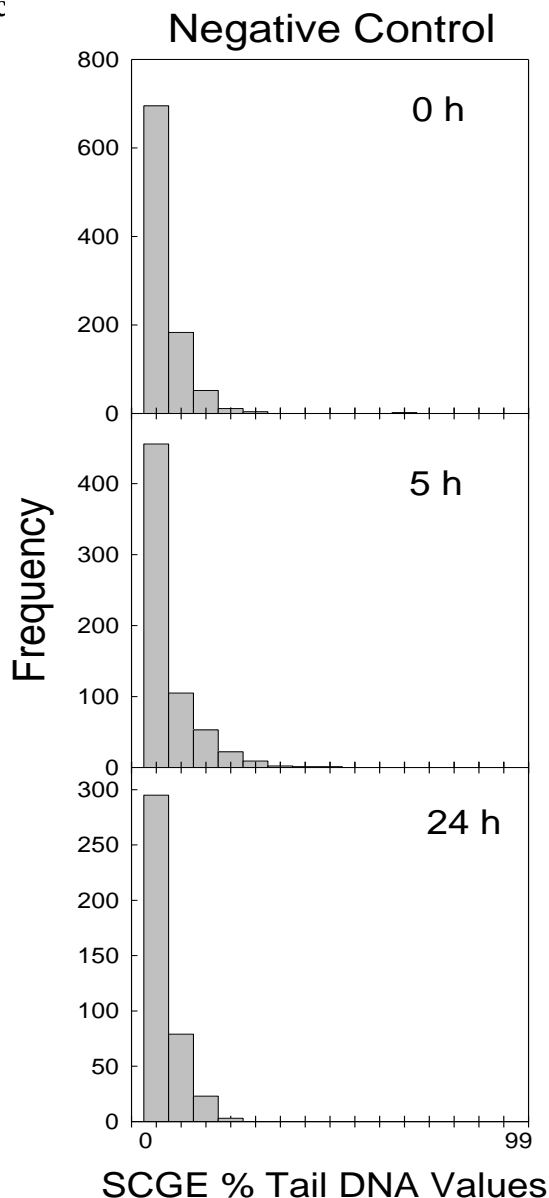


Source: Reprinted with permission from Komaki, Y.; Pals, J.; Wagner, E. D.; Marinas, B. J.; Plewa, M. J., *Environ. Sci. Technol.* 2009, 43, (21), 8437–8442. Copyright 2007, American Chemical Society.

Figure 6.1 CHO cell viability throughout a 60 h time period with cells maintained under liquid holding conditions (F12 medium without FBS).

DNA Repair Kinetics

DNA repair kinetics was determined for IAA, BAA, and CAA using SCGE and a liquid-holding protocol (Tice et al. 2000; Rundell, Wagner, and Plewa 2003). A distribution of genomic DNA damage was generated for each monoHAA. The negative control distributions at holding times of 0, 5 h and 24 h are presented in Figure 6.2. No significant difference was observed among the three negative c



Source: Reprinted with permission from Komaki, Y.; Pals, J.; Wagner, E. D.; Marinas, B. J.; Plewa, M. J., Environ. Sci. Technol. 2009, 43, (21), 8437–8442. Copyright 2007, American Chemical Society.

Figure 6.2 Histograms illustrating the distributions of SCGE % tail DNA values from the CHO cell negative controls at 0 h, 5 h and 24 h liquid-holding recovery.

The distributions of genomic DNA damage for the monoHAAs at the 0-h liquid holding recovery period (no re

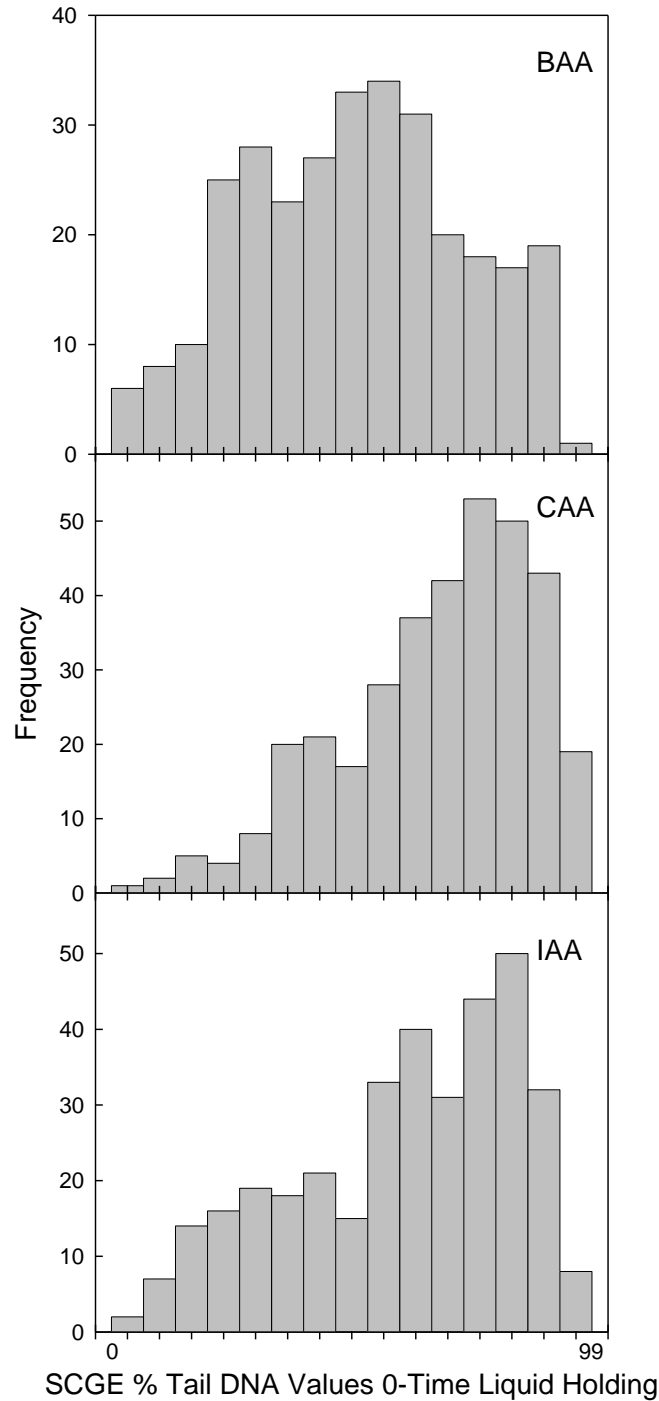


Figure 6.3 Histograms illustrating the distributions of SCGE % tail DNA values from CHO cells treated with bromoacetic acid (BAA), chloroacetic acid (CAA) and iodoacetic acid (IAA) at 0-h liquid-holding recovery.

The distributions of genomic DNA damage for the monoHAAs at the 1-h liquid holding recovery period is presented in Figure 6.4.

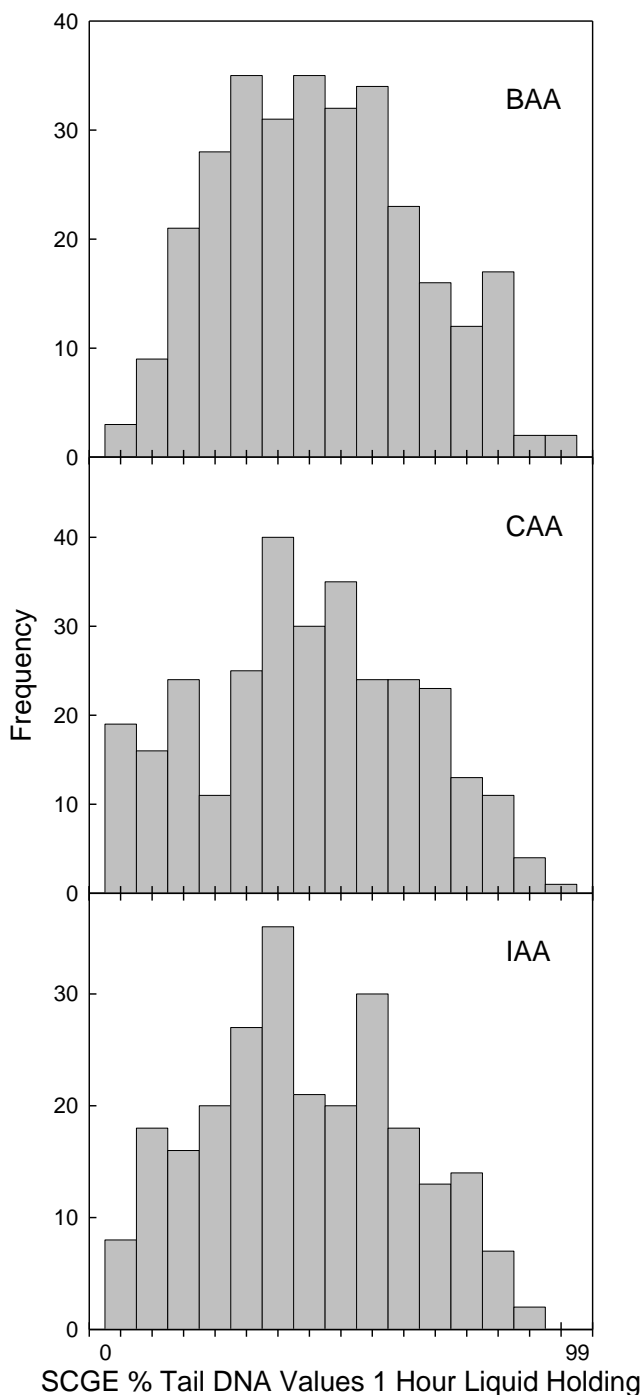


Figure 6.4 Histograms illustrating the distributions of SCGE % tail DNA values from CHO cells treated with bromoacetic acid (BAA), chloroacetic acid (CAA) and iodoacetic acid (IAA) at 1-h liquid-holding recovery.

The distributions of genomic DNA damage for the monoHAAs at the 2-h liquid holding recovery period is presented in Figure 6.5.

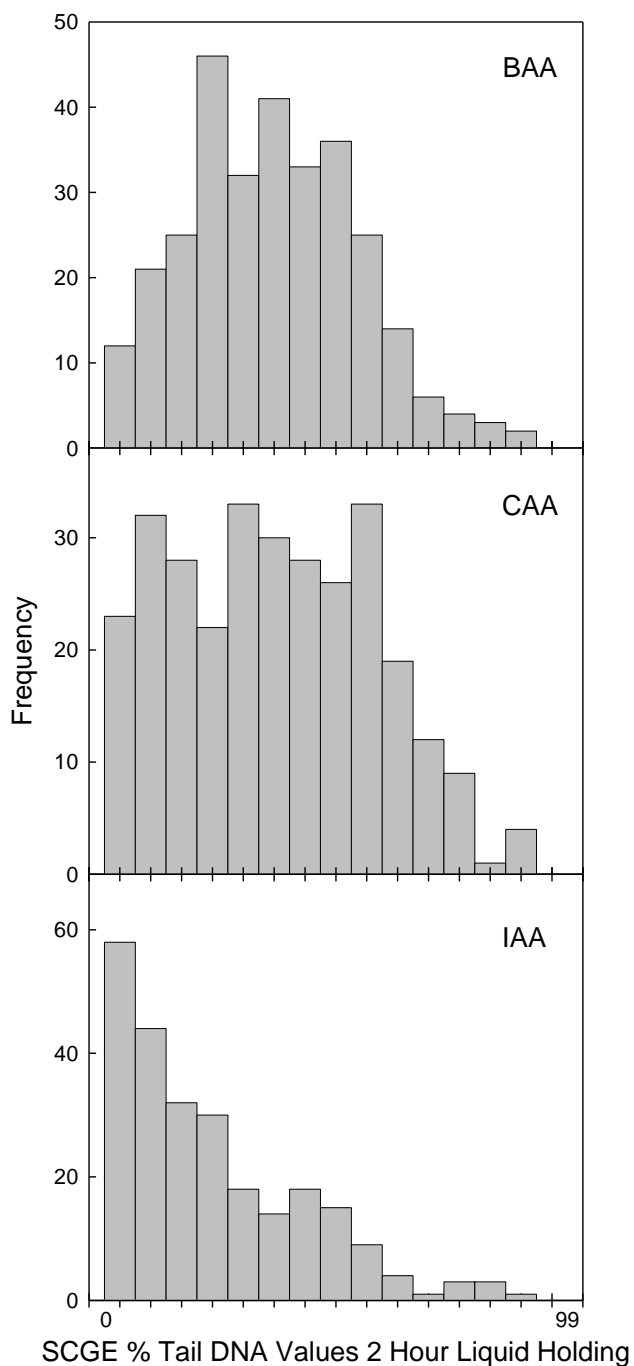


Figure 6.5 Histograms illustrating the distributions of SCGE % tail DNA values from CHO cells treated with bromoacetic acid (BAA), chloroacetic acid (CAA) and iodoacetic acid (IAA) at 2-h liquid-holding recovery.

The distributions of ge
period is presented in l

l holding recovery

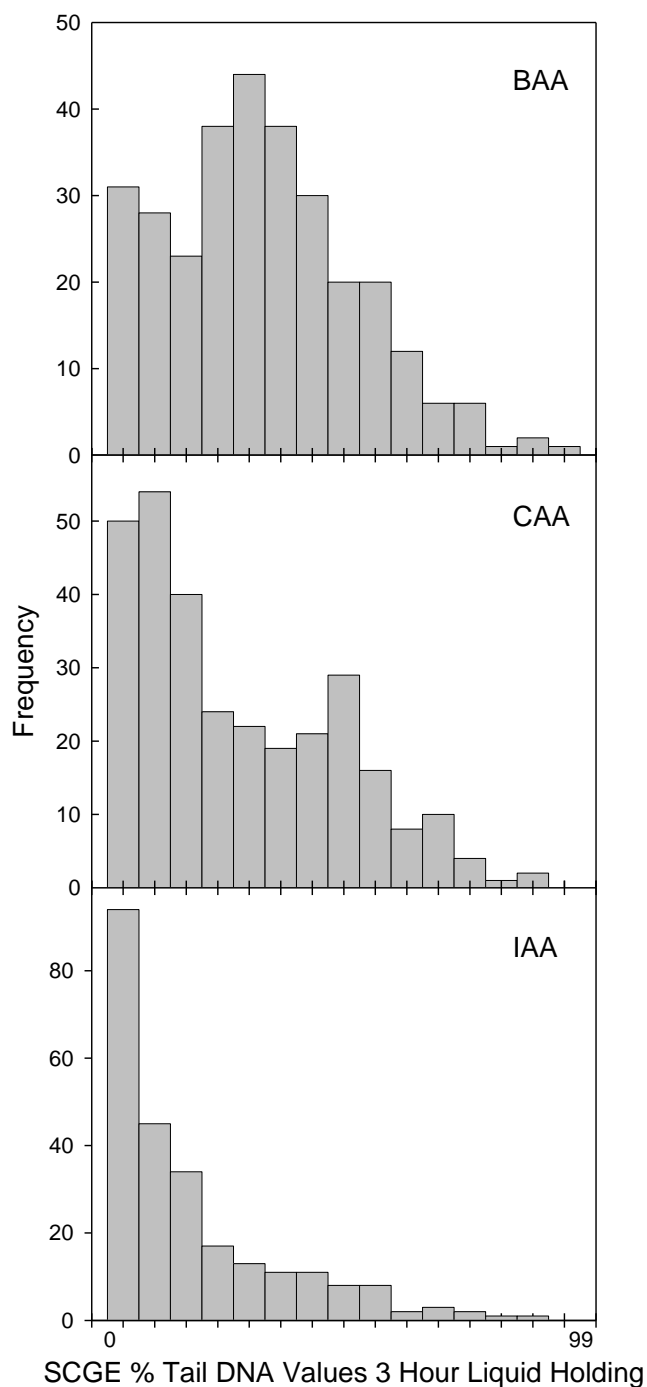


Figure 6.6 Histograms illustrating the distributions of SCGE % tail DNA values from CHO cells treated with bromoacetic acid (BAA), chloroacetic acid (CAA) and iodoacetic acid (IAA) at 3-h liquid-holding recovery.

The distributions of ger period is presented in F

1 liquid holding recovery

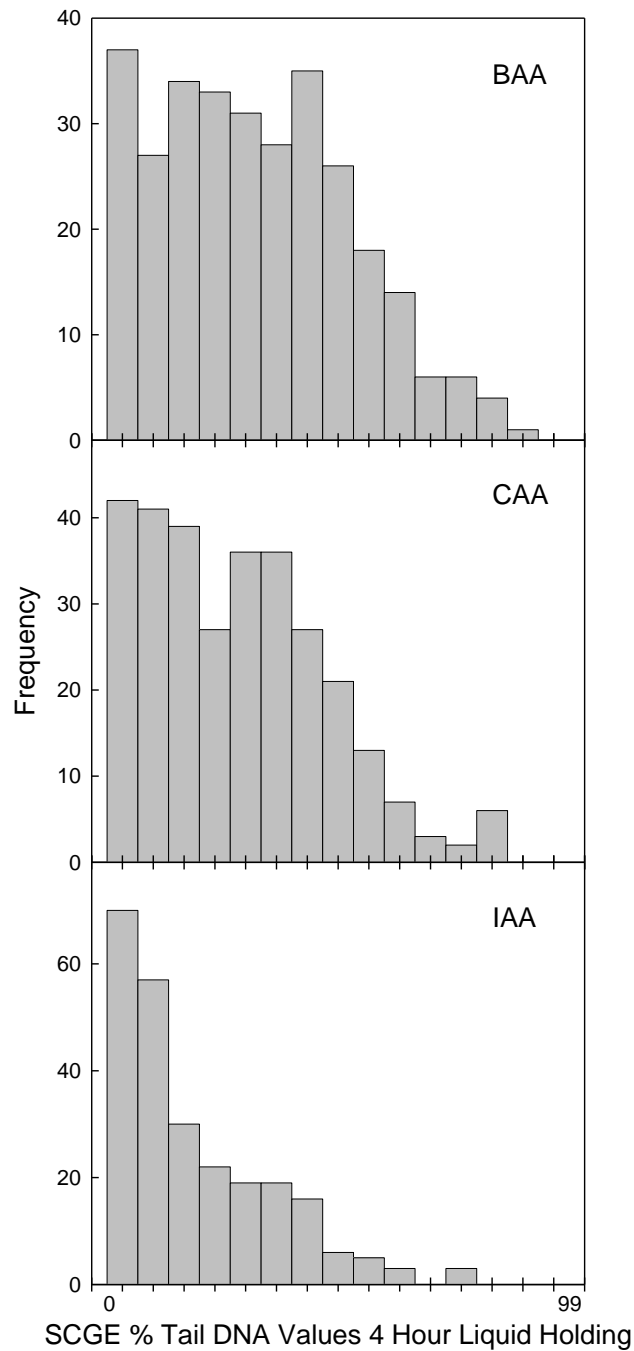


Figure 6.7 Histograms illustrating the distributions of SCGE % tail DNA values from CHO cells treated with bromoacetic acid (BAA), chloroacetic acid (CAA) and iodoacetic acid (IAA) at 4-h liquid-holding recovery.

The distributions of g_i period is presented in

quid holding recovery

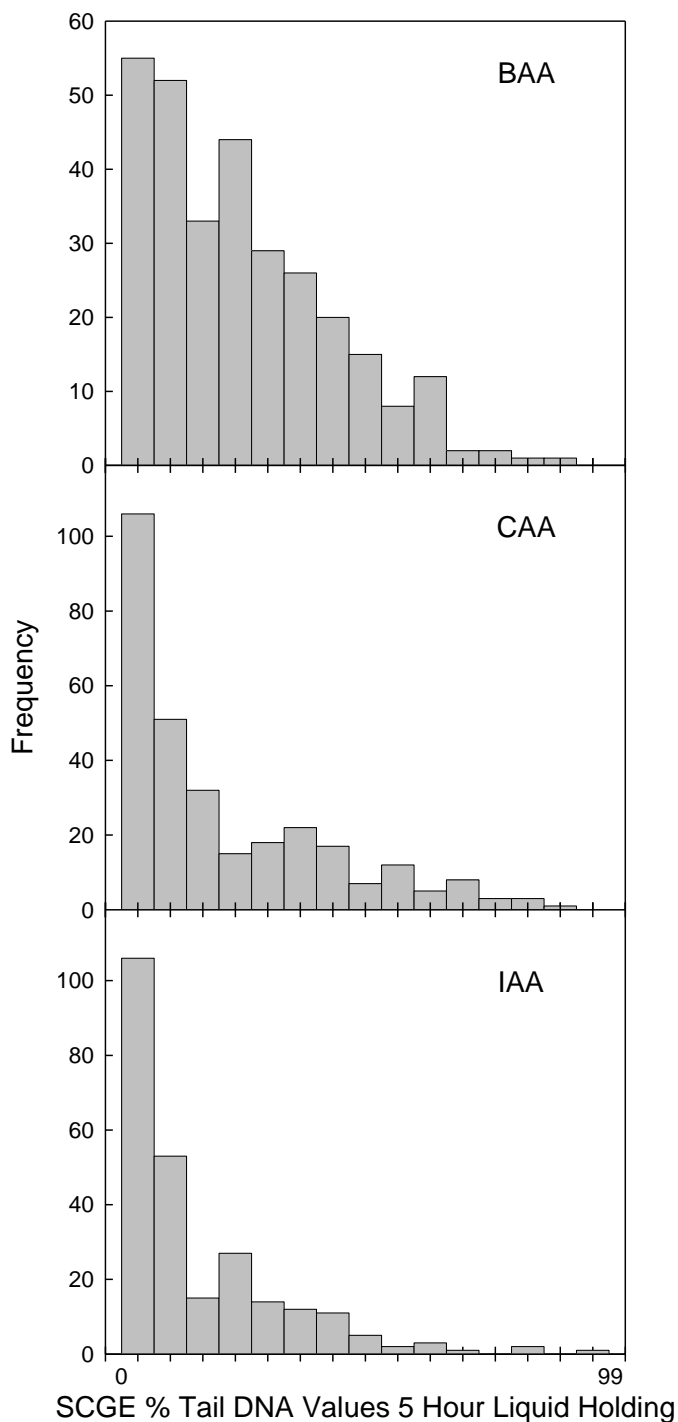


Figure 6.8 Histograms illustrating the distributions of SCGE % tail DNA values from CHO cells treated with bromoacetic acid (BAA), chloroacetic acid (CAA) and iodoacetic acid (IAA) at 5-h liquid-holding recovery.

The distributions of recovery period is pre

olding

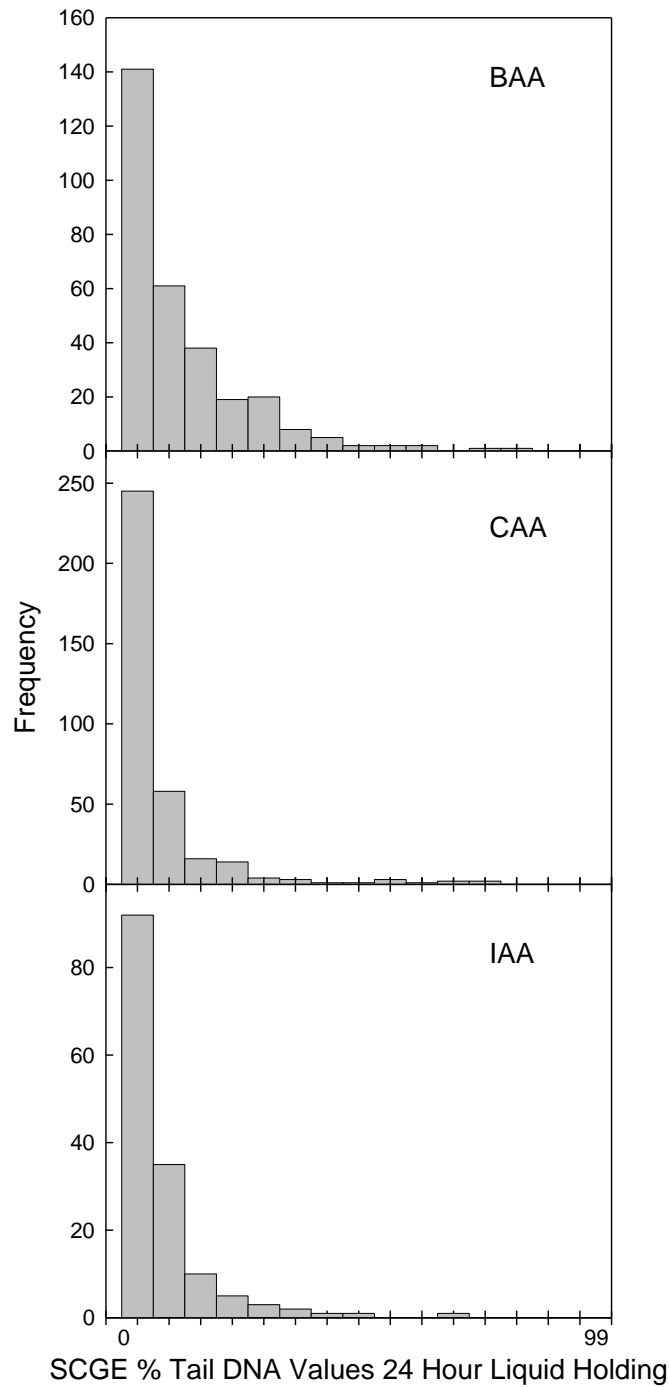


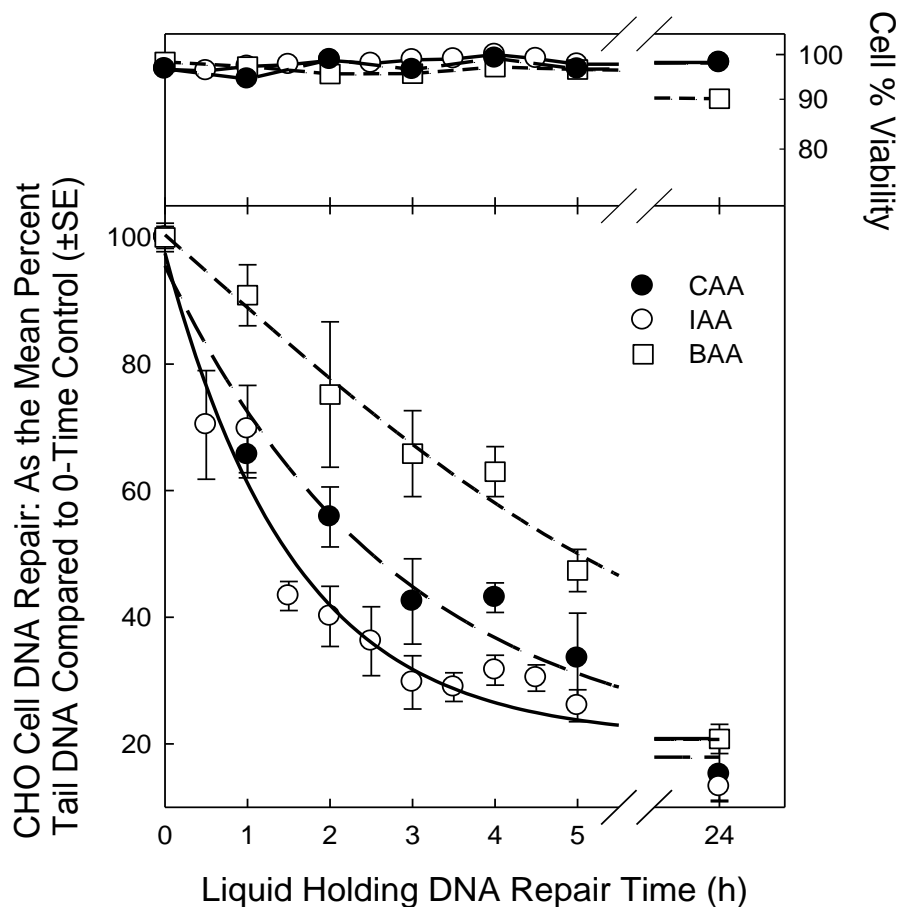
Figure 6.9 Histograms illustrating the distributions of SCGE % tail DNA values from CHO cells treated with bromoacetic acid (BAA), chloroacetic acid (CAA) and iodoacetic acid (IAA) at 24-h liquid-holding recovery.

Frequency Distribution of DNA Repair

The levels of damaged DNA that migrated from each nucleus into the microgel (% tail DNA) for each haloacetic acid as a function of liquid holding time were analyzed with frequency histograms (Figures 6.3 to 6.9). These figures illustrate the dynamics of genomic DNA repair in which the nucleus was the unit of measure. For each nucleus the distribution of DNA migration during each liquid holding time was plotted. The concentrations of haloacetic acids were chosen to generate approximately similar levels of biological damage. The 0-h liquid holding time (Figure 6.3) shows that CAA and IAA induced similar patterns of DNA damage. The damage induced by BAA with no liquid holding was much broader with fewer nuclei expressing the highest % tail DNA values but also many more nuclei with lower amounts of damage. As the liquid holding time progressed from 1 h (Figure 6.4), 2 h (Figure 6.5), 3 h (Figure 6.6), 4 h (Figure 6.7), 5 h (Figure 6.8) to 24 h (Figure 6.9), the levels of DNA damage in each treatment group steadily diminished. Figure 6.10 presents the comparative kinetics of DNA repair. Acute cytotoxicity was not observed throughout the liquid holding period (top panel, Figure 6.10). Although each monoHAA exhibited repair, it is notable that the cells treated with BAA showed less DNA repair as compared to CAA and IAA. Over a 24 h time period no difference in DNA damage distributions were observed in the negative controls (Figure 6.2). Finally, the level of completeness for the repair of DNA damage induced by each monoHAA can be observed by comparing the 24 h liquid holding distribution (Figure 6.9) with that of the 0-time liquid holding distribution (Figure 6.3).

With no liquid holding time for repair, the average % tail DNA values were 60.5, 50.3, and 67.3 for IAA, BAA and CAA, respectively (Figure 6.3). However, after 24 h of liquid holding, the respective mean % tail DNA values for these monoHAAs were 7.5, 12.0 and 7.2, respectively (Figure 6.9). Liquid-holding recovery significantly shifted the distributions to lower % tail DNA values; IAA showed the most rapid shift, CAA the next and BAA the slowest (Figure 6.10). The mean % tail DNA values of the negative controls did not change significantly over time, 4.8% without liquid holding, 4.1% after 5 h and 4.3% after 24 h liquid holding recovery time (Figure 6.2).

The data for each DNA repair curve were regressed using curvilinear curve fitting as well as regression based on first order kinetics (Table 6.1). The time required to affect 50% repair of the originally induced DNA damage (t_{50}) was calculated by sigmoidal or first order regression analysis of the data within the 0-5 h liquid holding time. Based on the calculation with sigmoidal regression, the t_{50} values for IAA, CAA and BAA were 84, 134 and 296 min, respectively (Table 6.1). The values were similar with first order regression. Using first order regression analysis, bimodal repair kinetics was observed. These bimodal repair curves may be the result of the diversity of DNA lesions induced by the haloacetic acids. Some DNA lesions such as apurinic sites, single strand DNA breaks, and damaged bases can be repaired more efficiently and relatively quickly as compared to DNA crosslinks and DNA double strand breaks. These latter lesions induce serious genomic damage and require more cellular processing for their repair (Friedberg, Walker, and Siede 1995). The calculated first order repair rates (during the first 3 h of liquid holding) for IAA, CAA and BAA were 0.842 h^{-1} , 0.763 h^{-1} and 0.187 h^{-1} , respectively. These calculations demonstrate that the rate of repair of BAA-induced lesions was different from the repair rates of CAA and IAA.



Source: (Reprinted with permission from Komaki, Y.; Pals, J.; Wagner, E. D.; Marinas, B. J.; Plewa, M. J., Environ. Sci. Technol. 2009, 43, (21), 8437–8442. Copyright 2007, American Chemical Society).

Figure 6.10 Comparative genomic DNA repair kinetics in CHO cells for chloroacetic acid (CAA), iodoacetic acid (IAA), and bromoacetic acid (BAA).

Table 6.1
DNA repair t_{50} values of genomic damage induced by IAA, BAA or CAA

Haloacetic Acid	Treatment Concentration	CAS Number	t_{50} (min, sigmoidal regression)	t_{50} (min, first order regression)
IAA	25 μ M	64-69-7	84	85
BAA	60 μ M	79-08-3	296	319
CAA	6 mM	79-11-8	134	135

Source: Reprinted with permission from Komaki, Y.; Pals, J.; Wagner, E. D.; Marinas, B. J.; Plewa, M. J., Environ. Sci. Technol. 2009, 43, (21), 8437–8442. Copyright 2007, American Chemical Society.

Statistical Analyses of DNA Repair

Cells treated with BAA expressed the lowest rate of DNA repair compared to IAA or CAA. By visual inspection the BAA repair curve appears to be different from those for IAA and CAA (Figure 6.10). To determine if there were significant differences in DNA repair amongst the three monoHAAs, we used a balanced multivariate analysis of variance (ANOVA) test statistic (Box, Hunter, and Hunter 1978). The DNA repair data for each haloacetic acid at 0, 1, 2, 3, 4 and 5 h liquid holding time periods were analyzed with a Holm-Sidak pairwise multiple comparison test (Table 6.2). A significant difference in the DNA repair kinetics was expressed by CHO cells exposed to BAA as compared to those exposed to IAA or CAA. The DNA repair kinetics for CAA and IAA were statistically similar.

Table 6.2
Two-way Analysis of Variance for DNA repair of CHO cells treated with IAA, BAA or CAA (Holm-Sidak pairwise multiple comparison)

Comparison	Liquid Holding Time (h)	Difference of Means	<i>P</i>
CAA vs. IAA	0	1.42×10^{-13}	0.99
CAA vs. BAA	0	4.26×10^{-14}	0.99
BAA vs. IAA	0	9.95×10^{-14}	0.99
CAA vs. IAA	1	4.08	0.58
CAA vs. BAA *	1	25.22	0.001
BAA vs. IAA *	1	21.14	0.005
CAA vs. IAA *	2	15.70	0.03
CAA vs. BAA *	2	19.35	0.009
BAA vs. IAA *	2	35.05	0.0001
CAA vs. IAA	3	12.79	0.08
CAA vs. BAA *	3	23.35	0.002
BAA vs. IAA *	3	36.136	0.0001
CAA vs. IAA	4	11.46	0.1
CAA vs. BAA *	4	19.90	0.007
BAA vs. IAA *	4	31.36	0.0001
CAA vs. IAA	5	7.49	0.3
CAA vs. BAA	5	13.87	0.06
BAA vs. IAA *	5	21.36	0.004

Source: (Reprinted with permission from Komaki, Y.; Pals, J.; Wagner, E. D.; Marinas, B. J.; Plewa, M. J., Environ. Sci. Technol. 2009, 43, (21), 8437–8442. Copyright 2007, American Chemical Society).

* DNA repair levels were statistically different between the treatment groups at $P < 0.05$.

The different rates of genomic repair that are expressed by IAA or CAA versus BAA suggest that different DNA lesions and/or different distributions of DNA lesions are induced. Since the concentration of each haloacetic acid was chosen to generate approximately the same level of genotoxic damage, the null hypothesis was that there would be no difference in the DNA repair kinetics if similar DNA lesions were induced by all three monoHAAs. The data do not support the null hypothesis.

In summary, the toxicogenomic data presented in this study indicate that noncytotoxic concentrations of the monoHAAs significantly modulate the expression of human genes involved in dsDNA break repair. Double strand breaks are one of the most toxic mutagenic lesions and require more time for repair than other types of DNA damage. dsDNA breaks must be repaired to restore the integrity, stability, and reproducibility of the genome. XRCC3-241 is a mutant allele for dsDNA break repair; humans who carry this allele express higher risks of bladder cancer. It is intriguing that bladder cancer is associated with the consumption of disinfected drinking water. The use of DNA repair coupled with genomic technologies may lead to the understanding of the biological and genetic mechanisms that are involved in toxic responses induced by DBPs. Such knowledge may lead to the identification of biomarkers that may be employed in feed-back loops to aid water chemists and engineers in the overall goal of producing safer drinking water.

CHAPTER 7

MONOHALOACETIC ACID GENOMIC DAMAGE, ALTERED GENE EXPRESSION AND DNA REPAIR KINETICS

POSSIBLE MECHANISMS TO INTEGRATE MONOHAA-MEDIATED DNA DAMAGE, ALTERED GENE EXPRESSION AND DNA REPAIR

Previous studies showed that the potent antioxidant butylated hydroxyanisole or the enzyme catalase substantially reduced IAA-induced mutagenicity in *S. typhimurium* and reduced genomic DNA damage in CHO cells (Cemeli et al. 2006). These results supported the hypothesis that oxidative stress-induced DNA lesions were a biological mechanism contributing to the genotoxicity of IAA. Oxidative stress has been linked with the toxicity of other DBPs such as 3-chloro-4-(dichloromethyl)-5-hydroxy-2(5H)-furanone (MX) (Yuan et al. 2006), bromate (Umemura et al. 1998; Umemura and Kurokawa 2006; Delker et al. 2006; Luan et al. 2007), and chloroacetonitrile (Ahmed et al. 2005). Oxidative stress-induced DNA damage ranges from damage to individual bases to the induction of single strand and double strand DNA breaks (Friedberg, Walker, and Siede 1995). DNA repair of oxidative stress-induced lesions may be relatively fast if mediated by DNA glycosylases (Fry, Begley, and Samson 2005) or require more time if the lesion is a double strand DNA break (Helleday et al. 2007).

Double strand DNA breaks are considered to be one of the most toxic and mutagenic lesions and require more time for repair as compared to other types of DNA damage (Helleday et al. 2007). dsDNA breaks are lesions that must be repaired to restore the integrity, stability and reproducibility of the genome. It is interesting to note that humans who carry a mutant allele for dsDNA break repair (XRCC3-241) express higher risks of bladder cancer (Andrew et al. 2008). Bladder cancer is associated with the consumption of disinfected drinking water (Villanueva et al. 2004).

For additional mechanistic information we compared the DNA repair kinetics of IAA, BAA and CAA in CHO cells. Concentrations of each monoHAA were employed that resulted in equivalent biological responses. Although IAA is a more potent genotoxin as compared to BAA, BAA-induced genomic DNA damage required more time to repair than damage induced by IAA (Figure 6.10) (Komaki et al. 2009). BAA may be inducing a higher frequency of unrepaired dsDNA lesions. However, as illustrated in Figure 5.8, the toxicogenomic data show that all of the monoHAAs cause the modulation of similar number of genes associated with dsDNA breaks (Attene-Ramos, Wagner, and Plewa 2010).

An alternative explanation is founded on the interesting correlation that the monoHAAs may cause different levels of cell cycle inhibition. The distribution of genomic DNA damage by the monoHAAs at equivalent levels of SCGE genotoxicity (Figure 5.4) also expressed differential levels of cell growth after exposure. Figure 3.6 shows both IAA and CAA generated a reduction in cell density without killing cells, while BAA did not exhibit a decline in cell density. This response may be associated with differential effects on cell cycle inhibition. That the toxicogenomic data demonstrated that IAA and CAA modulated a larger number of cell cycle control genes than BAA may be the foundation of this cellular response (Figure 5.8). We speculate that the slower rate of repair of BAA-induced lesions may, in part, be due to a lack of cell cycle inhibition. This effect may result in reducing the time available for error-free DNA repair.

CHAPTER 8 CONCLUSIONS

In general the data from this project generated the following conclusions.

1. The use of non-transformed (non-tumor) human cells in toxicogenomic analyses provided a robust concurrent control.
2. Treating cells with non-cytotoxic concentrations of the monoHAAs ensured that the RNA isolated for the generation of the transcriptome profiles were derived from cells that were not dead or dying.
3. Using monoHAA concentrations that induced equivalent genotoxic responses in treated human cells allowed for the direct comparison of the genomic effects of each DBP.
4. Using the Database for Annotation, Visualization and Integrated Discovery to analyze the gene array data, the majority of the altered transcriptome profiles were associated with genes responding to DNA damage or those regulating cell cycle or apoptosis.
5. The major pathways involved with altered gene expression were ATM, MAPK, p53, BRCA1, BRCA2, and ATR.
6. These latter pathways highlight the involvement of DNA repair, especially the repair of double strand DNA breaks.
7. All of the resolved pathways are involved in human cell stress response to DNA damage and regulate different stages in cell cycle progression or apoptosis.
8. The monoHAAs expressed different rates of DNA repair with BAA-induced lesions requiring significantly more time than genomic DNA damage induced by IAA or CAA.
9. A reduction in the control of cell cycle arrest in cells treated with BAA may slow the rate of genomic DNA repair as compared to IAA- and CAA-exposed cells.

Overall this work represents the first non-transformed human cell toxicogenomic study with regulated drinking water DBPs. We linked the biological endpoint of DNA damage (SCGE) with toxicogenomic arrays featuring primers for genes related to human DNA damage and repair, and general cellular responses to toxicity. This research is a leap forward in understanding the link between *in vitro* cytotoxicity and genotoxicity assays with that of investigating the impact of DBPs on the expression of human toxic response gene pathways that may be involved in the etiology of disease. In addition toxicogenomic research may provide information that could aid in identifying individuals who are especially sensitive to the toxic impacts of specific DBP classes. By appropriate intervention it may be possible to reduce even more the level of adverse health impacts associated with exposure to DBPs.

With the implementation of the U.S. EPA Stage 2 DBP Rule and with energy and cost considerations, drinking water utilities will continue providing high quality, tasteful potable water for the nation. However, there are health concerns for emerging DBPs especially iodinated DBPs and nitrogen-containing DBPs (N-DBPs). With the best characterized disinfectant, chlorine, only approximately 50% of the DBPs are chemically identified. Even less is known of

the DBPs generated with other disinfectants. Our knowledge concerning the toxicity of DBPs, although expanding, is woefully inadequate. Along with basic information that has accumulated on the adverse biological effects and health implications of DBPs, toxicogenomics provides insight into the impacts that DBPs impart upon the modulation of gene expression. With the information generated by the structure activity response between the chemistry and biology of DBPs coupled with the DBP-mediated transcriptome profiles, we have greater insight as to which molecular pathways impacted by DBPs may be associated with human disease.

In the future this information will be useful as part of the decision making process on the development and implementation of disinfection practices. Having an understanding of the unique characteristics of the source water, utilities ultimately will employ molecular markers for disease to choose disinfection methods that generate the least toxic DBPs in their finished drinking water.

We are now at the time in which a DBP toxicity library must be developed using both traditional short-term *in vitro* toxicology methods and quantitative high throughput screening methodologies as advocated by such agencies as the National Institutes of Health. The merger of analytical chemistry, analytical biology and toxicogenomics will allow for precisely tuning the disinfection of source waters to generate even higher quality, economic, and safe drinking water while protecting the public health and the environment.

REFERENCES

- Aardema, M. J., and J. T. MacGregor. 2002. Toxicology and genetic toxicology in the new era of "toxicogenomics": impact of "-omics" technologies. *Mutat. Res.* 499 (1):13-25.
- Ahmed, A. E., S. Jacob, G. A. Campbell, H. M. Harirah, J. R. Perez-Polo, and K. M. Johnson. 2005. Fetal origin of adverse pregnancy outcome: The water disinfectant by-product chloroacetonitrile induces oxidative stress and apoptosis in mouse fetal brain. *Dev. Brain Res.* 159 (1):1-11.
- Andrew, A. S., M. R. Karagas, H. H. Nelson, S. Guarrera, S. Polidoro, S. Gamberini, C. Sacerdote, J. H. Moore, K. T. Kelsey, E. Demidenko, P. Vineis, and G. Matullo. 2008. DNA repair polymorphisms modify bladder cancer risk: a multi-factor analytic strategy. *Hum. Hered.* 65 (2):105-118.
- Andrews, R. C., and M. J. Ferguson. 1996. Minimizing disinfection by-product formation while ensuring *Giardia* control. In *Disinfection By-products in Water Treatment: The Chemistry of Their Formation and Control*, edited by R. A. Minear and G. L. Amy. Boca Raton, FL: CRC Press.
- Annunziato, F., P. Romagnani, L. Cosmi, C. Beltrame, B. H. Steiner, E. Lazzeri, C. J. Raport, G. Galli, R. Manetti, C. Mavilia, V. Vanini, D. Chantry, E. Maggi, and S. Romagnani. 2000. Macrophage-derived chemokine and EBI1-ligand chemokine attract human thymocytes in different stage of development and are produced by distinct subsets of medullary epithelial cells: possible implications for negative selection. *J Immunol* 165 (1):238-46.
- Arikawa, E., G. Quellhorst, Y. Han, J. Yang, H. Pan, and J. Yang. 2006. PCR Array: A simple and quantitative method for gene expression profiling. Frederick, MD: SuperArray Bioscience Corp.
- Attene-Ramos, M. S., G. M. Nava, M. G. Muellner, E. D. Wagner, M. J. Plewa, and H. R. Gaskins. 2010. DNA damage and toxicogenomic analyses of hydrogen sulfide in human intestinal epithelial FHs 74 Int cells. *Environ. Mol. Mutagen.* 51:304-314.
- Attene-Ramos, M. S., E. D. Wagner, and M. J. Plewa. 2010. Comparative human cell toxicogenomic analysis of monohaloacetic acid drinking water disinfection byproducts. *Environ. Sci. Technol.* 44 (19):7206-7212.
- Barrett, T., D. B. Troup, S. E. Wilhite, P. Ledoux, D. Rudnev, C. Evangelista, I. F. Kim, A. Soboleva, M. Tomashevsky, and R. Edgar. 2007. NCBI GEO: mining tens of millions of expression profiles--database and tools update. *Nucleic Acids Res* 35 (Database issue):D760-5.
- Bichsel, Y., and U. von Gunten. 1999. Oxidation of iodide and hypiodous acid in the disinfection of natural waters. *Environ. Sci. Technol.* 33 (22):4040-4045.
- Bichsel, Y., and U. von Gunten. 2000. Formation of iodo-trihalomethanes during disinfection and oxidation of iodide containing waters. *Environ. Sci. Technol.* 34 (13):2784-2791.
- Bilsland, E., and J. A. Downs. 2005. Tails of histones in DNA double-strand break repair. *Mutagenesis* 20 (3):153-163.
- Boatright, K. M., and G. S. Salvesen. 2003. Mechanisms of caspase activation. *Curr Opin Cell Biol* 15 (6):725-31.

- Bootcov, M. R., A. R. Bauskin, S. M. Valenzuela, A. G. Moore, M. Bansal, X. Y. He, H. P. Zhang, M. Donnellan, S. Mahler, K. Pryor, B. J. Walsh, R. C. Nicholson, W. D. Fairlie, S. B. Por, J. M. Robbins, and S. N. Breit. 1997. MIC-1, a novel macrophage inhibitory cytokine, is a divergent member of the TGF-beta superfamily. *Proc Natl Acad Sci U S A* 94 (21):11514-9.
- Box, G. E. P., W. G. Hunter, and J. S. Hunter. 1978. *Statistics for Experimenters: An Introduction to Design, Data Analysis, and Model Building*. New York, NY.: Wiley & Sons Inc.
- Breitling, R., P. Armengaud, A. Amtmann, and P. Herzyk. 2004. Rank products: a simple, yet powerful, new method to detect differentially regulated genes in replicated microarray experiments. *FEBS Lett* 573 (1-3):83-92.
- Brugmans, L., R. Kanaar, and J. Essers. 2007. Analysis of DNA double-strand break repair pathways in mice. *Mutat. Res.* 614 (1-2):95-108.
- Caba, E., and J. Aubrecht. 2006. Genomic approaches for investigating mechanisms of genotoxicity. *Toxicol. Mech. Methods* 16 (2-3):69-77.
- Cahir-McFarland, E. D., D. M. Davidson, S. L. Schauer, J. Duong, and E. Kieff. 2000. NF-kappa B inhibition causes spontaneous apoptosis in Epstein-Barr virus-transformed lymphoblastoid cells. *Proc Natl Acad Sci U S A* 97 (11):6055-60.
- Carney, J. P., R. S. Maser, H. Olivares, E. M. Davis, M. Le Beau, J. R. Yates, 3rd, L. Hays, W. F. Morgan, and J. H. Petrini. 1998. The hMre11/hRad50 protein complex and Nijmegen breakage syndrome: linkage of double-strand break repair to the cellular DNA damage response. *Cell* 93 (3):477-86.
- Cartwright, R., C. E. Tambini, P. J. Simpson, and J. Thacker. 1998. The XRCC2 DNA repair gene from human and mouse encodes a novel member of the recA/RAD51 family. *Nucleic Acids Res* 26 (13):3084-9.
- Cemeli, E., E. D. Wagner, D. Anderson, S. D. Richardson, and M. J. Plewa. 2006. Modulation of the cytotoxicity and genotoxicity of the drinking water disinfection byproduct iodoacetic acid by suppressors of oxidative stress. *Environ. Sci. Technol.* 40 (6):1878-1883.
- Christmann, M., M. T. Tomicic, W. P. Roos, and B. Kaina. 2003. Mechanisms of human DNA repair: an update. *Toxicology* 193 (1):3-34.
- Davis, W., Jr., Z. J. Chen, K. E. Ile, and K. D. Tew. 2003. Reciprocal regulation of expression of the human adenosine 5'-triphosphate binding cassette, sub-family A, transporter 2 (ABCA2) promoter by the early growth response-1 (EGR-1) and Sp-family transcription factors. *Nucleic Acids Res* 31 (3):1097-107.
- Delker, D., G. Hatch, J. Allen, B. Crissman, M. George, D. Geter, S. Kilburn, T. Moore, G. Nelson, B. Roop, R. Slade, A. Swank, W. Ward, and A. DeAngelo. 2006. Molecular biomarkers of oxidative stress associated with bromate carcinogenicity. *Toxicology* 221 (2-3):158-165.
- Dennis, G., Jr., B. T. Sherman, D. A. Hosack, J. Yang, W. Gao, H. C. Lane, and R. A. Lempicki. 2003. DAVID: Database for Annotation, Visualization, and Integrated Discovery. *Genome Biol* 4 (5):P3.
- Dolphin, C., E. A. Shephard, S. Povey, C. N. Palmer, D. M. Ziegler, R. Ayyesh, R. L. Smith, and I. R. Phillips. 1991. Cloning, primary sequence, and chromosomal mapping of a human flavin-containing monooxygenase (FMO1). *J Biol Chem* 266 (19):12379-85.
- Edgar, R., M. Domrachev, and A. E. Lash. 2002. Gene Expression Omnibus: NCBI gene expression and hybridization array data repository. *Nucleic Acids Res.* 30 (1):207-210.

- Friedberg, E. C., G. C. Walker, and W. Siede. 1995. *DNA Repair and Mutagenesis*. Washington, D.C.: ASM Press.
- Fry, R. C., T. J. Begley, and L. D. Samson. 2005. Genome-wide responses to DNA-damaging agents. *Annu. Rev. Microbiol.* 59:357-377.
- Glaze, W., and H. Weinberg. 1993. *Identification and Occurrence of Ozonation By-products in Drinking Water*. Denver, CO: Am. Water Works Assoc. Res. Foundation.
- Gray, P. W., B. B. Aggarwal, C. V. Benton, T. S. Bringman, W. J. Henzel, J. A. Jarrett, D. W. Leung, B. Moffat, P. Ng, L. P. Svedersky, and et al. 1984. Cloning and expression of cDNA for human lymphotoxin, a lymphokine with tumour necrosis activity. *Nature* 312 (5996):721-4.
- Habu, T., T. Taki, A. West, Y. Nishimune, and T. Morita. 1996. The mouse and human homologs of DMC1, the yeast meiosis-specific homologous recombination gene, have a common unique form of exon-skipped transcript in meiosis. *Nucleic Acids Res* 24 (3):470-7.
- Hamadeh, H. K., R. P. Amin, R. S. Paules, and C. A. Afshari. 2002. An overview of toxicogenomics. *Curr. Issues Mol. Biol.* 4 (2):45-56.
- Hamadeh, H. K., P. R. Bushel, S. Jayadev, K. Martin, O. DiSorbo, S. Sieber, L. Bennett, R. Tennant, R. Stoll, J. C. Barrett, K. Blanchard, R. S. Paules, and C. A. Afshari. 2002. Gene expression analysis reveals chemical-specific profiles. *Toxicol. Sci.* 67 (2):219-231.
- Hansch, C., A. Leo, and D. Hoekman. 1995. *Exploring QSAR: Hydrophobic, Electronic, and Steric Constants*: American Chemical Society Washington DC.
- Harrison, J. C., and J. E. Haber. 2006. Surviving the breakup: The DNA damage checkpoint. *Ann. Rev. Genet.* 40:209-235.
- Hayes, F. D., R. D. Short, and J. E. Gibson. 1973. Differential toxicity of monochloroacetate, monofluoroacetate and monoiodoacetate in rats. *Toxicol. Appl. Pharmacol.* 26 (1):93-102.
- Helleday, T., J. Lo, D. C. van Gent, and B. P. Engelward. 2007. DNA double-strand break repair: From mechanistic understanding to cancer treatment. *DNA Repair* 6 (7):923-935.
- Hengartner, M. O. 2000. The biochemistry of apoptosis. *Nature* 407 (6805):770-6.
- Hollander, M. C., Q. Zhan, I. Bae, and A. J. Fornace, Jr. 1997. Mammalian GADD34, an apoptosis- and DNA damage-inducible gene. *J Biol Chem* 272 (21):13731-7.
- Hong, F., R. Breitling, C. W. McEntee, B. S. Wittner, J. L. Nemhauser, and J. Chory. 2006. RankProd: a bioconductor package for detecting differentially expressed genes in meta-analysis. *Bioinformatics* 22 (22):2825-7.
- Hsie, A. W., P. A. Brimer, T. J. Mitchell, and D. G. Gosslee. 1975. The dose-response relationship for ethyl methanesulfonate-induced mutations at the hypoxanthine-guanine phosphoribosyl transferase locus in Chinese hamster ovary cells. *Somatic Cell Genet.* 1 (3):247-261.
- Hsie, A. W., P. A. Brimer, T. J. Mitchell, and D. G. Gosslee. 1975. The dose-response relationship for ultraviolet-light-induced mutations at the hypoxanthine-guanine phosphoribosyltransferase locus in Chinese hamster ovary cells. *Somatic Cell Genet.* 1 (4):383-389.
- Hua, G. H., and D. A. Reckhow. 2007. Comparison of disinfection byproduct formation from chlorine and alternative disinfectants. *Water Res.* 41 (8):1667-1678.
- Huang, D. W., B. T. Sherman, and R. A. Lempicki. 2009. Systematic and integrative analysis of large gene lists using DAVID bioinformatics resources. *Nat Protoc* 4 (1):44-57.

- Hunter, E. S., 3rd, E. H. Rogers, J. E. Schmid, and A. Richard. 1996. Comparative effects of haloacetic acids in whole embryo culture. *Teratology* 54 (2):57-64.
- Ito, Y., A. Ando, H. Ando, J. Ando, Y. Saijoh, H. Inoko, and H. Fujimoto. 1998. Genomic structure of the spermatid-specific hsp70 homolog gene located in the class III region of the major histocompatibility complex of mouse and man. *J Biochem* 124 (2):347-53.
- Kargalioglu, Y., B. J. McMillan, R. A. Minear, and M. J. Plewa. 2002. Analysis of the cytotoxicity and mutagenicity of drinking water disinfection by-products in *Salmonella typhimurium*. *Teratogen. Carcinogen. Mutagen.* 22 (2):113-128.
- Karran, P. 2000. DNA double strand break repair in mammalian cells. *Curr. Opin. Genet. Dev.* 10 (2):144-150.
- Komaki, Y., J. Pals, E. D. Wagner, B. J. Marinas, and M. J. Plewa. 2009. Mammalian cell DNA damage and repair kinetics of monohaloacetic acid drinking water disinfection by-products. *Environ. Sci. Technol.* 43 (21):8437-8442.
- Krasner, S. W. 2009. The formation and control of emerging disinfection by-products of health concern. *Philos. Transact.R. Soc. A* 367 (1904):4077-4095.
- Krasner, S. W., H. S. Weinberg, S. D. Richardson, S. J. Pastor, R. Chinn, M. J. Scilimenti, G. D. Onstad, and A. D. Thruston, Jr. 2006. The occurrence of a new generation of disinfection by-products. *Environ. Sci. Technol.* 40 (23):7175-7185.
- Le Fevre, A. C., E. Boitier, J. P. Marchandau, A. Sarasin, and V. Thybaud. 2007. Characterization of DNA reactive and non-DNA reactive anticancer drugs by gene expression profiling. *Mutat. Res.* 619 (1-2):16-29.
- Lieber, M. R., Y. Ma, U. Pannicke, and K. Schwarz. 2003. Mechanism and regulation of human non-homologous DNA end-joining. *Nat. Rev. Mol Cell. Biol.* 4 (9):712-720.
- Lieberman, H. B., K. M. Hopkins, M. Nass, D. Demetrick, and S. Davey. 1996. A human homolog of the *Schizosaccharomyces pombe* rad9+ checkpoint control gene. *Proc Natl Acad Sci U S A* 93 (24):13890-5.
- Lindahl, T., and R. D. Wood. 1999. Quality control by DNA repair. *Science* 286 (5446):1897-905.
- Lio, Y. C., A. V. Mazin, S. C. Kowalczykowski, and D. J. Chen. 2003. Complex formation by the human Rad51B and Rad51C DNA repair proteins and their activities in vitro. *J Biol Chem* 278 (4):2469-78.
- Liu, N., J. E. Lamerdin, R. S. Tebbs, D. Schild, J. D. Tucker, M. R. Shen, K. W. Brookman, M. J. Siciliano, C. A. Walter, W. Fan, L. S. Narayana, Z. Q. Zhou, A. W. Adamson, K. J. Sorensen, D. J. Chen, N. J. Jones, and L. H. Thompson. 1998. XRCC2 and XRCC3, new human Rad51-family members, promote chromosome stability and protect against DNA cross-links and other damages. *Mol Cell* 1 (6):783-93.
- Liviak, D., A. Creus, and R. Marcos. 2009. Genotoxicity analysis of two halonitromethanes, a novel group of disinfection by-products (DBPs), in human cells treated in vitro. *Environ. Res.* 109 (3):232-238.
- Liviak, D., A. Creus, and R. Marcos. 2009. Genotoxicity analysis of two hydroxyfuranones, byproducts of water disinfection, in human cells treated in vitro. *Environ. Mol. Mutagen.* 50 (5):413-420.
- Loos, H., D. Roos, R. Weening, and J. Houwerzijl. 1976. Familial deficiency of glutathione reductase in human blood cells. *Blood* 48 (1):53-62.
- Loudon, G. M. 1995. *Organic Chemistry*. 3rd ed. Redwood, CA: Benjamin/Cummings Publ. Co.

- Lovell, D. P., and T. Omori. 2008. Statistical issues in the use of the comet assay. *Mutagenesis* 23 (3):171-182.
- Luan, Y., T. Suzuki, R. Palanisamy, Y. Takashima, H. Sakamoto, M. Sakuraba, T. Koizumi, M. Saito, H. Matsufuji, K. Yamagata, T. Yamaguchi, M. Hayashi, and M. Honma. 2007. Potassium bromate treatment predominantly causes large deletions, but not GC>TA transversion in human cells. *Mutat. Res.* 619 (1-2):113-123.
- Makeyev, A. V., and S. A. Liebhaber. 2000. Identification of two novel mammalian genes establishes a subfamily of KH-domain RNA-binding proteins. *Genomics* 67 (3):301-16.
- Malaguarnera, L., M. R. Pilastro, S. Quan, M. H. Ghattas, L. Yang, A. V. Mezentsev, T. Kushida, N. G. Abraham, and A. Kappas. 2002. Significance of heme oxygenase in prolactin-mediated cell proliferation and angiogenesis in human endothelial cells. *Int J Mol Med* 10 (4):433-40.
- Mao, Y. W., J. P. Liu, H. Xiang, and D. W. Li. 2004. Human alphaA- and alphaB-crystallins bind to Bax and Bcl-X(S) to sequester their translocation during staurosporine-induced apoptosis. *Cell Death Differ* 11 (5):512-26.
- Mazur, D. J., and F. W. Perrino. 1999. Identification and expression of the TREX1 and TREX2 cDNA sequences encoding mammalian 3'-->5' exonucleases. *J Biol Chem* 274 (28):19655-60.
- Miao, F., M. Bouziane, R. Dammann, C. Masutani, F. Hanaoka, G. Pfeifer, and T. R. O'Connor. 2000. 3-Methyladenine-DNA glycosylase (MPG protein) interacts with human RAD23 proteins. *J Biol Chem* 275 (37):28433-8.
- Moncada, S. 1999. Nitric oxide: discovery and impact on clinical medicine. *J R Soc Med* 92 (4):164-9.
- Muellner, M. G., M. S. Attene-Ramos, M. E. Hudson, E. D. Wagner, and M. J. Plewa. 2010. Human cell toxicogenomic analysis of bromoacetic acid: a regulated drinking water disinfection by-product. *Environ. Mol. Mutagen.* 51:205-214.
- Muellner, M. G., M. E. Hudson, E. D. Wagner, and M. J. Plewa. 2008. Human toxicogenomic analysis of bromoacetic acid: a regulated drinking water disinfection byproduct. In *Advances in Drinking Water Disinfection and Disinfection Byproducts*. New Orleans, LA: American Chemical Society.
- Nishida, T., N. Nishino, M. Takano, K. Kawai, K. Bando, Y. Masui, S. Nakai, and Y. Hirai. 1987. cDNA cloning of IL-1 alpha and IL-1 beta from mRNA of U937 cell line. *Biochem Biophys Res Commun* 143 (1):345-52.
- Papadopoulos, N., N. C. Nicolaides, Y. F. Wei, S. M. Ruben, K. C. Carter, C. A. Rosen, W. A. Haseltine, R. D. Fleischmann, C. M. Fraser, M. D. Adams, and et al. 1994. Mutation of a mutL homolog in hereditary colon cancer. *Science* 263 (5153):1625-9.
- Park, J. S., J. D. Luethy, M. G. Wang, J. Fagnoli, A. J. Fornace, Jr., O. W. McBride, and N. J. Holbrook. 1992. Isolation, characterization and chromosomal localization of the human GADD153 gene. *Gene* 116 (2):259-67.
- Paull, T. T., and M. Gellert. 1998. The 3' to 5' exonuclease activity of Mre 11 facilitates repair of DNA double-strand breaks. *Mol Cell* 1 (7):969-79.
- Phillips, H. J. 1973. Dye exclusion tests for cell viability. In *Tissue Culture: Methods and Applications*, edited by P. F. Kruse and M. J. Patterson. New York: Academic Press.
- Pitti, R. M., S. A. Marsters, S. Ruppert, C. J. Donahue, A. Moore, and A. Ashkenazi. 1996. Induction of apoptosis by Apo-2 ligand, a new member of the tumor necrosis factor cytokine family. *J Biol Chem* 271 (22):12687-90.

- Plewa, M. J., Y. Kargalioglu, D. Vanker, R. A. Minear, and E. D. Wagner. 2002. Mammalian cell cytotoxicity and genotoxicity analysis of drinking water disinfection by-products. *Environ. Mol. Mutagen.* 40 (2):134-142.
- Plewa, M. J., J. E. Simmons, S. D. Richardson, and E. D. Wagner. 2010. Mammalian cell cytotoxicity and genotoxicity of the haloacetic acids, a major class of drinking water disinfection by-products. *Environ. Mol. Mutagen* 51:871-878.
- Plewa, M. J., and E. D. Wagner. 2009. *Mammalian cell cytotoxicity and genotoxicity of disinfection by-products*. Denver, CO: Water Research Foundation.
- Plewa, M. J., E. D. Wagner, S. D. Richardson, A. D. Thruston, Jr., Y. T. Woo, and A. B. McKague. 2004. Chemical and biological characterization of newly discovered iodoacid drinking water disinfection byproducts. *Environ. Sci. Technol.* 38 (18):4713-4722.
- Powers, J. T., S. Hong, C. N. Mayhew, P. M. Rogers, E. S. Knudsen, and D. G. Johnson. 2004. E2F1 uses the ATM signaling pathway to induce p53 and Chk2 phosphorylation and apoptosis. *Mol. Cancer. Res.* 2 (4):203-214.
- Quellhorst, G., S. Prabhakar, Y. Han, and J. Yang. 2006. PCR Array: A simple and quantitative method for gene expression profiling. In *White Paper 1*. Frederick, MD,: SuperArray Bioscience Corp.
- Reddy, R. K., C. Mao, P. Baumeister, R. C. Austin, R. J. Kaufman, and A. S. Lee. 2003. Endoplasmic reticulum chaperone protein GRP78 protects cells from apoptosis induced by topoisomerase inhibitors: role of ATP binding site in suppression of caspase-7 activation. *J Biol Chem* 278 (23):20915-24.
- Richard, A. M., and E. S. Hunter, 3rd. 1996. Quantitative structure-activity relationships for the developmental toxicity of haloacetic acids in mammalian whole embryo culture. *Teratology* 53 (6):352-360.
- Richardson, S. D., F. Fasano, J. J. Ellington, F. G. Crumley, K. M. Buettner, J. J. Evans, B. C. Blount, L. K. Silva, T. J. Waite, G. W. Luther, A. B. McKague, R. J. Miltner, E. D. Wagner, and M. J. Plewa. 2008. Occurrence and mammalian cell toxicity of iodinated disinfection byproducts in drinking water. *Environ. Sci. Technol.* 42 (22):8330-8338.
- Richardson, S. D., M. J. Plewa, E. D. Wagner, R. Schoeny, and D. M. DeMarini. 2007. Occurrence, genotoxicity, and carcinogenicity of regulated and emerging disinfection by-products in drinking water: A review and roadmap for research. *Mutat. Res.* 636:178-242.
- Richardson, S.D. 2009. Water analysis: emerging contaminants and current issues. *Anal. Chem.* 81:4645-4677.
- Riches, L. C., A. M. Lynch, and N. J. Gooderham. 2008. Early events in the mammalian response to DNA double-strand breaks. *Mutagenesis* 23 (5):331-9.
- Rouault, J. P., N. Falette, F. Guehenneux, C. Guillot, R. Rimokh, Q. Wang, C. Berthet, C. Moyret-Lalle, P. Savatier, B. Pain, P. Shaw, R. Berger, J. Samarut, J. P. Magaud, M. Ozturk, C. Samarut, and A. Puisieux. 1996. Identification of BTG2, an antiproliferative p53-dependent component of the DNA damage cellular response pathway. *Nat Genet* 14 (4):482-6.
- Rundell, M. S., E. D. Wagner, and M. J. Plewa. 2003. The comet assay: genotoxic damage or nuclear fragmentation? *Environ. Mol. Mutagen.* 42 (2):61-67.
- Saiardi, A., E. Nagata, H. R. Luo, A. Sawa, X. Luo, A. M. Snowman, and S. H. Snyder. 2001. Mammalian inositol polyphosphate multikinase synthesizes inositol 1,4,5-trisphosphate and an inositol pyrophosphate. *Proc Natl Acad Sci U S A* 98 (5):2306-11.

- Scheuerer, B., M. Ernst, I. Durrbaum-Landmann, J. Fleischer, E. Grage-Griebenow, E. Brandt, H. D. Flad, and F. Petersen. 2000. The CXC-chemokine platelet factor 4 promotes monocyte survival and induces monocyte differentiation into macrophages. *Blood* 95 (4):1158-66.
- Schroeder, A., O. Mueller, S. Stocker, R. Salowsky, M. Leiber, M. Gassmann, S. Lightfoot, W. Menzel, M. Granzow, and T. Ragg. 2006. The RIN: an RNA integrity number for assigning integrity values to RNA measurements. *BMC Mol Biol* 7:3.
- Shrivastav, M., L. P. De Haro, and J. A. Nickoloff. 2008. Regulation of DNA double-strand break repair pathway choice. *Cell Res.* 18 (1):134-47.
- Singer, P. C. 2006. Regulation of only five haloacetic acids is neither sound science nor good policy. Paper read at Proceedings of Symposium on Safe Drinking Water: Where Science Meets Policy, Carolina Environmental Program, at Chapel Hill, NC.
- Smith, H. S. 1979. In vitro properties of epithelial cell lines established from human carcinomas and nonmalignant tissue. *J. Natl. Cancer Inst.* 62 (2):225-230.
- Stevens, A. A., L. A. Moore, C. J. Slocum, B. L. Smith, D. R. Seeger, and J.C. Ireland. 1989. *Water Chlorination: Chemistry, Environmental Impact and Health Effects*. Chelsea, MI: Lewis Publishers.
- Su, Tin Tin. 2006. Cellular responses to DNA damage: one signal, multiple choices. *Ann. Rev. Genet.* 40:187-208.
- Susin, S. A., H. K. Lorenzo, N. Zamzami, I. Marzo, B. E. Snow, G. M. Brothers, J. Mangion, E. Jacotot, P. Costantini, M. Loeffler, N. Larochette, D. R. Goodlett, R. Aebersold, D. P. Siderovski, J. M. Penninger, and G. Kroemer. 1999. Molecular characterization of mitochondrial apoptosis-inducing factor. *Nature* 397 (6718):441-6.
- Thai, S. F., J. W. Allen, A. B. DeAngelo, M. H. George, and J. C. Fuscoe. 2003. Altered gene expression in mouse livers after dichloroacetic acid exposure. *Mutat. Res.* 543 (2):167-180.
- Thybaud, V., A. C. Le Fevre, and E. Boitier. 2007. Application of toxicogenomics to genetic toxicology risk assessment. *Environ. Mol. Mutagen.* 48 (5):369-379.
- Tice, R. R., E. Agurell, D. Anderson, B. Burlinson, A. Hartmann, H. Kobayashi, Y. Miyamae, E. Rojas, J. C. Ryu, and Y. F. Sasaki. 2000. Single cell gel/comet assay: guidelines for in vitro and in vivo genetic toxicology testing. *Environ. Mol. Mutagen.* 35 (3):206-221.
- Tindall, K. R., and L. F. Stankowski, Jr. 1989. Molecular analysis of spontaneous mutations at the gpt locus in Chinese hamster ovary (AS52) cells. *Mutat. Res.* 220 (2-3):241-253.
- Tindall, K. R., L. F. Stankowski, Jr., R. Machanoff, and A. W. Hsie. 1984. Detection of deletion mutations in pSV2gpt-transformed cells. *Mol. Cell Biol.* 4 (7):1411-1415.
- Tomkinson, A. E., and Z. B. Mackey. 1998. Structure and function of mammalian DNA ligases. *Mutat Res* 407 (1):1-9.
- Tully, D. B., J. C. Luft, J. C. Rockett, H. Ren, J. E. Schmid, C. R. Wood, and D. J. Dix. 2005. Reproductive and genomic effects in testes from mice exposed to the water disinfectant byproduct bromochloroacetic acid. *Reprod. Toxicol.* 19 (3):353-366.
- Tzang, B. S., Y. C. Lai, M. Hsu, H. W. Chang, C. C. Chang, P. C. Huang, and Y. C. Liu. 1999. Function and sequence analyses of tumor suppressor gene p53 of CHO.K1 cells. *DNA Cell Biol.* 18 (4):315-321.
- U. S. Environmental Protection Agency. 1998. National primary drinking water regulations: Disinfectants and disinfection byproducts; Final rule. *Federal register* 63 (241):69390-69476.

- U. S. Environmental Protection Agency. 2006. National primary drinking water regulations: Stage 2 disinfectants and disinfection byproducts rule. *Fed. Reg.* 71 (2):387-493.
- Umemura, T., and Y. Kurokawa. 2006. Etiology of bromate-induced cancer and possible modes of action-studies in Japan. *Toxicology* 221 (2-3):154-157.
- Umemura, T., A. Takagi, K. Sai, R. Hasegawa, and Y. Kurokawa. 1998. Oxidative DNA damage and cell proliferation in kidneys of male and female rats during 13-weeks exposure to potassium bromate (KBrO₃). *Archives of Toxicology* 72 (5):264.
- Villanueva, C. M., K. P. Cantor, S. Cordier, J. J. Jaakkola, W. D. King, C. F. Lynch, S. Porru, and M. Kogevinas. 2004. Disinfection byproducts and bladder cancer: a pooled analysis. *Epidemiology* 15 (3):357-367.
- Wagner, E. D., and M. J. Plewa. 2009. Microplate-based comet assay. In *The Comet Assay in Toxicology*, edited by A. Dhawan and D. Anderson. London: Royal Society of Chemistry.
- Wagner, E. D., A. L. Rayburn, D. Anderson, and M. J. Plewa. 1998. Analysis of mutagens with single cell gel electrophoresis, flow cytometry, and forward mutation assays in an isolated clone of Chinese hamster ovary cells. *Environ. Mol. Mutagen.* 32 (4):360-368.
- Wagner, E. D., A. L. Rayburn, D. Anderson, and M. J. Plewa. 1998. Calibration of the single cell gel electrophoresis assay, flow cytometry analysis and forward mutation in Chinese hamster ovary cells. *Mutagenesis* 13 (1):81-84.
- Wang, X., C. H. McGowan, M. Zhao, L. He, J. S. Downey, C. Fearn, Y. Wang, S. Huang, and J. Han. 2000. Involvement of the MKK6-p38gamma cascade in gamma-radiation-induced cell cycle arrest. *Mol Cell Biol* 20 (13):4543-52.
- Wang, Y. G., C. Nnakwe, W. S. Lane, M. Modesti, and K. M. Frank. 2004. Phosphorylation and regulation of DNA ligase IV stability by DNA-dependent protein kinase. *J Biol Chem* 279 (36):37282-90.
- Waters, M. D., M. Jackson, and I. Lea. 2010. Characterizing and predicting carcinogenicity and mode of action using conventional and toxicogenomics methods. *Mutat. Res.* in press.
- Woo, Y. T., D. Lai, J. L. McLain, M. K. Manibusan, and V. Dellarco. 2002. Use of mechanism-based structure-activity relationships analysis in carcinogenic potential ranking for drinking water disinfection by-products. *Environ. Health Perspect.* 110 Suppl 1:75-87.
- Xu, X., T. M. Mariano, J. D. Laskin, and C. P. Weisel. 2002. Percutaneous absorption of trihalomethanes, haloacetic acids, and halo ketones. *Toxicol. Appl. Pharmacol.* 184 (1):19-26.
- Yang, C. R., S. Yeh, K. Leskov, E. Odegaard, H. L. Hsu, C. Chang, T. J. Kinsella, D. J. Chen, and D. A. Boothman. 1999. Isolation of Ku70-binding proteins (KUBs). *Nucleic Acids Res* 27 (10):2165-74.
- Yoshikawa, Y. M., S. Shudo, K. Sanui, and N. Ogata. 1986. Active transport of organic acids through poly (4-vinylpyridine-co-acrylonitrile) membranes. *J. Membr. Sci.* 26 (1):51-61.
- Yu, X., and R. Baer. 2000. Nuclear localization and cell cycle-specific expression of CtIP, a protein that associates with the BRCA1 tumor suppressor. *J Biol Chem* 275 (24):18541-9.
- Yuan, J., H. Liu, L. H. Zhou, Y. L. Zou, and W. Q. Lu. 2006. Oxidative stress and DNA damage induced by a drinking-water chlorination disinfection byproduct 3-chloro-4-(dichloromethyl)-5-hydroxy-2 (5H)-furanone (MX) in mice. *Mutat. Res.* 609:129-136.
- Zhang, H. S., and S. Q. Wang. 2006. Ginsenoside Rg1 inhibits tumor necrosis factor-alpha (TNF-alpha)-induced human arterial smooth muscle cells (HASMCs) proliferation. *J Cell Biochem* 98 (6):1471-81.

- Zhang, S. H., D. Y. Miao, A. L. Liu, L. Zhang, W. Wei, H. Xie, and W. Q. Lu. 2010. Assessment of the cytotoxicity and genotoxicity of haloacetic acids using microplate-based cytotoxicity test and CHO/HGPRT gene mutation assay. *Mutat. Res.* 703 (2):174-179.
- Zhang, X., S. Echigo, R. A. Minear, and M. J. Plewa. 2000. Characterization and comparison of disinfection by-products of four major disinfectants. In *Natural Organic Matter and Disinfection By-Products: Characterization and Control in Drinking Water*, edited by S. E. Barrett, S. W. Krasner and G. L. Amy. Washington, D.C.: American Chemical Society.
- Zhao, G. Y., E. Sonoda, L. J. Barber, H. Oka, Y. Murakawa, K. Yamada, T. Ikura, X. Wang, M. Kobayashi, K. Yamamoto, S. J. Boulton, and S. Takeda. 2007. A critical role for the ubiquitin-conjugating enzyme Ubc13 in initiating homologous recombination. *Mol Cell* 25 (5):663-75.
- Zilberstein, A., R. Ruggieri, J. H. Korn, and M. Revel. 1986. Structure and expression of cDNA and genes for human interferon-beta-2, a distinct species inducible by growth-stimulatory cytokines. *Embo J* 5 (10):2529-37.

ABBREVIATIONS

α	alpha value is the acceptable probability of incorrectly rejecting the null hypothesis
Å	angstrom
ANOVA	analysis of variance
AS52	a transgenic clone of CHO cells derived from line K1 BH4
AWWA	American Water Works Association
AwwaRF	Awwa Research Foundation
BAA	bromoacetic acid
Br	a chemical element with the symbol Br, an atomic number of 35, and an atomic mass of 79.904.
°C	degrees Celsius
CAA	chloroacetic acid
cDNA	complementary DNA
CHO	Chinese hamster ovary cells
Cl	a chemical element with the symbol Cl, an atomic number 17, and an atomic mass of 35.453.
DAVID	Database for Annotation, Visualization and Integrated Discovery
DBP	disinfection by-product
DMSO	dimethylsulfoxide
dsDNA	double strand DNA
EDTA	ethylenediaminetetraacetic acid disodium salt dehydrate
EGF	epidermal growth factor
EI	electron ionization
ELUMO	lowest unoccupied molecular orbital
EMS	ethylmethanesulfonate
<i>ex vivo</i>	tissue or organ from a living organism
F12	Hams F12 medium
<i>F</i> value	the ratio of population of variances of normal populations
FBS	fetal bovine serum
FHs 74 Int	non-transformed fetal human intestinal cells
g	gram
GC	gas chromatography
GSH	glutathione
GSTT1-1	glutathione-S-transferase-theta 1-1
h	hour
HAA	haloacetic acid

HBSS	Hank's balanced salt solution
I	a chemical element that has the symbol I and the atomic number 53, and an atomic mass of 126.9045.
IAA	iodoacetic acid
IARC	International Agency for Research on Cancer
ICR	U.S. EPA's Information Collection Rule
i.d.	internal diameter
<i>in vitro</i>	in an artificial environment outside the living organism
<i>in vivo</i>	within a living organism
K1-BH4	CHO cell parental line to CHO cell line AS52, clone 11-4-8
kcal	kilocalories
KV	kilovolt
L	liter
log <i>P</i>	octanol-water partition coefficient
M	molar
m	meter
MCL	maximum contaminant level
MCN	micronucleus
μg	microgram
μL	microliter
μM	micromolar
μm	micrometer
mg	milligram
mL	milliliter
mM	millimolar
mm	millimeter
min	minute
mol	mole
monoHAA	monohaloacetic acid
mRNA	massager RNA
MS	mass spectrometry
NA	not applicable
N-DBP	nitrogen-containing DBP
ng	nanogram
NS	not statistically significant
PBS	phosphate-buffered saline
%C _{1/2} value	the calculated DBP concentration that induced a CHO cell density that was 50% of the negative control
% tail DNA	the amount of DNA that migrated from the nucleus into the microgel
power	the probability that the statistical test will detect a difference if there really is a difference

pH	the logarithm of the reciprocal of hydrogen-ion concentration in gram atoms per liter
pKa	the negative logarithm of the equilibrium constant for the dissociation $HA \leftrightarrow H^+ + A^-$
qRT-PCR	quantitative real time polymerase chain reaction
R^2	the fit of the regression analysis
r	Pearsons Product Moment correlation coefficient
RIN	RNA Integrity Number
S9	hepatic 9000 $\times g$ supernatant
SAR	structure activity relationship
SCGE	single cell gel electrophoresis
SN2	alkylation potential
ssDNA	single strand DNA
t_{50}	the time during liquid holding needed to allow for 50% of the repair of genomic DNA
.txt	text file
TOC	total organic carbon
TOX	total organic halide
U.S. EPA	United States Environmental Protection Agency
v/v	volume to volume
V	volt